1-1-2018

Optimal Planning of Microgrid-Integrated Battery Energy Storage

Ibrahim S. Alsaidan
University of Denver

OPTIMAL PLANNING OF MICROGRID-INTEGRATED BATTERY ENERGY STORAGE

_____

A Dissertation

Presented to

the Faculty of the Daniel Felix Ritchie School of Engineering and Computer Science

University of Denver

_____

In Partial Fulfillment

of the Requirements for the Degree

Doctor of Philosophy

_____

by

Ibrahim S. Alsaidan

March 2018

Advisor: Dr. David Wenzhong Gao

Co-Advisor: Dr. Amin Khodaei

Author: Ibrahim S. Alsaidan
Title: OPTIMAL PLANNING OF MICROGRID-INTEGRATED BATTERY ENERGY STORAGE
Advisors: David Wenzhong Gao, Amin Khodaei
Degree Date: March 2018

Abstract

Battery energy storage (BES) is a core component in reliable, resilient, and cost-effective operation of microgrids. When appropriately sized, BES can provide the microgrid with both economic and technical benefits. Besides the BES size, it is found that there are mainly three planning parameters that impact the BES performance, including the BES integration configuration, technology, and depth of discharge.

In this dissertation, the impact of each one of these parameters on the microgrid-integrated BES planning problem is investigated. Three microgrid-integrated BES planning models are developed to individually find the optimal values for the aforementioned parameters. These three microgrid-integrated BES planning models are then combined and extended, by including the impact of microgrid islanding incidents on the BES planning solution, to develop a comprehensive planning model that can be used by microgrid planners to simultaneously determine the installed BES optimal size, integration configuration, technology, and maximum depth of discharge.

Besides applications in microgrids, this dissertation investigates the integration of BES to provide other types of support in distribution networks such as load management of commercial and industrial customers, distribution network expansion, and solar PV ramp rate control.

Acknowledgements

This dissertation would not have been completed without the help of my advisors, Dr. David Gao and Dr. Amin Khodaei. Dr. Gao's courses provided me with the knowledge required to peruse my PhD research. His guidance, support, encouragement, and understanding were of great help in completing this work. Dr. Gao helped me in conducting this advanced and interesting research by providing an intellectually stimulating environment and interactions. I consider myself lucky having the opportunity to work with Dr. Khodaei. I owe a lot to Dr. Khodaei for what I have learned about microgrid and power system planning. I am highly grateful to the time he made himself available to answer my inquiries and to the expertise he shared with me that made solving the research challenges possible.

I would also like to thank my committee members; Dr. David Gao, Dr. Amin Khodaei, Dr. Mohammed Matin, and Dr. Ron Throupe for taking time to review this dissertation and providing the valuable comments that will improve the dissertation quality. I am also grateful to numerous researchers whose papers are listed in the reference section.

This dissertation is dedicated to the memory of Norah Al-Khames, an exceptional mother, a wonderful woman, and an inspirational figure. My mother was a great person who dedicated her life to her family. I find myself obliged to thank Mr. Saleh Al-Khames, who, although no longer with us, continues to inspire by his wisdoms and dedication to his beloved ones. Many thanks are due to my family members for their support and love. Last but not least, I would like to express my special gratitude to my wife Alhanof Albuhairi and my son Saad for their patience and support during my PhD studies.

Table of Contents

List of Figures

List of Tables

List of Symbols

Symbol	Definition
Chapter 2	
Indices:	
ch	Superscript for BES charging.
dch	Superscript for BES discharging.
d	Index for day.
h	Index for hour.
i	Index for distributed energy resources.
n	Index for BES number.
Sets:	
S	Set of BES units.
G	Set of dispatchable DGs.
W	Set of renewable DGs.
Parameters:	
BL	Investment budget.
CE^a	Annualized energy rating cost.
CP^a	Annualized power rating cost.
CL	Critical load demand.
L	Load demand.
D	BES depth of discharge.
$P^{M,\max}$	Maximum power that can be transferred to/from the main grid.
r	interest rate.
T	BES lifetime.
v	Value of lost load.
DR,UR	Ramp down and ramp up rates.
DT, UT	Minimum down and up times.
ρ	Real electricity price.
η	BES round trip efficiency.
δ	Microgrid type identifier (1 if grid-tied, 0 if isolated).
Variables:	
C	Stored energy in the BES at each interval.
C^R	BES rated energy.
P^R	BES rated power.
P^M	Power exchanged with main grid.
LS	Load curtailment.
I	State of dispatchable DG (1 if committed, 0 otherwise).
P	DER output power.
R	DER available online reserve.
T^{on}, T^{off}	Number of consecutive ON and OFF times.
u	BES operating state (1 if discharging, 0 otherwise).

ξ	A variable that represents the performed BES cycle (1 if BES cycle is completed, 0 otherwise).

Chapter 3

Indices*:*

ch	Superscript for BES charging.
dch	Superscript for BES discharging.
d	Index for day.
h	Index for hour.
i	Index for distributed energy resources.
m	Index for considered depth of discharge values.
n	Index for incremental steps in the BES size.

Sets:

S	Set of BES units.

Parameters:

N	BES number of cycles.
T	BES lifetime.
η	BES round trip efficiency.
σ	BES charging/discharging period.
ψ	BES degradation factor.

Variables:

C	Stored energy in the BES at each interval.
C^R	BES rated energy.
P^R	BES rated power.
D	BES depth of discharge.
P	DER power.
P^{ch},P^{dch}	BES charging and discharging power.
u	BES operating state (1 if discharging, 0 otherwise).
ξ	A variable that represents the performed BES cycle (1 if BES cycle is completed, 0 otherwise).
w	Binary variable that represents the chosen value of the BES depth of discharge (1 if chosen, 0 otherwise).
x	BES investment state (1 if installed, 0 otherwise).
γ	BES state of charge at each time interval.
z	BES depth of discharge indicator (1 at the actual depth of discharge, 0 otherwise).
λ	Estimated BES degradation factor at each cycle.

Chapter 4

Indices

b	Index for bus.
d	Index for day.
h	Index for hour.
i	Index for distributed energy resources.

l	Index for lines.
m	Index for depth of discharge segments.
s	Index for scenarios.
~	Index for forecasted parameter.

Sets

B	Set of BES technologies.
K	Set of microgrid buses.
L	Set of microgrid distribution lines.
N	Set of maximum depth of discharge segments.
G	Set of dispatchable units.
W	Set of renewable generation units.
Φ	Set of uncertain parameters.

Parameters

BL	BES investment budget limit.
CE_i^a, CP_i^a	BES annualized energy/power capital cost.
CI_i^a	BES annualized installation cost.
CM_i	BES annual operating and maintenance cost.
D_{bdh}, CD_{bdh}	Total load demand and critical load demand at bus b, day d, hour h.
DR_i, UR_i	Ramp down and ramp up rates.
DT_i, UT_i	Minimum down and up times.
$f_l^{\max}$	Maximum power capacity of distribution lines.
$P^{M,\max}$	Maximum power capacity of the line connecting the microgrid to the utility grid.
r	Interest rate.
T	Project lifetime.
pr_s	Probability of islanding scenarios.
v	Value of lost load, $/kWh.
z_{dhs}	Microgrid/utility grid connection state.
$\alpha_i^{\max}, \alpha_i^{\min}$	Maximum and minimum BES energy rating to power rating ratio.
γ_{ibm}	BES maximum depth of discharge.
κ_{im}	BES lifecycle.
ρ_{dh}	Electricity market price, $/kWh.
η_i	BES round trip efficiency.
μ_{ib}	Element of generation-bus incidence matrix (1 if unit i is connected to bus b, 0 otherwise).
ψ_{lb}	Element of line-bus incidence matrix (1 if line l is connected to bus b, 0 otherwise).

Variables

C_{ibdhs}	Stored energy in the BES at each interval.
C_{ib}^R, P_{ib}^R	BES rated energy and rated power.
$P_{ibdhs}^{ch}, P_{ibdhs}^{dch}$	BES charging and discharging power.

F_i	Cost function of the microgrid local DG units.
f_{ldhs}	Distribution line power flow.
LS_{bdhs}	Load curtailment.
I_{idhs}	Commitment state of dispatchable units.
P_{idhs}	DER output power.
P_{dhs}^{M}	Power transferred to/from the utility grid.
$T_{idh}^{\text{on}}, T_{idh}^{\text{off}}$	Number of consecutive ON and OFF times.
u_{ibdhs}	BES operating state.
x_{ib}	BES investment state (1 if installed, 0 otherwise).
w_{ibm}	Binary variable that represents the chosen value of the BES maximum depth of discharge for discharge segment *m* (1 if chosen, 0 otherwise).
ξ_{ibdhs}	BES cycle indicator.
$\chi^{g}, \chi^{l}, \chi^{p}$	Auxiliary binary variables for renewable DGs generation, load demand, and electricity price.

Chapter 5

Indices:

ch	Superscript for BES charging.
dch	Superscript for BES discharging.
k	Index for the depth of discharge segments.
m	Index for month.
h	Index for hour.
t	Index for time intervals.
i,j	Index for buses.
s	Index for candidate BES units.
^	Index for calculated variables.

Sets:

B_i	Set of buses adjacent to bus *i*.
S_i	Set of candidate DES units installed at bus *i*.
L_e	Set of existing distribution lines.
L_c	Set of candidate distribution lines.

Parameters:

b	Line susceptance.
BL	Budget limit.
CL	Distribution line annualized investment cost.
CC^E	Annualized energy rating capital cost.
CC^P	Annualized power rating capital cost.
D	BES depth of discharge.
g	Line conductance.
K	Large positive constant number.
L	Load demand.

T	BES/project lifetime.
PL^{max}	Distribution line capacity.
P^{PV}	Solar photovoltaic output power.
PD	Load active power.
PQ	Load reactive power.
v	Value of lost load.
ρ	Energy rate/price ($/kWh).
λ	Demand rate/price ($/kW).
η	BES roundtrip efficiency.
α	BES charging/discharging duration.

Variables:

C^B	BES investment cost.
C^E	Consumer energy cost.
C^P	Consumer peak demand cost.
C^R	BES rated energy.
E^B	Stored energy in the BES.
E^R	BES rated energy.
LS	Load curtailment.
P^B	BES net output power.
P^R	BES rated power.
P^{dch}	BES discharging power.
P^{ch}	BES charging power.
P^M	Active power exchange with the utility grid in MW.
P^{max}	Commercial customer monthly peak load.
PL	Line active flow.
Q^M	Reactive power exchange with the utility grid in MWh.
QL	Line reactive flow.
N	BES number of cycles.
u	BES operating state (1 if discharging, 0 otherwise).
V	Bus voltage magnitude.
ξ	BES cycles indicator (1 if the cycle is completed, 0 otherwise)
w	BES depth of discharge indicator (1 if a specific depth of discharge segment is selected, 0 otherwise).
x	BES investment state (1 if installed, 0 otherwise)
z	Distribution line investment state (1 if installed, 0 otherwise).
θ	Bus voltage angle.

Chapter 1. Introduction

1.1 Theoretical Background

The deployment of energy storage systems in distribution network has considerably increased in recent years. Installed distributed energy storages (DES) are owned by electric utilities or customers and used to provide a variety of services. For example, utilities deploy DES to defer distribution network upgrades, improve reliability, or enhance voltage profile in their system. The customers on the other hand, install DES to reduce their electricity payment by taking advantage of electricity price variations through an energy arbitrage or by reducing their potential demand charges.

The attention toward DES has also increased with the development of microgrids. The urgent need for reducing greenhouse gas emissions, improving the system reliability and power quality, and upgrading the aging transmission and distribution infrastructure, have led to a significant increase in the deployment of microgrids in power systems. The U.S. Department of Energy defines a microgrid as "a group of interconnected loads and distributed energy resources (DERs) with clearly defined electrical boundaries that acts as a single controllable entity with respect to the grid and can connect and disconnect from the grid to enable it to operate in both grid-connected or islanded modes" [1].

Based on this definition, microgrids can be divided into two types: grid-tied microgrids and isolated microgrids. In the first type, the microgrid is connected to the main distribution network through a connection point known as point of common coupling

(PCC). Grid-tied microgrids can disconnect themselves from the distribution network and operate in islanded mode, protecting their demand from being affected by any external faults. The second microgrid type (i.e., isolated microgrid) is used to supply remote areas demand for electricity where the connection to the utility grid is not available.

Microgrids are considered as viable enablers of DERs integration, and in particular, would facilitate an efficient and reliable integration of emission free renewable distributed generators (DGs) to support the environmental agenda. Renewable DGs, however, produce a variable output power that may impose several challenges to the microgrid operation and control, especially during the islanded operation. Various methods are studied to mitigate the generation intermittency and volatility associated with renewable DGs, including but not limited to demand response [2], generation curtailment [3], provisional microgrids [4] [5], and DES deployment [6]. The demand response and renewable generation curtailment methods are argued to reduce the microgrid's economic value and/or reliability as they are based on either reducing the available renewable DGs generation or supplied demand (e.g., load shedding or load shifting). Provisional microgrids significantly facilitate the integration of renewable DGs, however, they require additional investments and control mechanism to ensure a reliable and economic operation. The DES, among the rest, is discussed to be the best option for mitigating the challenges imposed by renewable generation and improving microgrid reliability while at the same time reducing the microgrid operation cost.

DES can store the excess renewable generation to be utilized when it is beneficial from either an economic perspective (e.g., energy arbitrage) or a technical perspective (e.g., frequency and voltage regulation) [7]. DES applications in microgrids can be further

categorized into energy applications and power applications [8]. DES technologies that have high power density and fast response are known to be best suited for power quality and frequency regulation applications. On the other hand, DES technologies that have high energy density and long discharging time are well suited for long-term applications including peak shaving and energy arbitrage. Figure 1.1 shows several existing DES technologies that can be used in microgrid applications. Among these technologies, battery energy storage (BES) technology is considered to be the most attractive option due to its technological maturity and ability to provide both sufficient energy and power densities [9].

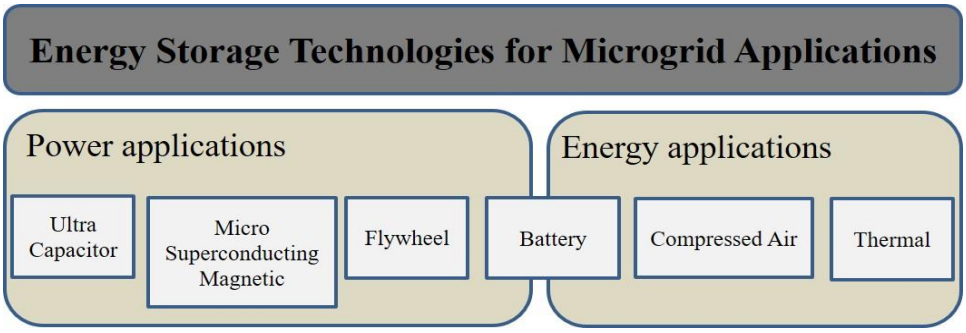

Figure 1.1 DES technologies for microgrid applications

1.2 Literature Review

Different methods have been proposed in literature to solve the microgrid-integrated BES planning problems. In this section, a comprehensive literature review of existing methods is presented. Based on the planning objective, the existing methods are categorized into: a) cost-based BES planning methods and b) non-cost-based BES planning methods. In the cost-based methods, the BES planning problem is solved to either minimize the total cost or maximize the total benefits associated with installing the BES within the microgrid. In the non-cost-based methods, the BES planning problem is solved to provide

technical services such as frequency control, voltage regulation, and power smoothing. In such methods, the economic aspect of the problem is ignored.

1.2.1 Cost-Based BES Planning Methods

The investment cost associated with purchasing, installing, operating, and disposing the BES is greatly related to their size. Thus, most of the existing works in literature are concentrated on finding the optimal size for the installed BES. A few works, however, include other parameters such as technology and location into the microgrid-integrated BES planning problem. The installation of the BES is economically justifiable only if the provided economic benefits outweigh the investment cost. Most of the reviewed papers formulate the BES planning problem as an optimization problem whose objective is either to minimize the microgrid total expansion planning cost or to maximize the total benefits (i.e., a cost-benefit analysis). The BES parameters are considered as a design variables whose optimal value is determined by solving the optimization problem. Figure 1.2 shows the typical microgrid total expansion planning cost components, which are divided into two categories: microgrid operation cost and BES investment cost. The former includes any operation cost needed to supply the microgrid local load such as the fuel cost and the cost of energy exchanged with the utility grid. It must be noted that the cost or benefit of exchanging power with the utility grid is only considered for grid-tied microgrids. Nevertheless, the reviewed papers may include all or some of the microgrid total cost components depicted in Figure 1.2.

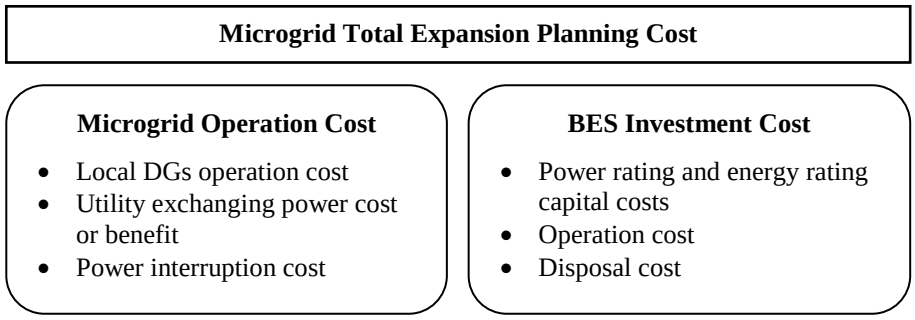

Figure 1.2 Microgrid total expansion planning cost components [10]

The works in [11]-[14] implement mixed integer linear programming (MILP) to formulate the BES planning problem. In [11], the renewable generation is not considered and the BES is sized for a microgrid containing only dispatchable DGs which reduces the potential economic benefits of the BES and ignores one of the most important aspects of microgrids. However, this work is expanded in [12] to consider not only renewable generation but also a reliability criterion. Different scenarios for the power system conditions such as generator outages and line contingencies as well as renewable generation are stochastically produced using Monte Carlo Simulation (MCS). After that, the large number of generated scenarios is reduced by a scenario reduction technique. A loss of load expectation (LOLE) index is used to evaluate the reliability of the studied microgrid. A BES capacity expansion model is developed in [13] for an isolated microgrid. In this work, the selected BES size is not considered fixed and is updated through the planning time horizon. It is found that the developed model reduces the associated cost by 10% as compared to fixed BES size methods. Similar to [12], this paper uses MCS to model the stochastic nature of wind speed, microgrid load, and DG availability, followed by a scenario reduction technique. The Ah-throughput is used as a measure for the BES lifetime, which is defined as the total amount of Ah or Wh that the BES is expected to deliver

throughout the project lifetime before it needs to be replaced. The Ah-throughput is normally made readily available by the BES manufacturer. However, this method is not able to accurately determine the BES lifetime as the impact of important factors such as depth of discharge and number of cycles are overlooked. The work in [14] includes the installation year into the expansion problem and determines the optimal size and installation year for BES in an isolated microgrid that minimizes the total microgrid cost.

A genetic algorithm (GA) is employed in [15] to develop the knowledge base for a fuzzy expert system that is used to manage the BES output power and solve a daily unit commitment problem in order to minimize the microgrid operation cost. In this work, the BES is sized using GA while its charging/discharging schedules are determined based on a fuzzy expert system. For economic reasons, the model proposed in [15] does not impose a minimum state of charge limit on the BES. Instead, a new cost associated with operating the BES at low state of charge is introduced to the objective function to prevent unnecessary deep discharge incidents. Similar to [13], the aging of the installed BES is modeled based on the weighted Ah-throughput. In this model, a weighting factor corresponding to the BES state of charge is multiplied by the amount of the actual Ah delivered to obtain what is called the effective cumulative Ah. This effective cumulative Ah is divided by the expected Ah that the BES is presumed to deliver when it is first installed to determine the BES loss of life. In [16], a hybrid GA-sequential quadratic programming (SQP) is used to optimize the size and the location of the BES units and capacitors in a smart grid. The SQP is used to solve the optimal power flow while the GA is used to determine the optimal size and location of the BES units and the capacitors that minimize the overall planning cost. A non-dominated sorting genetic algorithm II (NSGA-

II) is employed in [17] to solve a multi-objective BES sizing problem in presence of demand response (DR). The considered objectives are to maximize the photovoltaic consumptive rate and the net profit of the microgrid. In [18] a clustering techniques are adopted to generate a number of scenarios associated to the wind speed, solar radiation, and load daily patterns to be used in BES sizing. GA is implemented to solve the proposed optimization problem as well.

The work in [19] studies BES sizing considering the stochastic nature of wind generation. A Here-and-Now approach is implemented to model the variability of wind generation by including new constraints to the microgrid unit commitment formulation. Particle swarm optimization (PSO) method is used to find the optimal BES size that maximize the microgrid total benefit in the grid-connected mode and minimize the microgrid total cost in the islanded mode. By decomposing the BES sizing problem into two subproblems (i.e., a planning subproblem and an energy management subproblem), the work in [20] develops a two-stage optimization strategy in order to reduce the computation time required to find the optimal BES size. An improved PSO is applied to solve the planning subproblem while Mesh Adaptive Direct Search black box optimization algorithm is implemented to solve the microgrid energy management subproblem. The authors of [21] and [22] study the optimal BES sizing in the presence of DR to regulate the frequency and voltage of a grid-tied microgrid during islanding. A multi-objective function is developed aiming to minimize the BES capital cost, maintenance and operating cost, as well as the size required to maintain the microgrid stability. A quantum-behaved particle swarm optimization (QSPO) is used in [23] to optimize the size of a hybrid energy storage system (HESS) that is composed of batteries and ultracapacitors. The authors compare the

obtained results by the one obtained using conventional PSO and find that the QSPO is faster in solving the optimization problem.

A new evolutionary optimization algorithm is improved and adopted by the authors in [24] to determine the optimal energy rating of a BES installed in a grid-tied microgrid. The new algorithm is called Bat Algorithm (BA) and is described as a population-iterative based method. The proposed improved BA (IBA) results are compared to other optimization methods such as conventional BA, teaching-learning-based optimization, and artificial bee colony in terms of the resulted error from conducted test functions. In general, it is shown that the IBA yields smaller error values, in terms of best value, mean value, and standard deviation, compared to the other methods. Another new evolutionary optimization algorithm known as grey wolf optimization (GWO) is applied in [25] to solve the BES sizing problem in a microgrid. The obtained microgrid operation cost at the optimal BES size along with other optimization parameters such as standard deviation and simulation time are compared to those obtained by different optimization methods including the aforementioned IBA. GWO shows a superior performance compared to other optimization methods. The stochastic nature of the microgrid demand, renewable generation, and electricity price is considered in [26]. A scenario based model is developed to formulate the unit commitment problem. The impact of the DES size on the microgrid operation cost is further investigated.

An iterative based method is implemented in [27]–[30] to determine the optimal BES size. The microgrid unit commitment problem is solved for different BES sizes within predetermined minimum and maximum values as shown in Figure 1.3. The unit commitment problem is solved by implementing dynamic programming (DP) in [27],

knowledge based expert system controller (KBES) in [28], mixed integer nonlinear programming (MINLP) in [29], and MILP in [30]. The work in [27] focuses on determining the optimal power rating and energy rating of a Vanadium Redox Battery (VRB) taking into account the nonlinear relationship between the VRB power and efficiency. Different energy storages technologies, including BES, are considered in [28] and it is found that lead acid battery yields the minimum energy cost and hence it is the optimal energy storage technology choice. The problem of reserve sizing and BES sizing is investigated in [31]. The authors propose a two-stage probabilistic co-optimization method that determines the optimal BES size as well as the reserve amount that minimizes the microgrid total cost with the consideration of the system reliability. The sizing problem is decomposed into a master problem in which the BES size is fixed and a subproblem in which the optimal reserve size is calculated. The BES size is then updated and the process is repeated. The optimal solution (i.e., the BES optimal size and the optimal reserve) would be the one that minimizes the microgrid total cost. In order to reduce the calculation time, a Markovian steady state analysis is implemented to solve the subproblem and find the optimal reserve value.

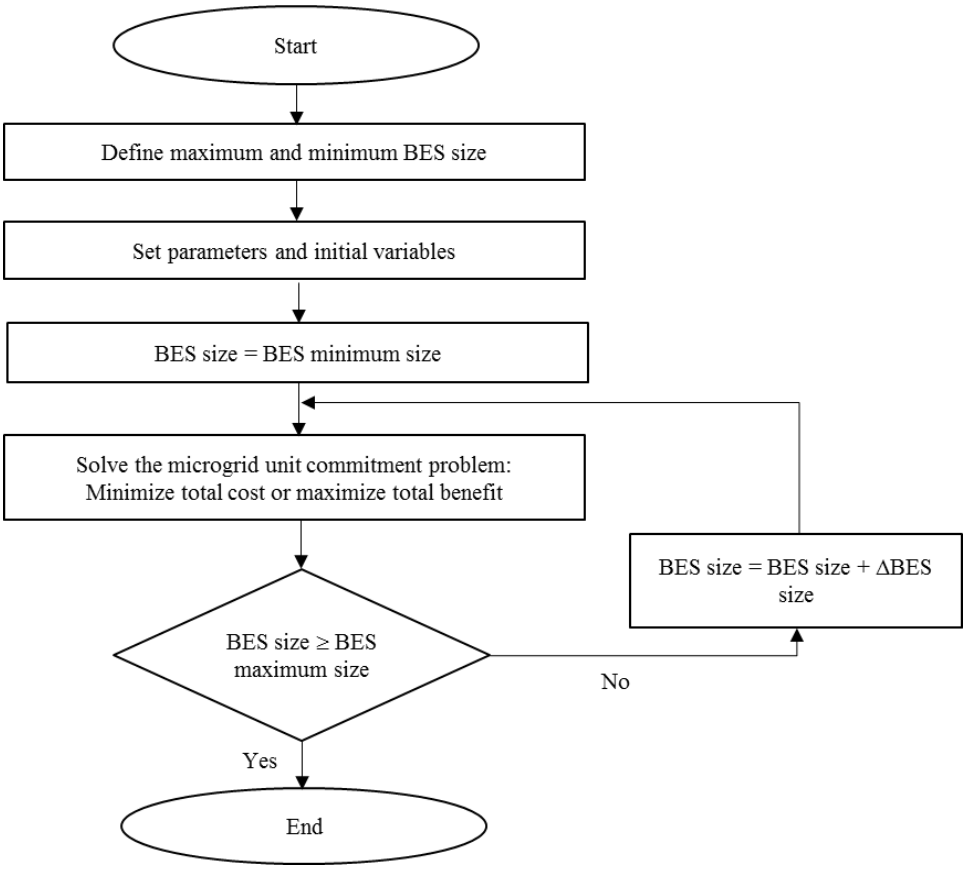

Figure 1.3 General flowchart for sizing BES using iterative based methods [10]

1.2.2 Non-Cost-Based BES Planning Methods

The common aspect of the previous reviewed works is that they solve the microgrid-integrated BES planning problem based on an economic objective. However, the following papers approach the BES planning problem from a different perspective. A duty cycle based sizing method is used in [32] in order to determine the size of a BES to be used for peak shaving applications. The BES cycling and the temperature impact on the sizing problem are considered and included as factors that adjust the determined size. However, it is not clear how the authors determine the values of these factors. In [33], the installed BES is analytically sized in order to smooth the power oscillation seen by the utility grid. A control algorithm is also developed to protect the BES from being over

charged or discharged. The authors in [34] size the BES in order to minimize the power transferred through the line connecting the microgrid to the utility grid. The idea behind this is to reduce the dependency of the microgrid on the utility grid which will lead to improved microgrid reliability during islanded operation. The BES size and location are determined in [35] for both grid-connected and islanded microgrids simultaneously. A GA is used to solve the microgrid AC power flow. The fitness function is selected to minimize the power losses and improve the voltage profile. In [36], authors use a HESS which consists of batteries and supercapacitors to improve the power quality when integrating wind power in islanded microgrids. Supercapacitors can smooth the wind power with high frequency whereas the low frequency part of wind power is smoothed by batteries. The optimization problem is modeled by Back Propagation neural network approach and solved in short term (to test the wind power smoothing) and long term (to prove the economic viability of the model).

The appropriate size for BES to regulate the frequency of an islanded microgrid is investigated in [37]–[41]. In [37] a BES size optimization method based on an artificial neural network (ANN) model is proposed. The model inputs are the islanded microgrid frequency and voltage, and the output is the optimal BES size that is obtained after training the data using a multilayer perceptron structure. The multilayer perceptron structure can ensure high accuracy of data fitting so the error of obtained optimal sizing is very small. Moreover, the effect of the BES location has been investigated and it is found that the optimal location should be close to local loads to minimize power losses. In [38], the BES is optimized by analyzing the value of power ramp rate (PRR) of the microgrid. The case study shows the effect of the BES on the frequency control with and without considering

the PRR. It is shown that the energy of BES that is essential for frequency control is remarkably reduced with the PRR consideration. The BES in [39] is used as a primary frequency controller to utilize the overloading characteristics of BES to restore the mismatch power during islanding transition in microgrids. The optimal BES capacity should be able to capture the maximum mismatch power. So, the mismatch power is calculated first to determine the BES overload capacity. The largest overloading charge or discharge power to restore the mismatch power is considered as the optimal power rating of the BES. An inertia based method is proposed in [40] to size the BES considering primary control (arrest the deviated frequency) and secondary control (restore the deviated frequency). The inertia deficiency for primary and secondary controls are measured as the key parameter of the BES sizing. The provided power from the BES may result in voltage violation, hence, the voltage stability is enhanced by using power electronics. It is discussed that the proposed method performs better in low resistance/reactance distribution networks. A HESS is presented in [41] as an islanded microgrid frequency controller. The frequency is controlled based on hysteretic loop control to prolong battery lifetime by preventing small charge/discharge cycles, while a statistical model based on MCS is applied to determine the optimal capacity distributions of the HESS. The HESS output power is determined and analyzed through simulation process on the system data. The optimal rated power of the battery is determined to depend on the maximum charging or discharging power in all cycles, while the optimal rated energy is the integration of all charging and discharging power in each single cycle. Similar to battery, the supercapacitor distributions capacity is found. The reviewed microgrid-integrated BES planning methods are summarized in Table 1.1 in terms of considered microgrid type, BES optimized

parameters and planning timeframe. A single day planning timeframe or less is labeled as short term whereas one year planning timeframe or longer is labeled as long term.

Table 1.1 Summary of existing microgrid-integrated BES planning methods [10]

Reference Number	Microgrid Operation Mode		BES Optimized Characteristics					Planning Timeframe	
	Grid-connected	Isolated or Islanded	Power Rating	Energy Rating	Depth of Disch.	Technology	Location	Short	Long
[11]	√	×	√	×	×	×	×	×	√
[12]	√	×	√	√	×	×	×	×	√
[13]	×	√	√	×	×	×	×	×	√
[14]	×	√	√	√	×	×	×	×	√
[15]	√	×	√	√	×	×	×	√	×
[16]	√	×	√	×	×	×	√	×	√
[17]	√	×	×	√	×	×	×	×	√
[18]	×	√	×	√	×	×	×	√	×
[19]	√	√	×	√	×	×	×	√	×
[20]	√	√	√	√	×	×	×	×	√
[21]	×	√	√	×	×	×	×	√	×
[22]	×	√	√	×	×	×	×	√	×
[23]	×	√	×	√	×	×	×	√	×
[24]	√	×	×	√	×	×	×	√	×
[25]	√	×	×	√	×	×	×	√	×
[26]	√	×	×	√	×	×	×	√	×
[27]	√	√	√	√	×	×	×	√	×
[28]	×	√	√	√	×	√	×	×	√
[29]	×	√	×	√	×	×	×	√	×
[30]	√	√	×	√	×	×	×	√	×
[31]	√	√	×	√	×	×	×	×	√
[32]	×	√	×	√	×	×	×	√	×
[33]	√	×	√	√	×	×	×	√	×
[34]	√	×	√	×	×	×	×	√	×
[35]	√	√	√	×	×	×	√	√	×
[36]	×	√	×	√	×	×	×	√	×
[37]	×	√	√	×	×	×	×	√	×
[38]	×	√	√	√	×	×	×	√	×
[39]	×	√	√	×	×	×	×	√	×
[40]	×	√	√	√	×	×	×	√	×
[41]	×	√	√	√	×	×	×	√	×

1.3 Research Motivation, Dissertation Organization, and Main Contributions

It is found that the reviewed microgrid-integrated BES planning methods in the previous section have either one or more of the following shortfalls: (i) Short time frame (e.g., one day) or static models (i.e., operation snapshots) are used to calculate the optimal BES size, which reduce the accuracy and the practicality of the obtained results; (ii) A single BES technology is considered while ignoring the wide range of available BES with various technical and economical characteristics; (iii) The impact of some decisive factors on the BES lifetime is overlooked, such as the BES depth of discharge, number of charging/discharging cycles, and centralized vs. distributed installations; and (iv) On merely one operation mode (i.e., either grid-connected or islanded) is focused while the required coordination is not taken into account.

To overcome these shortfalls, five microgrid-integrated BES planning models are developed in this research. Chapter 2 presents the general outlines for the developed microgrid-integrated BES planning models and specifically discusses the first two models which are used to determine the optimal BES size, integration configuration, and technology. The impact of the BES depth of discharge on its lifetime is explained in Chapter 3 and accordingly two BES planning models that enable the microgrid planners to consider such impact on the microgrid expansion results are proposed. A comprehensive microgrid-integrated planning model which determines the installed BES technology, size, integration configuration, and maximum depth of discharge taking into consideration the probability of microgrid islanding operation is presented in Chapter 4.

Chapter 5 investigates the benefits of utilizing the BES for non-microgrid applications such as commercial and industrial (C&I) customers installation, distribution

network expansion, and PV ramp rate control. Three BES planning models that are suited for the aforementioned applications are developed and tested using numerical studies. This dissertation is written using a collection of articles published during the Ph.D. studies. These articles are listed at the end of this dissertation under "List of Publications" and cited in the reference section.

The main contributions of this dissertations are as follow:

- The consideration of important planning parameters in microgrid-integrated BES planning problems. These parameters include: BES size, integration configuration, technology, and depth of discharge.
- Improving the accuracy and practicality of BES planning problems results by including the impact of BES operation on its lifetime in the planning problem formulation.
- A comprehensive microgrid-integrated BES planning model is developed in this dissertation. The developed model enables the microgrid planner to simultaneously determine the optimal BES size, technology, maximum depth of discharge, and integration configuration taking into accounts both microgrid operation modes (i.e., grid connected and islanded operation modes).
- Besides microgrid services, BES planning models for other types of support in distribution networks are presented.

Chapter 2. Microgrid-Integrated BES Optimal Planning

2.1 Introduction

The optimal BES parameters are determined based on economic objective. This objective is selected to be the minimization of the microgrid total expansion planning cost as shown in Figure 1.2. Expansion planning problems are commonly formulated using Mixed Integer Linear Programming (MIP) [42]–[44]. In MIP, an objective function is typically needed to be either maximized or minimized. This objective function is composed of variables (continuous, integers, or binaries) called decision variables and is solved subject to a set of constraints. If the studied expansion problem consists of nonlinear constraints, these constraints must be linearized first before solving the problem. An example of how to linearize bilinear terms is given in Appendix A.

A commonly used approach to solve MIP problems is branch and bound approach. This approach is based on two processes: 1) bounding process, in which the solution of a relaxed MIP problem (e.g., transforming MIP problem into LP problem by removing integrality restrictions) is found and imposed as lower bound for minimization problems or upper bound for maximization problems; 2) branching process, in which the problem is split into a number of subproblems. A comprehensive discussion on the branch and bound approach is given in Appendix B [45]. Powerful solvers such as CPLEX, Xpress-MP, and SYMPHONEY implement a combination of branch and bound techniques and cutting-

plane techniques to accelerate the computation time associated with solving MIP problems, which allows large MIP problems to be solved using personal computers.

Compared with MIP, using nonlinear programming to model the microgrid expansion problem will have two major impacts on the results: (1) solution optimality, as nonlinear programming models may get stuck in a local optimal solution and never reach the global optimal solution, which is not the case in linear programming models; (2) solution time, nonlinear programming models have higher computation time compared to linear programming models, especially when binary variables are introduced to the problem, which is the case in the proposed microgrid expansion formulation in this paper. In general, it can be said that mixed integer nonlinear programming (MINLP) are hard to be solved and can be numerically intractable [46]. Thus, the developed BES planning models in this dissertation are formulated using MIP and the resulted optimization problems are solved using General algebraic modeling system (GAMS).

2.2 General Models Outlines

The objective of the developed microgrid-integrated BES planning models is to minimize the microgrid total expansion planning cost which can be defined as:

$$Min\left\{\begin{array}{l}\sum_{i\in \mathrm{G}}\sum_{d}\sum_{h}F_i(P_{idh}I_{idh})+\sum_{d}\sum_{h}\rho_{dh}P_{dh}^{M}+\sum_{d}\sum_{h}LS_{dh}v\\+\sum_{i\in \mathrm{S}}\left(P_i^{\mathrm{R}}CP_i^{\mathrm{a}}+C_i^{\mathrm{R}}CE_i^{\mathrm{a}}\right)\end{array}\right\} \quad (2.1)$$

The first term in (2.1) represents the DGs generation cost. This cost is normally considered for dispatchable DGs only as renewable DGs generation is free of cost. The cost or benefit of exchanging power with the main grid is given in the second term. In grid-connected mode, local load can be partially supplied by the utility grid, however in islanded

mode or in isolated microgrids the microgrid must rely solely on its local DERs. Any generation shortage in this case results in load curtailment, which reduces the microgrid reliability. Therefore, the third term which indicates the cost of unserved energy is imposed as a penalty for failing to supply the local demand. The value of lost load (VOLL) is used to quantify the economic loss associated with the unserved energy [47]. The VOLL represents a customer's willingness to pay for reliable electricity service [48]. This value depends on the customer type and location in addition to the outage time and duration. The BES investment cost, which is the last term in (2.1), is composed of annualized power rating and energy rating capital costs. It is assumed that the power conversion system cost and the BES annual maintenance cost are embedded in the power rating capital cost. Both the BES capital costs (i.e., power rating cost and energy rating cost) are annualized using (2.2)

$$\text{Annualized cost} = \frac{r(1+r)^T}{(1+r)^T - 1} \times \text{One time cost} \tag{2.2}$$

The objective function of the microgrid expansion planning problem given in (2.1) is subject to several operation and technical constraints, associated with the microgrid, dispatchable DGs, and the BES, that must be taken into account as discussed in the following.

2.2.1 Microgrid Operation Constraints

Microgrid's system level constraints include power balance equality equation, power exchange with the utility grid limit, and limits on load curtailment. The microgrid operation constraints are given as follow:

$$\sum_{i\in\{\mathrm{G,W,S}\}} P_{idh} + P_{dh}^{\mathrm{M}} + LS_{dh} = L_{dh} \qquad \forall d, \forall h \qquad (2.3)$$

$$-P^{\mathrm{M,max}}\delta \le P_{dh}^{\mathrm{M}} \le P^{\mathrm{M,max}}\delta \qquad \forall d, \forall h \qquad (2.4)$$

$$0 \le LS_{dh} \le \left(L_{dh} - CL_{dh}\right)\left(1-\delta\right) \qquad \forall d, \forall h \qquad (2.5)$$

$$\sum_{i\in\{G,B\}} R_{idh} \ge R_{dh}^{\mathrm{target}}\left(1-\delta\right) \qquad \forall d, \forall h \qquad (2.6)$$

The load balance equation (2.3) ensures that the total generation in the microgrid, the BES output power, and the power that are either purchased from (i.e., positive) or sold to (i.e., negative) the main grid matches the demand at all times. If the line connecting the microgrid to the main grid is disconnected or if the considered microgrid is isolated, the total available generation within the microgrid may not be sufficient to supply the demand. In this case, load would be curtailed to satisfy the power balance and the load curtailment variable (*LS*) will have a positive value. The exchanged power with the main grid is restricted by both the capacity of the line that connects the microgrid to the main grid and by the capacity of the substation transformer as given in (2.4). It is also possible to limit the volatility of the power exchanged with the main grid by imposing certain cap values on P^M value [49]. The parameter δ is used to define the microgrid type. That is, δ is 1 if grid tied microgrid is considered and 0 if isolated microgrid is considered. One of the motivations for microgrid deployment is the continuity of service for critical loads. The critical loads are typically associated with high VOLL so it is not economically advisable to consider them for the load curtailment. Keeping this in mind, the load curtailment limits can be defined as in (2.5). In order to maintain a reliable operation of the isolated microgrid, some reserve must be available to compensate for any sudden shortage in the generation or

increase in the load. This reserve will only be used to supply the critical load when needed. In other words, a load curtailment may occur even if there is a reserve in the microgrid. The dispatchable units and the BES units can provide this reserve for the microgrid. There are different methods to quantify the required reserve. Here, the required reserve must be at least equal to a value R^{target} which depends on the microgrid critical load at each interval (2.6).

2.2.2 Dispatchable DGs Operational and Physical Constraints

These constraints represent the physical limitations of the dispatchable DGs which differ upon the DG technology and can be expressed as:

$$P_i^{\min} I_{idh} \le P_{idh} \le P_i^{\max} I_{idh} \qquad \forall i \in G, \forall d, \forall h \qquad (0.7)$$

$$P_{idh} - P_{id(h-1)} \le UR_i \qquad \forall i \in G, \forall d, \forall h \qquad (2.8)$$

$$P_{id(h-1)} - P_{idh} \le DR_i \qquad \forall i \in G, \forall d, \forall h \qquad (2.9)$$

$$T_{idh}^{OFF} \ge DT_i \left(I_{id(h-1)} - I_{idh}\right) \qquad \forall i \in G, \forall d, \forall h \qquad (2.10)$$

$$T_{idh}^{ON} \ge UT_i \left(I_{idh} - I_{id(h-1)}\right) \qquad \forall i \in G, \forall d, \forall h \qquad (2.11)$$

$$R_{idh} \le P_i^{\max} I_{idh} - P_{idh} \qquad \forall i \in G, \forall d, \forall h \qquad (2.12)$$

The output power of the dispatchable DGs is limited by maximum and minimum capacity (2.7). The generation variation between two successive periods is limited by ramp up and ramp down constraints (2.8)-(2.9). When the DG shuts down, it must stay off for a certain minimum down time (2.10). Similarly, when the DG starts up, it must remain on for a certain minimum up time (2.11). The contribution of each DG in the online reserve is given in (2.12). The DGs that participate in providing reserve must be online and ready to

generate as fast as they receive the output change signal. Note that if the microgrid operates in grid tied operation mode, the required reserve in (2.6) will be 0 as the main grid will pick up any difference between generation and demand, and therefore the DGs do not need to participate in the online reserve.

2.2.3 Microgrid Expansion Planning Budget Limit

Any expansion planning project normally has a budget limit that cannot be exceeded. Investing in BES is no exception. Thus, the BES investment cost is limited by the available budget. The available budget limit imposes a higher cap on the BES size and can be expressed as:

$$\sum_{i\in S}\left(P_i^{R} CP_i^{a} + C_i^{R} CE_i^{a}\right) \le BL \tag{2.13}$$

2.3 Microgrid-Integrated BES Optimal Planning Focused on Size and Integration Configuration

The BES can be integrated into the microgrid as an aggregated or community unit or as distributed units as shown in Figure 2.1. In the aggregated configuration, one BES with a relatively large size is installed next to the utility substation. In the distributed configuration, however, multiple smaller-sized BESs units are connected to several busses in the microgrid. The BES units may have identical or different power and energy ratings. A performance comparison between the aggregated configuration and distributed configuration in wind farm application is performed in [50]-[51]. This comparison is focused only on the technical side ignoring the economic issues of the problem. Moreover, the optimal size of the BES is not determined in the proposed methods even though it is an important factor in the assessment of the BES performance. It is very important for

microgrid planners to decide which configuration is best suited for their microgrids. Moreover, if distributed BES configuration is chosen, the optimal number of the installed BES units as well as the optimal size for each unit must be found.

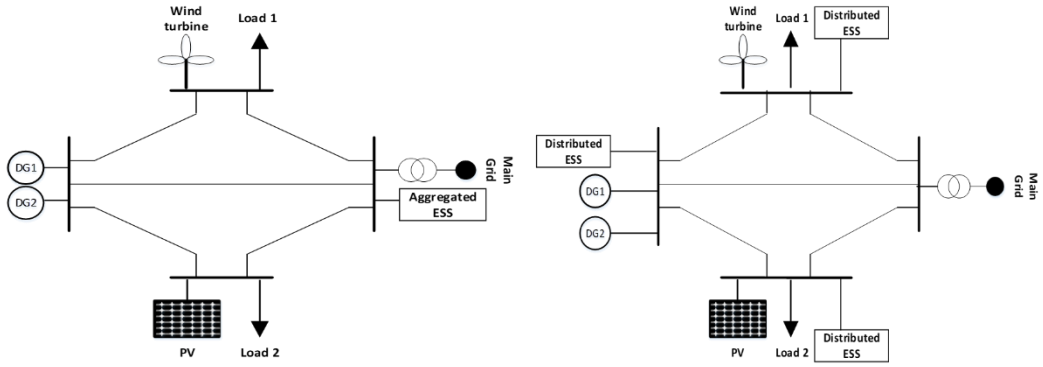

(a) (b)

Figure 2.1 Integrating BES in the microgrid; (a) aggregated configuration, (b) distributed configuration [52]

2.3.1 Problem Formulation

In order to determine the optimal BES size and units number, the objective function in (2.1) is solved subject to the previous set of constraints (2.3)-(2.13) as well as the following constraints that represent the BES operation:

$$P_i^{\min} x_{in} \le P_{in}^R \le P_i^{\max} x_{in} \qquad \forall i \in \mathrm{S}, \forall n \qquad (2.14)$$

$$C_i^{\min} x_{in} \le C_{in}^R \le C_i^{\max} x_{in} \qquad \forall i \in \mathrm{S}, \forall n \qquad (2.15)$$

$$P_{indh} = P_{indh}^{\mathrm{dch}} + P_{indh}^{\mathrm{ch}} \qquad \forall i \in \mathrm{S}, \forall n, \forall d, \forall h \qquad (2.16)$$

$$0 \le P_{indh}^{\mathrm{dch}} \le P_{in}^R u_{indh} \qquad \forall i \in \mathrm{S}, \forall n, \forall d, \forall h \qquad (2.17)$$

$$-P_{in}^R (1 - u_{indh}) \le P_{indh}^{\mathrm{ch}} \le 0 \qquad \forall i \in \mathrm{S}, \forall n, \forall d, \forall h \qquad (2.18)$$

$$\xi_{indh} = \left(u_{indh} - u_{ind\,(h-1)}\right)\ u_{indh} \qquad \forall i \in \mathrm{S}, \forall n, \forall d, \forall h \qquad (2.19)$$

$$\sum_{h} \xi_{indh} \le K \qquad \forall i \in \mathrm{S}, \forall n, \forall d \tag{2.20}$$

$$C_{indh} = C_{ind\,(h-1)} - \frac{P_{indh}^{\mathrm{dch}} \tau}{\eta_i} - P_{indh}^{\mathrm{ch}} \tau \qquad \forall i \in \mathrm{S}, \forall n, \forall d, \forall h \tag{2.21}$$

$$\left(1 - D_i\right) C_{in}^{R} \le C_{indh} \le C_{in}^{R} \qquad \forall i \in S, \forall n, \forall d, \forall h \tag{2.22}$$

$$R_{indh} \le -P_{indh}^{\mathrm{ch}} + \min\left\{\frac{C_{indh}}{\tau}, P_{in}^{R}\right\} \qquad \forall i \in S, \forall n, \forall d, \forall h \tag{2.23}$$

The BES size (i.e., the power rating and the energy rating) are restricted by given maximum and minimum values as represented in (2.14) and (2.15), respectively. The binary variable x_{in} denotes the BES installation state for BES unit *n*. If the BES unit is installed x_{in} is 1, otherwise it is 0. The BES power is defined as the summation of its discharging and charging powers (2.16), where it is made sure that only one is active in any given time period using the BES binary operation state *u*. If *u* is 1, the BES is discharging, otherwise it is either idle or charging. The BES discharging power is positive (2.17) whereas the charging power is negative (2.18). A cycles indicator ξ_{int} is added to the BES operation model as given in (2.19). Every time the BES begins new discharging cycle, the value of ξ_{int} will be 1, otherwise it is zero. By this way, the BES performed cycles over the expansion planning horizon can be determined. The number of BES performed cycles has a significant impact on the BES lifetime [53]. In this BES planning model, a cycle limit is imposed on the BES daily cycles in order to prolong its lifetime (2.20). The stored energy in each BES is calculated by (2.21) and restricted by (2.22). Equation (2.23) is used to model the BES participation in the online reserve requirement. The BES Charging power can be included in the reserve availability since the charging process can be quickly interrupted and the power that was used to charge the battery can be used toward supplying

the load. Moreover, the minimum of either the available stored energy in the BES at each interval and the rated power is considered as available reserve. In grid connected mode of operation, the BES does not participate in the online reserve application as any mismatch between the microgrid generation and demand will be covered by the main grid.

2.3.2 Case Study

Microgrid and BES Data

A test grid-tied microgrid consisting of two gas turbine units, a PV array, a wind generator, and an aggregated load is used to investigate and validate the proposed model. The technical characteristics of the gas units are given in Table 2.1. The PV array power rating is 1.5 MW and the wind generator power rating is 1 MW. The hourly output power of the PV array, the hourly output power of the wind generator, the hourly microgrid aggregated load, and the hourly electricity market price are obtained from [54]. The maximum power that can be transferred to the main grid is assumed to be 10 MW. The BES characteristics are shown in Table 2.2. Two cases are considered: base case operation (without BES installation) and BES case. The results are given below:

Table 2.1 Dispatchable generation units' characteristics

Unit	Cost Coefficient ($/MWh)	Min.-Max. Capacity (MW)	Ramp Up/Down Rate (MW/h)	Min Up/Down Time (hour)
1	75.7	0.8-8	2.5	1
2	80.1	0.5-5	2.5	1

Table 2.2 BES characteristics

Maximum Power Rating (MW)	Maximum Energy Rating (MWh)	Power Rating Capital Cost ($/MW/year)	Energy Rating Capital Cost ($/MWh/year)	Fixed Cost ($/year)	Round Trip Efficiency (%)

10	20	20,000	11,000	10,000	90

Results and Discussion

In the first case (i.e., base case) the only cost considered is the microgrid operation cost since the BES is not installed. The total generation cost is $2,163,984/year. The microgrid profit of exchanging energy with the main grid is $823,862/year. This yields a total microgrid operation cost of $1,340,122/year.

However, in the second case (i.e., BES Installation Case), the proposed model is used to find the optimal size and number of installed BES units that minimizes the microgrid total expansion planning cost. The maximum number of BES units that can be installed in the system is assumed to be 4 to reduce the computation burden. The discharged cycles of each BES is limited to two cycles per day as imposed by (i.e., K=2 in (2.20)). The optimal number of installed BES units in this case is 2. The power rating and energy rating of each BES unit is given in Table 2.3. The microgrid total cost reduces to $1,266,863/year compared to the base case. This cost is composed of a total BES investment cost of $420,000/year, the generation cost of $1,689,341/year, and the benefit of exchanging energy with the main grid of $842,478/year.

Table 2.3 Installed BES units optimal size [52]

Installed BES unit number	Rated Power (MW)	Rated Energy (MWh)
1	4.05	9
2	4.95	11

The installed BES units charging/discharging cycles for one sample day are depicted in Figure 2.2. Both BES units are charged during low price periods (hours 1, 2,

and 3) and discharged during high price periods (hours 17-20). This helps the microgrid to reduce its operation cost by selling the low price energy to the main grid during high price hours (i.e., an energy arbitrage). The BES units also follow a rather similar patterns in other days.

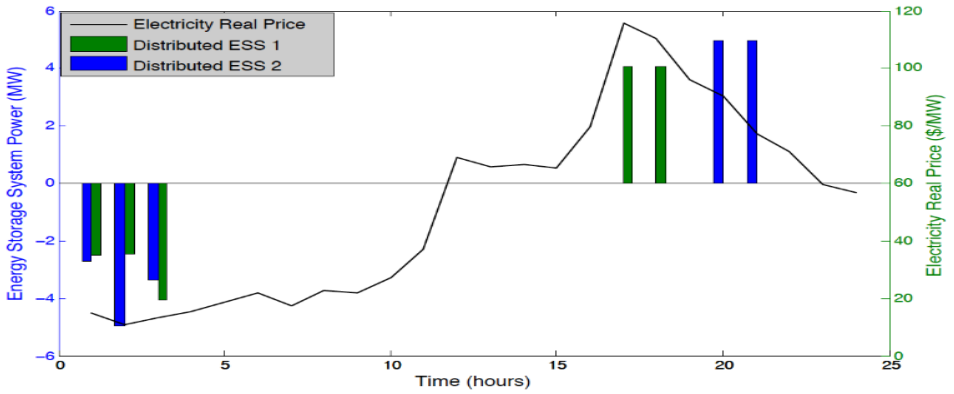

Figure 2.2 The charging/discharging power of installed BES units and the electricity price [52]

To further investigate the impact of the number of the installed BES units, different scenarios with various number of BES units installations are studied. The results are shown in Figures 2.3-2.5. The investment cost increases with increasing the number of BES units as shown in Figure 2.3. From Figure 2.4, it can be seen that the microgrid operation cost decreases as n increases until n reaches 2 and then increases again. Same behavior is observed at the microgrid total expansion planning cost as can be seen in Figure 2.5. The minimum total expansion planning cost occurs at n = 2 which is similar to the solution obtained by the proposed microgrid-integrated BES planning model. This validates the ability of the proposed model to determine both the optimal number and the optimal size of the ESS in the microgrid. Detailed cost analysis for all scenarios is given in Table 2.4.

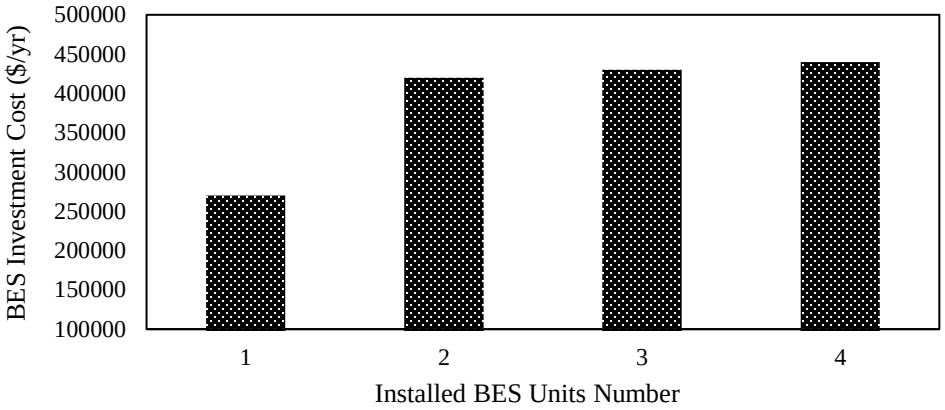

Figure 2.3 Investment cost with different number of installed BES units

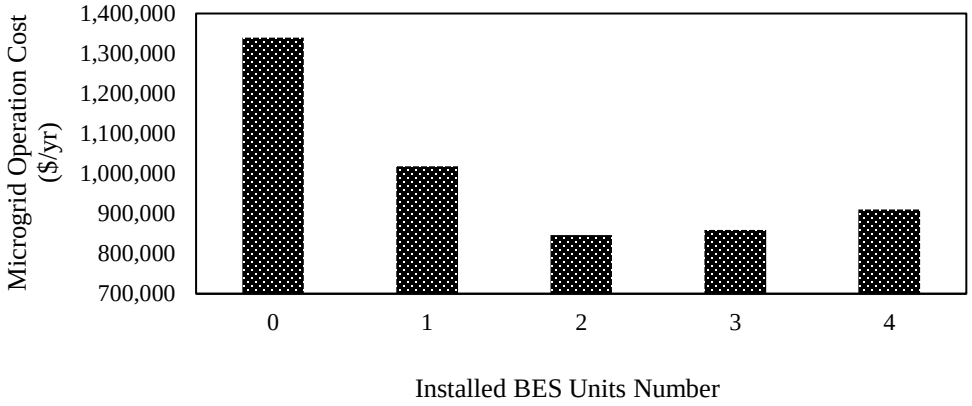

Figure 2.4 Microgrid operating cost with different number of installed BES units

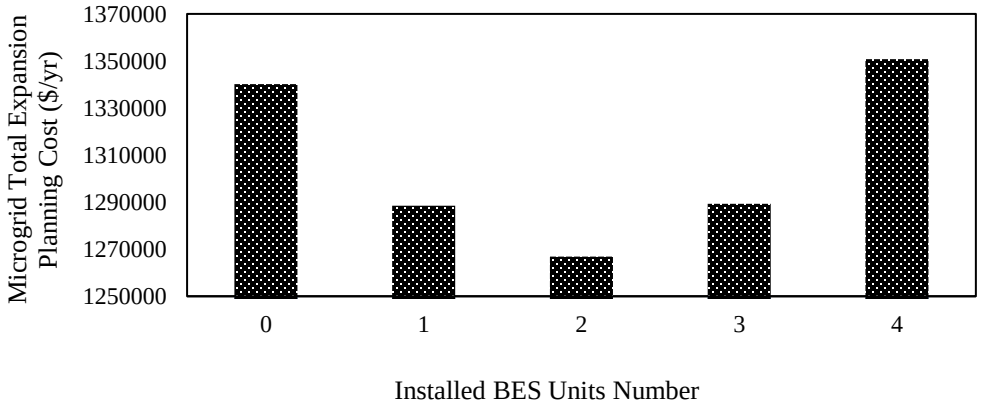

Figure 2.5 Microgrid total expansion planning cost with different number of installed BES units

Table 2.4 Detailed cost analysis for different BES units number [52]

Installed BES Units Number	BES Investment Cost ($/yr)	Generation Cost ($/year)	Profit of Power Exchanged ($/year)	Operation Cost ($/year)	Expansion Planning Cost ($/year)
0	0	2,163,984	823,862	1,340,122	1,340,122
1	270,000	1,815,074	796,585	1,018,489	1,288,489
2	420,000	1,689,341	842,478	846,863	1,266,863
3	430,000	1,719,841	860,563	859,278	1,289,278
4	440,000	1,693,881	783,122	910,759	1,350,759

When aggregated BES configuration is adopted, the optimal BES power rating and energy rating is found to be 5.85 MW and 13 MWh, respectively. However, the lack of flexibility in aggregated configuration, especially when the discharging cycles are limited, prevent the microgrid from taking advantage of the electricity price variations to increase its benefit compared to the distributed BES configuration. Moreover, it is observed that the cost of local generation is the highest in aggregated case while the benefit of exchanging power with the main grid is the lowest. Increasing the discharging cycles limit will enhance the economic viability of aggregated configuration but it will also reduce its lifetime. Distributed BES configuration, on the other hand, tends to cope better with price electricity variations while prolonging the BES lifetime.

2.4 Microgrid-Integrated BES Optimal Planning Focused on Size and Technology

Different BES technologies possess different characteristics including power rating cost, energy rating cost, round trip efficiency, depth of discharge, and cycle lifetime. Thus, it is very critical to select the appropriate BES technology for the planned microgrid considering the required investment and the resultant operational and reliability benefits

[55]. The majority of existing methods commonly consider merely one type of energy storage while ignoring the impact of their distinct technology characteristics on the optimal solution. The studies in [28] and [56] consider the BES technology in sizing, however the proposed methods are either based on iterative process or genetic algorithm, which are known for high computation burden [57]. In this section, a developed mathematical model is presented to determine the BES technology (or a combination of technologies) along with their optimal sizes that minimize a standalone microgrid expansion planning cost given in (2.1). Even though we examine the problem from an economic perspective, the presence of the cost of energy of not supplied in the objective function implies that the microgrid reliability is also taken into consideration when the optimal solution is found. Four BES technologies are considered: Lead Acid, Sodium Sulphur (NaS), Vanadium Redox (VRB), and Nickel Cadmium (NiCd). The proposed model, however, can be used to solve any combination of BES technologies as long as their characteristics are known. The considered characteristics are power rating cost, energy rating cost, round trip efficiency, life cycle, and depth of discharge. The contribution of this work is the provision of expansion planning model that takes into account different BES technologies, which expands the range of options for microgrid developers. The proposed model further considers practical factors that affect the BES operation such as depth of discharge, lifetime, and round trip efficiency in the optimization process. Unlike the previous expansion model, this model considers stand-alone microgrid (i.e., δ=0). Moreover, different BES technologies are considered in this model compared to the previous model where only one BES technology is considered.

2.4.1 Case Study

Microgrid and BES Data

A standalone microgrid, as in Figure 2.6, is used to test the proposed model. The technical characteristics of the diesel generator are given in Table 2.5. The hourly actual output power for a 1.5 MW PV and a 1 MW wind turbine as well as the hourly aggregated local load are retrieved from [54]. The microgrid local peak load is 8 MW, where 40% of this load is assumed to be critical that must be supplied at all times. The required reserve is assumed to be 10% of the critical load at each hour (i.e., R_{dh}^{target}=0.1*CL_{dh}) A VOLL of $20,000/MWh is used in the studies considering a combination of residential and small commercial customers. Table 2.6 shows the characteristics of the considered BES technologies in this paper, which are borrowed from [58] and [59]. Note that the BES capital costs are converted to annual bases using (2) with the assumption of 5% interest rate and 10 years project lifetime. The minimum energy rating limits is assumed to be zero for the considered BES technologies. For the maximum energy rating limits, maximum discharge duration of 4 hours is assumed. The maximum energy rating can be found by multiplying the maximum power rating limit of each BES technology with the maximum discharge duration time. The expansion planning budget is restricted to $1 million.

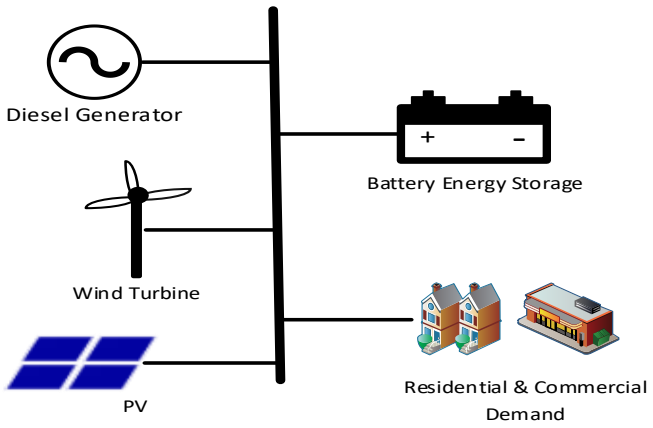

Figure 2.6 Standalone microgrid structure [60]

Table 2.5 Diesel generator characteristics

Cost Coefficients ($/kWh)	Maximum Power Capacity (MW)	Minimum Power Capacity (MW)	Min Up/Down Time (hour)
0.36	8	1.6	1

Table 2.6 BES technologies characteristics

BES Technology	Power Rating Min./Max (MW)	Power Rating Capital Cost ($/MW-yr)	Energy Rating Capital Cost ($/MWh-yr)	Cycles Lifetime (Cycles/yr)	D (%)	η (%)
Lead-acid	0/20	38,800	25,900	200	70	78
NaS	0.5/8	129,500	38,800	250	100	89
VRB	0.3/3	77,700	19,400	1000	75	85
NiCd	0/40	64,700	103,600	300	100	78

Results and Discussion

Three cases with different microgrid components are studied in the simulation.

Case 1: In this case the microgrid demand is met solely by the diesel generator. This case represents the worse-case scenario when only one power source is supplying the load. It is found that 50.033 MWh/year of demand is not supplied. The cost of not supplying

this demand is $1,000,656/year. The DG operation cost is $15,134,704/year. The summation of these two costs yields a microgrid total cost of $16,135,360/year.

Case 2: In order to improve the reliability and reduce the microgrid operation cost, BES units are considered for installation. The objective is to find the appropriate BES technology, or a combination of technologies, as well as their optimal size. Based on the simulation results, the optimal solution yields when NaS battery is installed with 0.5 MW power rating and 3 MWh energy rating. The microgrid expansion planning cost is $15,352,480/year. This cost is composed of cost of energy not supplied ($18,180/year), BES investment cost ($181,149/year), and diesel generator operation cost ($15,153,151/year).

Case 3: In this case renewable DGs are further considered in the microgrid. To examine the renewable DGs impact on the BES technology selection and sizing, different penetration levels are considered. The renewable penetration is changed by multiplying renewable DGs output power by a renewable generation factor. Four renewable generation factors are considered in the simulation: 50%, 100%, 150%, and 200%. The 100% renewable generation represents a penetration level of 31.25% (considering the peak load of 8 MW and total renewable generation capacity of 2.5 MW). The obtained results for different renewable penetration scenarios as well as for Cases 1 and 2 are given in Table 2.7 and Table 2.8. It can be seen from the results that the renewable penetration has a great impact on the BES technology selection and size. Generally, it is observed that as the renewable penetration increases, the amount of unmet demand decreases which means that the overall microgrid reliability improves. Increasing the renewable penetration also

reduces the microgrid expansion planning cost. However, this may not be true for higher penetration since relatively larger scale BES units are required to absorb the excess power, which imposes higher investment cost to the microgrid. It is also found that the combination of different BES technologies is not economic for the considered microgrid.

Table 2.7 Detailed cost analysis for the studied cases [60]

Case Number		MG Components	Unmet Demand (MWh/yr)	Cost of Energy Not Supplied ($/yr)	Diesel Generator Cost ($/yr)	Expansion planning Cost ($/yr)
1		Diesel Generator	50.033	1,000,656	15,134,704	16,135,360
2		Diesel Generator and BESs	0.909	18,180	15,153,151	15,352,480
3	50% Renewable	Diesel Generator, BESs, and Renewable DGs	0.30	6,000	13,964,794	14,013,504
	100% Renewable		0.740	14,800	12,711,213	12,834,743
	150% Renewable		0.248	4,960	11,572,004	11,674,548
	200% Renewable		0.20	4,000	10,405,626	10,567,642

Table 2.8 Installed BES technology information for the studied cases [60]

Case Number		Installed BES Technology	Power Rating (MW)	Energy Rating (MWh)	BES Investment Cost ($/yr)	Number of Cycles (Cycles/yr)
1		-	-	-	-	-
2		NaS	0.5	3	181,149	250
3	50% Renewable	VRB	0.3	1	42,710	126
	100% Renewable	NaS	0.540	1	108,730	249

	150% Renewable	Lead Acid	1.18	2	97,584	172
	200% Renewable	Lead Acid	2.07	3	158,016	200

For the sake of comparison and assurance of the model's ability to find the optimal solution, the simulation is performed for different BES technologies with 100% renewable penetration. The obtained results are shown in Table 2.9. It can be seen that the microgrid minimum expansion planning cost is found when NaS battery is installed which conforms to the proposed model results.

Table 2.9 Simulation results for different BES technology with 100% renewable penetration

Installed BES Technology	Optimal Power Rating (MW)	Optimal Energy Rating (MWh)	Unmet Demand (MWh/yr)	BES Investment Cost ($/yr)	MG Expansion Planning Cost ($/yr)
Lead-acid	0.546	1	2.326	47,085	12,843,823
NaS	0.540	1	0.740	108,730	12,834,743
VRB	0.320	1	2.850	44,264	12,844,585
NiCd	0.540	1	0.740	138,538	12,864,714

Chapter 3. Consideration of BES Degradation in Microgrid-Integrated BES Planning Problems

3.1 Introduction

The BES degradation is greatly related to its operation. How deep the BES is discharged and how many charging/discharging cycles are performed have a significant impact on the BES rate of degradation. The relationship between these operation parameters and the BES lifetime must be taken into account when the BES operation or planning problems are investigated. One of the common approaches used to consider the BES degradation phenomena in the BES operation problem is to add an extra term to the objective function that represents the BES degradation cost in $/kWh (i.e., based on its charged/discharged energy) [61]–[64]. In BES planning problem, however, the Ah-throughput model is normally used to estimate the BES lifetime [15], [65]. In this model, the total delivered energy by the BES during the planning time horizon is computed and compared with the expected Ah (i.e., current-hour) that the BES can deliver during its lifetime, which is typically provided by the manufacturer. This, however, may yield inaccurate estimation of the BES lifetime as the relation between the BES depth of discharge and number of cycles are not taken into consideration.

Different methods are proposed to estimate the BES lifecycle [66]–[68]. However, it is not uncommon for BES manufacturer to provide the relationship between lifecycle and depth of discharge. This information is normally presented in a curve as the one depicted

in Figure 3.1. As the depth of discharge increases, the BES lifecycle decreases. Different BES technologies have different lifecycle versus depth of discharge relationships. In lead acid batteries, for example, this relationship tends to exhibit an exponential form whereas in lithium ion batteries a linear relationship is normally observed.

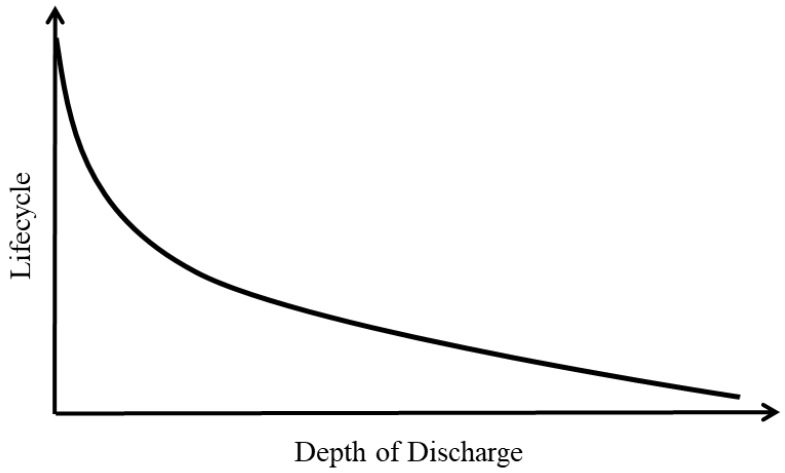

Figure 3.1 An example of BES depth of discharge and lifecycle relationship [69]

3.2 Optimal BES Maximum Depth of Discharge Determination

3.2.1 Problem Formulation

This model uses the relationship between the BES depth of discharge and lifecycle to determine not only the optimal size of the installed BES but also the optimal maximum depth of discharge. The microgrid expansion planning problem is solved for isolated microgrid, which means the microgrid type definer (δ) is set to be 0 in (2.4), (2.5), and (2.6). The total cost given in (2.1) is minimized subject to the common constraints (2.3)-(2.13). The following equations are used to model the installed BES operation and the impact of the depth of discharge on the BES lifetime:

$$0 \le P_{idh}^{dch} \le P_i^R u_{idh} \qquad \forall i \in \mathrm{S}, \forall d, \forall h \qquad (3.1)$$

$$-P_i^R (1-u_{idh}) \le P_{idh}^{ch} \le 0 \qquad \forall i \in \mathrm{S}, \forall d, \forall h \qquad (3.2)$$

$$P_{idh} = P_{idh}^{ch} + P_{idh}^{dch} \qquad \forall i \in \mathrm{S}, \forall d, \forall h \qquad (3.3)$$

$$\xi_{idh} = \left(u_{idh} - u_{id(h-1)}\right) u_{idh} \qquad \forall i \in \mathrm{S}, \forall d, \forall h \qquad (3.4)$$

$$\sum_d \sum_h \xi_{idh} \le N(i, D, T) \qquad \forall i \in \mathrm{S} \qquad (3.5)$$

$$(1-\sum_m D_m w_m) \le C_{idh} \le C_i^R \qquad \forall i \in \mathrm{S}, \forall d, \forall h \qquad (3.6)$$

$$\sum_m w_m \le 1 \qquad \forall i \in S \qquad (3.7)$$

$$C_{idh} = C_{id(h-1)} - \frac{P_{idh}^{dch} \tau}{\eta} - P_{idh}^{ch} \tau \qquad \forall i \in \mathrm{S}, \forall d, \forall h \qquad (3.8)$$

$$0 \le P_i^R \le P_i^{\max} \qquad \forall i \in \mathrm{S} \qquad (3.9)$$

$$C_i^R = P_i^R \sigma_i \qquad \forall i \in \mathrm{S} \qquad (3.10)$$

The relationship between the BES depth of discharge and number of cycles, which is normally provided by the BES manufacturer, is used in this microgrid-integrated BES planning model to determine the optimal size and depth of discharge for the installed BES. As MIP is used to formulate the expansion problem in this research, the depth of discharge curves are linearized by using a piecewise linearization approximation as depicted in Figure 3.2. It is worth noting that increasing the number of depth of discharge segments reduces the approximation error but at the same time increases the computational requirements. Index *m* is used to represent the selected segment for the depth of discharge value in a step-wise depth of discharge curve.

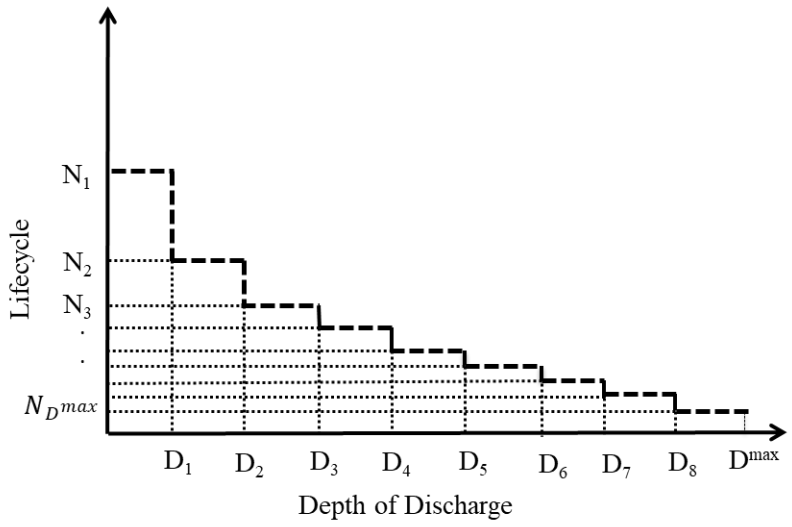

Figure 3.2 Piece wise linearization of BES depth of discharge-lifecycle curve [69]

As can be seen from (3.6), the installed BES cannot be discharged beyond the determined optimal depth of discharge value and cannot be charged above the optimal energy rating. The binary variable *w* determines the optimal depth of discharge value. The summation of *w* over *m* must be less than or equal to 1 to ensure that only one value of the BES depth of discharge is chosen (3.7). The BES energy rating is determined based on the optimal power rating and continuous charging/discharging duration (3.10).

3.2.2 Case Study

Microgrid and BES Data

A standalone microgrid that contains one diesel generator, one PV unit, one wind turbine, and one aggregated local load, is used to show the practicality and the merits of the proposed microgrid expansion model. The characteristics of the microgrid generation units are given in Table 3.1. The historical data for the microgrid load and renewable generation are obtained from [54] for one year. The microgrid peak load is 8.49 MW. A

combination of residential and commercial customers is assumed for this microgrid with a value of lost load of $30,000/MWh [48]. The critical load is 40% of the microgrid load at each time interval. The microgrid online reserve must be greater than or equal to 10% of the critical load to compensate for any sudden decrease in generation or increase in demand. Figure 3.3 shows the difference between the microgrid load and available generation taking into account the required online reserve. A negative difference means that the microgrid has sufficient generation to meet the load and the required online reserve. On the other hand, the positive values represent the unserved load due to the shortage in the available generation.

Table 3.1 Microgrid generation units characteristics

Unit	Cost Coefficient ($/MWh)	Minimum Capacity (MW)	Maximum Capacity (MW)
Diesel Engine	200	1.4	7
Wind turbine	-	-	1
PV	-	-	1.5

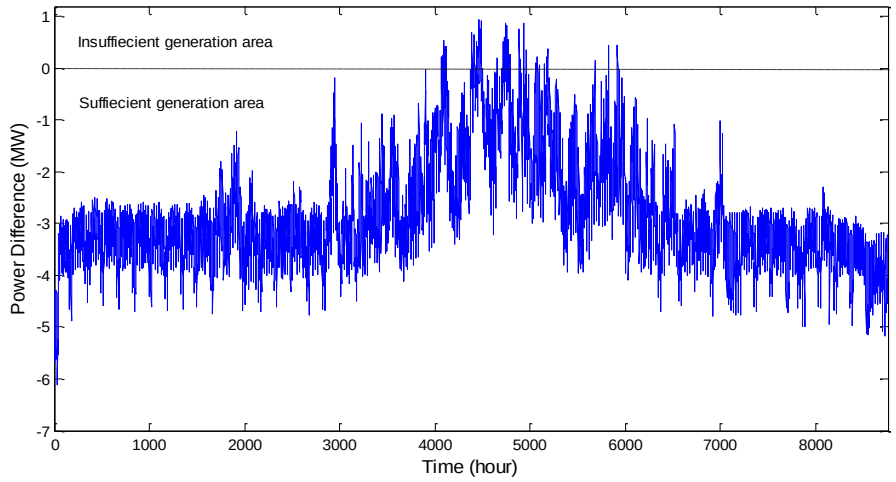

Figure 3.3 Difference between microgrid load and installed generation capacity

According to [28], lead acid battery is found to be one of the best BES technologies for standalone microgrid applications. Lead acid battery is known to have a low investment cost as well as a low life cycle. Thus, it is very important to optimize the battery depth of discharge which in turn impacts the number of cycles before the battery reaches its end of life time. Even though lead acid battery is used in this simulation, the proposed model can be applied to any other battery technology without loss of generality. Table 3.2 provides the annualized costs associated with purchasing and installing the lead acid battery in the microgrid for different BES lifetimes [70]. The amount of money that can be spent investing on the BES is limited by the available budget limit which is assumed to be $3 million. This budget limit is also annualized and given in Table 3.2 for each BES lifetime. The costs are computed based on a 4% interest rate. The round trip efficiency of the lead acid battery is assumed to be 80% and the charging/discharging periods are assumed to be 3 hours. The relationship between the lead acid battery cycles and its depth of discharge is taken from the manufacturer data sheet [71] and presented in Table 3.3. The number of cycles for each depth of discharge value must be divided by the BES lifetime to get the annual number of cycles for each BES lifetime.

Table 3.2 Lead acid battery annualized costs and budget limit

Lead acid Battery Lifetime (yr)	Annualized Power Rating Related Cost ($/MW/yr)	Annualized Energy Rating Related Cost ($/MWh/yr)	Annualized Budget Limit ($/yr)
10	74,658	8,629	396,873
20	64,716	5,150	220,745
30	61,566	4,047	173,490

Table 3.3 Lead acid battery cycles at different depth of discharge

Depth of Discharge (%)	Number of Cycles	Depth of Discharge (%)	Number of Cycle
5	30000	55	650
10	7900	60	580
15	4000	65	520
20	2500	70	490
25	1800	75	450
30	1500	80	430
35	1200	85	400
40	950	90	380
45	800	95	370
50	700	100	350

Results and discussion

Two cases are studied: in the first case, the microgrid operation without the integration of the lead acid battery is studied; in the second case, the expansion model is applied to determine the optimal size and depth of discharge for the installed lead acid battery that yields the minimum expansion cost. This case is solved for various BES life time scenarios. The obtained results for each case are discussed below:

Case 1: The microgrid load is supplied by the diesel generator and renewable DGs. It can be seen from Figure 3.3 that the microgrid load is higher than the installed generation capacity during the peak periods, which occurs rarely during the year. As mentioned before, the diesel generator fuel consumption and efficiency depend on the diesel generator output power compared to its rated power and therefore it is not economically and technically advisable to oversize the diesel engine only to supply those rarely occurred demands. The unserved demand in this case is found to be 23.4 MWh/year. The computed costs associated with this case are given in Table 3.4.

Case 2: A lead acid battery is integrated into the microgrid in order to reduce the unserved load (i.e., to improve the microgrid reliability) as well as the operation cost. Three BES lifetime scenarios, including 10 years, 20 years, and 30 years, are considered in this case. The costs and optimal values for each BES lifetime scenario are given in Table 3.4 and Table 3.5 respectively. From the results presented Table 3.4 in it is clear that the integration of the lead acid battery is economically justifiable regardless of the considered BES life time, as the reduction in the microgrid operation cost is higher than the investment cost imposed by the battery installation. The 20-year BES life time yields the minimum microgrid total expansion planning cost. However, if more weight is put on the microgrid reliability, then a 10-year BES lifetime would be the more desirable solution. It is further noticed that a larger battery size and a lower depth of discharge are needed as the BES life time increases. This comes from the fact that higher depth of discharge and BES life time reduce the cycles that can be performed by the BES. Thus, a trade off between the size and depth of discharge must be performed to reach the optimal solution.

Table 3.4 Cost analysis for the considered cases [69]

Case Number	Project lifetime (years)	Lead Acid Battery Investment Cost ($/year)	Operation Cost ($/year)		Microgrid Total Expansion Planning Cost ($/year)
			Diesel Generation Cost	Unserved Energy Cost	
1	-	-	6,987,198	702,000	7,689,198
2	10	61,332	6,990,960	202,639	7,254,931
	20	51,662	6,990,917	207,720	7,250,299
	30	60,057	6,990,833	216,000	7,266,891

Table 3.5 Determined optimal values for case 2 [69]

Project lifetime (years)	Optimal Size		Optimal Depth of Discharge (%)	Number of Performed Cycles	Unserved Energy (MWh)
	Power Rating (MW)	Energy Rating (MWh)			
10	0.61	1.83	95	34	6.75
20	0.64	1.93	75	22	6.92
30	0.81	2.44	45	26	7.20

Another representation for the BES depth of discharge value is the minimum state of charge, which defines the minimum amount of energy that must be stored in the battery at each time interval. For example, a 75% depth of discharge value is equivalent to a 25% minimum state of charge. The state of charge for the installed BES is given in Figure 3.4 for a sample day. It is clear that the lead acid battery state of charge remains above the minimum state of charge value determined by the model.

To further check the accuracy of the obtained results and examine the impact of the depth of discharge value on the expansion cost, the simulation is run with a variety of depth of discharge values while the lead acid battery size is kept at the determined optimal value. Figure 3.5 shows the microgrid total expansion planning costs for the considered BES lifetimes. The expansion cost decreases as the depth of discharge increases until it reaches the optimal depth of discharge determined by the proposed expansion model after which the expansion cost increases again. For a 10-year BES lifetime, the expansion cost is almost the same for depth of discharge values larger than 80%.

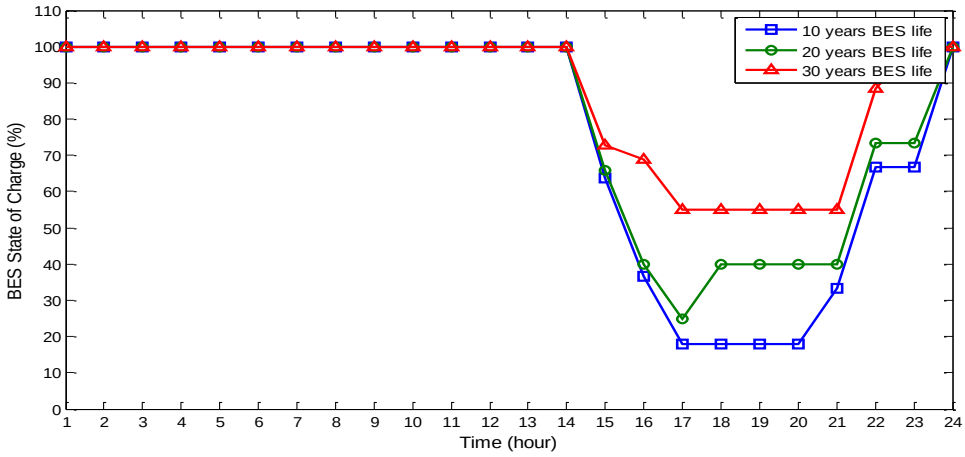

Figure 3.4 Lead acid battery state of charge for one sample day [69]

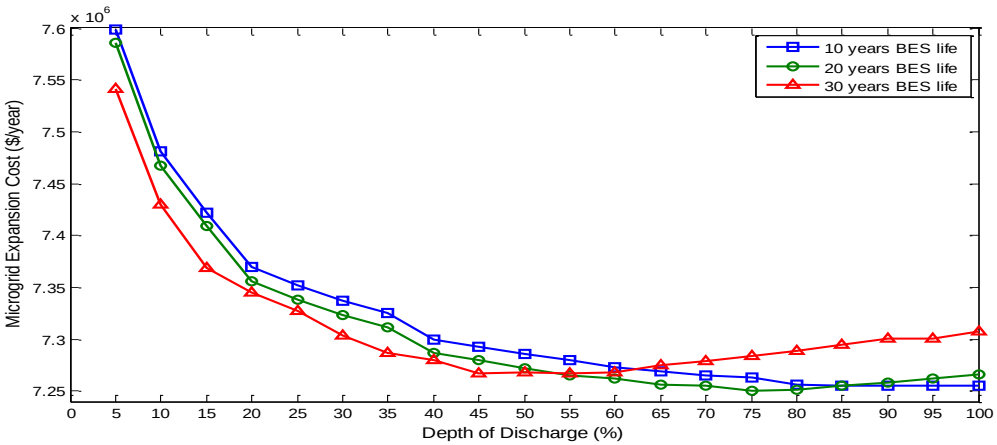

Figure 3.5 Microgrid total expansion planning cost for different lead acid battery life and depth of discharge values at the determined optimal size [69]

3.3 Variable Depth of Discharge impact on BES Degradation

Since different BES cycles will have different depth of discharge values, it is essential to find a BES planning model that can determine the actual depth of discharge at each performed cycle and utilizes this value to accurately estimate the associated BES degradation. For this reason, a new factor that represents the depth of discharge impact on the BES lifetime is introduced in this model. The new factor is called the BES degradation

factor and denoted by ψ. This factor is derived from the BES depth of discharge versus lifecycle curve given in Figure 3.2 and calculated using (3.11).

$$\psi_{im} = \frac{N_{D^{\max}}}{N_{D_m}} \qquad \forall i \in S, \forall m \tag{3.11}$$

Where $N_{D^{\max}}$ and N_{D_m} represent the maximum number of cycles that the BES can perform at the maximum depth of discharge ($D^{\max}$) and the calculated depth of discharge (D_m), respectively. An example of the derived degradation factor is shown in Figure 3.6. If the BES is discharged at the maximum depth of discharge, ψ will be 1, otherwise it will be smaller than 1. It is worth noting that the number of segment for linearization present a tradeoff between the solution accuracy and computation time. A larger number of segments ensures a more accurate solution at the expense of increased computation time. A desired number of segments will be selected based on the microgrid planner's discretion.

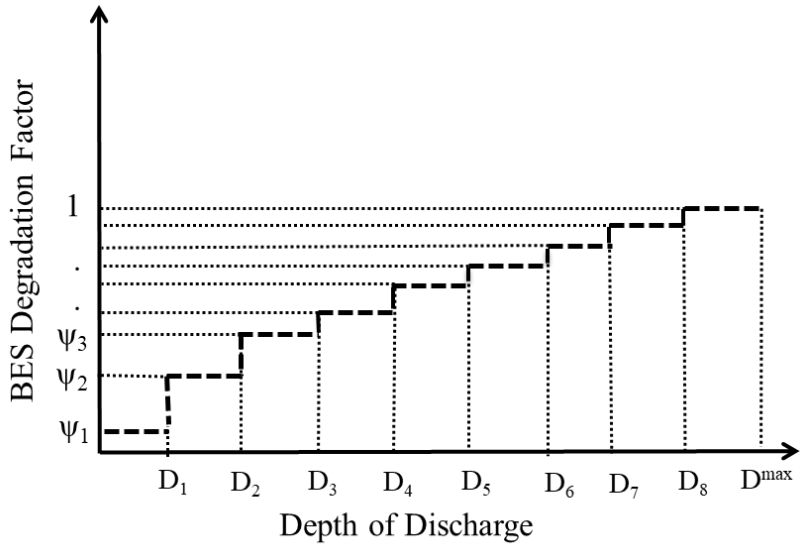

Figure 3.6 An example of linearized BES degradation factor [72]

3.3.1 Problem Formulation

Similar to previous section, the microgrid expansion objective is to minimize the total cost as given in (2.1) taking into consideration a set of constraints that represents the microgrid operation limits, the DGs operational and physical limits, and the available budget limit (i.e., Equations (2.3)-(2.13)). The BES operation are modelled using the following equations:

$$C_i^{\min} \le C_i^R \le C_i^{\max} \qquad \forall i \in S \tag{3.12}$$

$$C_i^R = \sum_n x_{in}\left(C_i^{\min} + k_n \Delta C_i\right) \qquad \forall i \in S \tag{3.13}$$

$$\sum_n x_{in} \le 1 \qquad \forall i \in S \tag{3.14}$$

$$\frac{C_i^R}{\sigma_i^{\max}} \le P_i^R \le \frac{C_i^R}{\sigma_i^{\min}} \qquad \forall i \in S \tag{3.15}$$

$$0 \le P_{idh}^{dch} \le P_i^R u_{idh} \qquad \forall i \in S, \forall d, \forall h \tag{3.16}$$

$$-P_i^R\left(1 - u_{idh}\right) \le P_{idh}^{ch} \le 0 \qquad \forall i \in S, \forall d, \forall h \tag{3.17}$$

$$\xi_{idh} = \left(u_{idh} - u_{id(h+1)}\right)u_{idh} \qquad \forall i \in S, \forall i \in d, \forall i \in h \tag{3.18}$$

$$C_{idh} = C_{id(h-1)} - \frac{P_{idh}^{\text{dch}}\tau}{\eta_i} - P_{idh}^{\text{ch}}\tau \qquad \forall i \in S, \forall d, \forall h \tag{3.19}$$

$$\left(1 - D_i^{\max}\right)C_i^R \le C_{idh} \le C_i^R \qquad \forall i \in S, \forall d, \forall h \tag{3.20}$$

$$\gamma_{idh}\, C_i^R = C_i^R - C_{idh}\xi_{idh} \qquad \forall i \in S, \forall d, \forall h \tag{3.21}$$

$$\gamma_{idh} = \sum_m \left(1 - D_{im}\right)\, z_{imdh} \qquad \forall i \in S, \forall d, \forall h \tag{3.22}$$

$$\sum_m z_{imdh} \le 1 \qquad \forall i \in S, \forall d, \forall h \tag{3.23}$$

$$\lambda_{idh} = \sum_{\mathrm{m}} z_{imdh} \ \psi_{im} \qquad \forall i \in S, \forall d, \forall h \qquad (3.24)$$

$$\sum_{d} \sum_{h} \lambda_{idh} \ \xi_{idh} \leq \frac{N_{D^{\max}}}{T} \qquad \forall i \in S \qquad (3.25)$$

The BES unit are commonly manufactured in modules. That is, the optimal size of the installed BES will be an integer multiple of the BES manufactured base modular size. In this model, an incremental step (ΔC) that represents the BES modular energy rating size is used. The optimal energy rating size of the installed BES is limited by a minimum value (the base modular size) and a maximum value which is imposed due to economic reasons (e.g., budget limit) and/or physical reasons (e.g., available space) as in (3.12). The optimal energy rating size is determined using (3.13) where k_n is an integer variable that starts from 0 and increases by 1 with each incremental step n. That is, $k_n = k_{n-1} + 1$ and $k_1 = 0$. The binary variable x is used to determine the selected optimal energy rating size for the installed BES. Equation (3.14) ensures that only one energy rating size is selected. If the installation of the BES is not feasible, x will be zero. The BES power rating size is determined based on the desired discharging time as in (3.15). Different BES technologies have different discharging time capabilities. The BES discharging and charging limits can be expressed using (3.16) and (3.17), respectively. The binary variable u represents the operation state of the BES (i.e., 1 if BES is discharging and 0 if the BES is charging or idling). This binary variable is used in (3.18) to indicate the end of each charging/discharging cycle. The BES cycles indicator (ξ) is 1 each time the BES completes a full charging/discharging cycle, otherwise it is 0. The stored energy in the BES at each time interval is determined using (3.19). The amount of stored energy cannot exceed the optimal BES energy rating size and

cannot be less than a minimum capacity limit whose value is determined based on the BES maximum depth of discharge (3.20). However, the BES is not discharged at the maximum depth of discharge value at each cycle and therefore the actual depth of discharge value must be determined. Equations (3.21) and (3.22) are used to calculate the variable depth of discharge value of each BES charging/discharging cycle. In (3.21), the BES state of charge, which represents how much energy stored in the BES compared to the energy rating size, is calculated. Note that this value is only determined at the end of the charging/discharging cycle (i.e., ξ=1). The state of charge variable is then used to find the depth of discharge value from (3.22). It is worth noting that if ξ=0 in (3.21), the value of the state of charge variable (γ) must be 1, which forces the value of depth of discharge (D) to be 0 (i.e., the charging/discharge cycle is not completed). The binary variable z in (3.22) is used to define the depth of discharge segment (m) so it can be used in (3.24) to determine the depth of discharge impact on lifetime factor (λ). At each time interval, only one depth of discharge is found (3.23). If the BES is discharged at the maximum depth of discharge value, λ will be 1, otherwise λ will be less than 1. The exact value of the parameter ψ is obtained from (3.11). The summation of the depth of discharge impact on lifetime over the planning horizon must be less than the number of cycles that the BES can perform at the maximum depth of discharge divided by the project lifetime as in (3.25). Satisfying (3.25) is important to ensure that the BES will be in service during the considered project lifetime.

3.3.2 Case Study

Microgrid and BES Data

The proposed model is tested on a standalone brownfield microgrid that is composed of three DGs (1 fuel-based and 2 renewables). The microgrid demand as well as the renewable DGs generation are obtained from [54]. The microgrid DGs characteristics are given in Table 3.6. It is assumed that 30% of the demand is critical and cannot be curtailed. The value of lost load is chosen to be $30/kWh.

Table 3.6 Microgrid generation units' characteristics

Unit	Cost Coefficient ($/MWh)	Minimum Capacity (MW)	Maximum Capacity (MW)
Fuel-based DG	150	0.2	7.2
PV	-	0	1.5
Wind	-	0	1

The standalone microgrid is planned to be expanded with BES to improve its reliability and reduce its operation cost. A Lithium-ion (Li-ion) battery is selected in this simulation as the desired BES technology. The Li-ion battery capital costs and efficiency are shown in Table 3.7. It must be noted that a 4% interest rate and a 40-year project lifetime are assumed when the annualized BES capital costs are calculated. The Li-ion battery modular size is assumed to be 0.2 MWh and 20 incremental size steps (i.e., n=20) is considered in the simulation.

Table 3.7 Li-ion battery costs and technical characteristics

Power Rating Capital Cost ($/kW)	Energy Rating Capital Cost ($/kWh)	Round Trip Efficiency (%)	Min./Max Depth of Discharge (%)	Min./Max Discharging Time (hour)
900	600	95	55/90	1/4

The relationship between the Li-ion battery depth of discharge and number of cycle is taken from a manufacturer data sheet [73]. After using the piece-wise linearization technique, the number of cycles and the associated degradation factor (ψ) are given in Table 3.8. The proposed expansion model is then used to find the optimal BES size and operation, taken into consideration the impact of variable depth of discharge and number of cycles on the BES lifetime. It must be noted that, the BES is needed to be in service for the considered project lifetime (i.e., 40 years).

Table 3.8 Li-ion battery cycles and degradation factor at different depth of discharge

Depth of Discharge (%)	Number of Cycles	Degradation Factor
55	7500	0.493
60	6900	0.536
65	6200	0.596
70	5800	0.637
75	5000	0.740
80	4500	0.822
85	4100	0.902
90	3700	1.000

Results and discussion

The obtained simulation results for two cases (with and without the BES) are tabulated in Table 3.9. It can be seen that installing the BES reduces the amount of unserved energy by 99.7%. This huge enhancement in the microgrid reliability is combined with a significant reduction in the microgrid total cost. The optimal Li-ion battery energy rating size is found to be 1 MWh while the optimal power rating size is found to be 0.418 MW. The installed Li-ion battery performed 108 cycles/year to improve the microgrid reliability and reduce the operation cost. Note that based on the information given in Table 3.8 along with (3.25), the Li-ion battery cannot perform more than 92 cycles/year at the maximum

depth of discharge if it is to stay in service for the entire project lifetime. However, due to the ability of the proposed model to determine the actual depth of discharge impact on the Li-ion battery lifetime, more cycles per year are performed.

Table 3.9 Operation cost analysis for the standalone microgrid before and after the expansion take place [72]

Microgrid Expansion State	Microgrid Operation Cost		Energy Not Supplied (MWh/yr)	Li-ion battery Investment Cost	Total Cost ($/yr)
	DGs Generation Cost ($/yr)	Load Interruption Cost ($/yr)			
No BES	7,521,174	1,580,400	52.680	-	9,101,574
With BES	7,527,893	4500	0.150	591,577.7	8,123,970

Figure 3.7 shows the Li-ion power and cycle indicator for a one-day sample. It is shown that the battery charging/discharging cycles can be accurately calculated using (41) in the proposed model. In the examined day, three complete charging/discharging cycles are performed by the installed Li-ion battery. The amount of energy stored in the Li-ion battery at each time interval is given in Figure 3.8. Figure 3.9 shows the actual depth of discharge at each completed cycle which is determined using (44) and (45). The battery is discharged with two different depth of discharge values: 70% and 60%. The impact of the depth of discharge on the battery lifetime is shown in Figure 3.10.

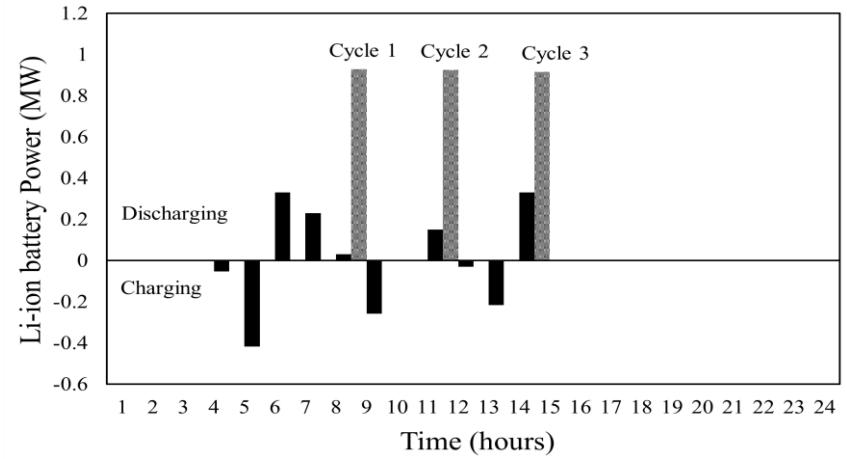

Figure 3.7 Li-ion battery power and cycle indicator [72]

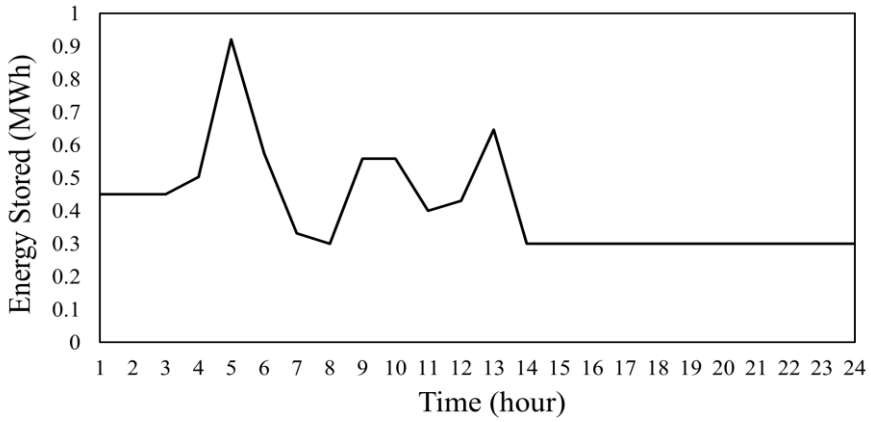

Figure 3.8 Li-ion battery stored energy for a sample day [72]

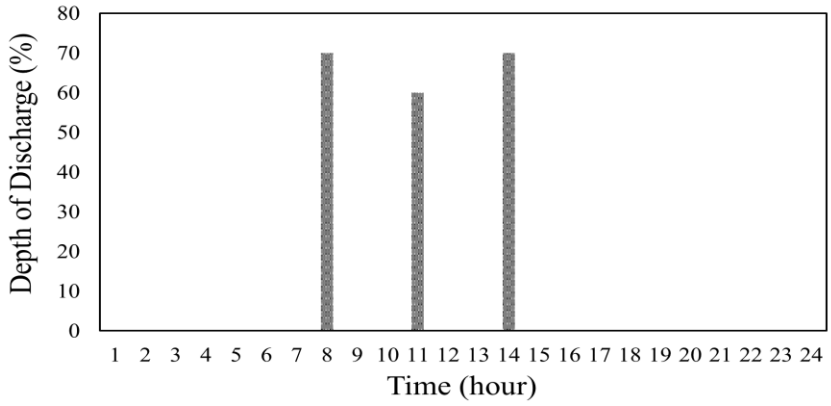

Figure 3.9 The calculated depth of discharge at each performed cycle [72]

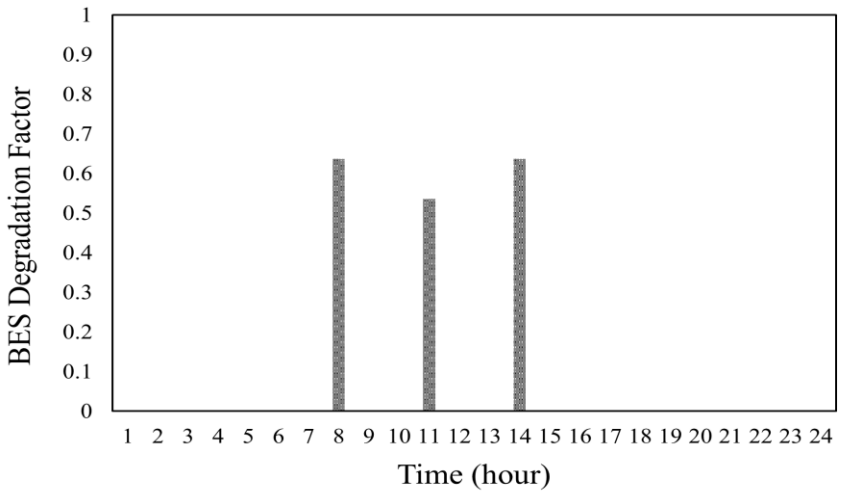

Figure 3.10 The impact of the depth of discharge on the Li-ion battery lifetime [72]

Chapter 4. Comprehensive Microgrid-Integrated BES Planning Model

4.1 Introduction

The comprehensive microgrid-integrated BES planning model takes all of the previous BES parameters (i.e., BES technology, size, units number, depth of discharge) into consideration when the microgrid expansion problem is solved. Moreover, both grid tied microgrid operation modes are considered in this model (i.e., grid connected and islanded). Under the grid-connected mode operation, the BES is used to increase the economic viability of the microgrid as they store energy at low price periods and generate the stored energy back to the system to be either used by local demand or sold to the utility grid at high price periods. In the islanded mode, however, BES units are used to improve the microgrid reliability by minimizing the curtailed load and the cost of unserved energy. Robust optimization is implemented in this model to consider the uncertainty associated with the renewable DGs and microgrid demand.

4.2 Problem Formulation

Similar to the previously discussed BES planning models, the objective of the proposed BES optimal comprehensive planning problem is to minimize the microgrid total expansion planning cost. However, in this model a new index (s) that represents the islanding scenarios is included in the expansion problem. In addition, more accurate mathematical equations are used to model the microgrid power flow. The total microgrid expansion cost is rewritten as follow:

$$Min\left\{\begin{array}{l}\sum_{i\in \mathrm{G}}\sum_{d}\sum_{h} F_i\left(P_{idh0} I_{idh0}\right)+\sum_{d}\sum_{h}\rho_{dh} P_{dh0}^{M}+\sum_{s} pr_s \sum_{b\in K}\sum_{d}\sum_{h} LS_{bdhs} v \\ +\sum_{i\in \mathrm{B}}\sum_{b\in K}\left(P_{ib}^{\mathrm{R}}\left(CP_i^{\mathrm{a}}+CM_i\right)+C_{ib}^{\mathrm{R}}\left(CE_i^{\mathrm{a}}+CI_i^{\mathrm{a}}\right)\right)\end{array}\right\} \tag{4.1}$$

The objective function comprises the microgrid operation cost (first and second terms), the cost of unserved energy (third term), and the annualized BES investment cost (last term). The microgrid operation cost incorporates the local generation cost and the cost of power exchange with the utility grid. This cost is determined only for the microgrid grid-connected mode, i.e., during the normal operation. Thus, the index for the islanding scenario is set to 0 in the operation cost terms in (4.1). In grid-connected mode, local load can be partially supplied by the utility grid, however in islanded mode the microgrid must rely solely on its local DERs. Any generation shortage in this case results in load curtailment, which reduces the microgrid reliability. Therefore, the cost of unserved energy is imposed as a penalty for failing to supply the local demand in each islanding scenario. To consider the probability of occurrence of each islanding scenario, pr_s is added as a weighting factor for each scenario. The BES investment cost is composed of power rating and energy rating capital costs, annual maintenance cost, and installation cost. It is assumed that the power conversion system cost is embedded in the power rating capital cost. The annual maintenance cost is normally given in terms of the BES power rating whereas the installation cost is given in term of the BES energy rating.

This objective is subject to several operation and technical constraints, associated with the microgrid, dispatchable DGs, and the BES, that must be taken into account as discussed in the following.

4.2.1 Microgrid Constraints

$$\sum_{i\in\{\mathrm{G,W}\}}\mu_{ib}\,P_{idhs}+\sum_{i\in\mathrm{B}}\left(P^{\mathrm{ch}}_{ibdhs}+P^{\mathrm{dch}}_{ibdhs}\right)+\sum_{l\in\mathrm{L}}\psi_{ib}\,f_{ldhs}+P^{\mathrm{M}}_{dhs}+LS_{bdhs}=D_{bdh}\qquad\forall b,\forall d,\forall h,\forall s \tag{4.2}$$

$$-P^{\mathrm{M,max}}z_{dhs}\le P^{\mathrm{M}}_{dhs}\le P^{\mathrm{M,max}}z_{dhs}\qquad\forall d,\forall h,\forall s \tag{4.3}$$

$$0\le LS_{bdhs}\le\left(D_{bdh}-CD_{bdh}\right)\qquad\forall b,\forall d,\forall h,\forall \mathrm{s} \tag{4.4}$$

$$-f_l^{\max}\le f_{ldhs}\le f_l^{\max}\qquad\forall l\in L,\forall d,\forall h,\forall \mathrm{s} \tag{4.5}$$

The nodal power balance (4.2) ensures that at each bus the power generated form DERs located at that bus plus/minus power flowing to/from the bus equals local demand. If the generation is not sufficient, load would be curtailed to satisfy the power balance. The BES power is positive when discharging and negative when charging. The utility grid power is positive when the power flows from the utility grid to the microgrid, and negative otherwise. Note that the utility grid power is zero at all buses except at the point of common coupling (PCC). Equation (4.3) imposes a maximum limit on the power transferred through the line connecting the microgrid to the utility grid. This equation is modified by including a binary parameter *z* that indicates the microgrid islanding state. That is, if the value of *z* is 0, the microgrid is disconnected from the utility grid and operated in the islanded mode, while if it is equal to 1, the microgrid is grid-connected. The value of *z* is set by the microgrid planner before solving the expansion planning problem and reflects how many hours in a year the microgrid operates in the islanded mode. There is a tradeoff between the number of considered islanding scenarios and the reliability of the obtained results and the computation burden. Increasing the number of considered islanding scenarios in the proposed model will increase both the results accuracy and the time required to solve the

problem, while ensuring more reliable operational solutions. One of the motivations for microgrid deployment is the continuity of service for critical loads. The critical loads are typically associated with high VOLL so it is not economically advisable to consider them for the load curtailment. Keeping this in mind, the load curtailment limits can be defined as in (4.4). The power flow in the microgrid distribution network is limited by the lines capacities (4.5). A radial distribution network is considered, hence (4.2) and (4.5) can efficiently model the power flow in the microgrid distribution network.

In the proposed model, it is assumed that the microgrid generations and loads are in close proximity, thus active losses as well as the bus voltage magnitude and angle are ignored in this work. A linear power flow model is needed to be combined with the proposed model in order to solve the full AC power flow without introducing nonlinear equations. Thus, existing power flow models presented in literature (e.g.,[74]–[77]) are not suitable to be used with the proposed model. The model needs to consider both active and reactive powers (i.e., a full AC power flow) to determine all bus voltage angles and magnitudes, and accordingly, active and reactive losses. The challenge is that the current distribution network power flow models are not linear, thus cannot be readily integrated to the proposed MILP model. There are certainly available linear power flow models in the literature, which however are mainly based on ZIP models, hence not very useful in the proposed model in this paper as studies here are focused on active and reactive power injections, in line with data collection/measurement and studies of many electric utilities.

4.2.2 Dispatchable DGs Constraints

$$P_i^{\min} I_{idh} \le P_{idhs} \le P_i^{\max} I_{idh} \qquad \forall i \in \mathrm{G}, \forall d, \forall h, \forall s \tag{4.6}$$

$$P_{idhs} - P_{id(h-1)s} \le UR_i \qquad \forall i \in \mathrm{G}, \forall d, \forall h, \forall s \qquad (4.7)$$

$$P_{id(h-1)s} - P_{idhs} \le DR_i \qquad \forall i \in \mathrm{G}, \forall d, \forall h, \forall s \qquad (4.8)$$

$$T_{idh}^{\mathrm{on}} \ge UT_i (I_{idh} - I_{id(h-1)}) \qquad \forall i \in \mathrm{G}, \forall d, \forall h \qquad (4.9)$$

$$T_{idh}^{\mathrm{off}} \ge DT_i (I_{id(h-1)} - I_{idh}) \qquad \forall i \in \mathrm{G}, \forall d, \forall h \qquad (4.10)$$

Dispatchable DGs output power is limited by maximum and minimum capacities (4.6), variations across two successive intervals, i.e., ramp up and ramp down (4.7), (4.8), and minimum up/down time limits (4.9), (4.10). Other constraints such as emission and fuel limits can be easily included. It must be noted that *h*-1 values at the first hour of each day (i.e., when *h*=1) are considered equal to the values of the last hour of the previous day (i.e., *h*=24 in *d*-1).

4.2.3 BES Constraints

$$P_i^{\min} x_{ib} \le P_{ib}^{\mathrm{R}} \le P_i^{\max} x_{ib} \qquad \forall i \in \mathrm{B}, \forall b \qquad (4.11)$$

$$\sigma_i^{\min} P_{ib}^{\mathrm{R}} \le C_{ib}^{\mathrm{R}} \le \sigma_i^{\max} P_{ib}^{\mathrm{R}} \qquad \forall i \in \mathrm{B}, \forall b \qquad (4.12)$$

$$0 \le P_{ibdhs}^{\mathrm{dch}} \le P_{ib}^{\mathrm{R}} u_{ibdhs} \qquad \forall i \in \mathrm{B}, \forall d, \forall h, \forall s \qquad (4.13)$$

$$-P_{ib}^{\mathrm{R}} (1 - u_{ibdhs}) \le P_{ibdhs}^{\mathrm{ch}} \le 0 \qquad \forall i \in \mathrm{B}, \forall b, \forall d, \forall h, \forall s \qquad (4.14)$$

$$\xi_{ibdhs} = (u_{ibdhs} - u_{ibd(h-1)s}) u_{ibdhs} \qquad \forall i \in \mathrm{B}, \forall b, \forall d, \forall h, \forall s \qquad (4.15)$$

$$\sum_d \sum_h pr_s \xi_{ibdhs} \le \frac{1}{T} \sum_{m \in \mathrm{N}} \kappa_{im} w_{ibm} \qquad \forall i \in \mathrm{B}, \forall b, \forall s \qquad (4.16)$$

$$\sum_{m \in \mathrm{N}} w_{ibm} \le x_{ib} \qquad \forall i \in \mathrm{B}, \forall b \qquad (4.17)$$

$$C_{ibdhs} = C_{ibd(h-1)s} - \frac{P_{ibdhs}^{\mathrm{dch}} \tau}{\eta_i} - P_{ibdhs}^{\mathrm{ch}} \tau \qquad \forall i \in \mathrm{B}, \forall b, \forall d, \forall h, \forall s \qquad (4.18)$$

$$\left(1-\sum_{m\in \mathrm{N}} \gamma_{ibm} w_{ibm}\right) C_{ib}^{\mathrm{R}} \le C_{ibdhs} \le C_{ib}^{\mathrm{R}} \qquad \forall i \in \mathrm{B}, \forall b, \forall d, \forall h, \forall s \qquad (4.19)$$

The BES power rating is limited by maximum and minimum values (4.11). For some BES technologies, such as those considered in this research, the energy rating is correlated to the power rating and cannot be sized independently. A capacity to power ration is used to size the BES capacity and determine the maximum discharge time at rated power (4.12). If flow batteries such as vanadium redox battery are considered, this constraint can be easily modified to decouple the power rating and the energy rating. The binary variable *x* is used to indicate the investment state of a BES technology. The BES charging/discharging powers are limited by the installed rated power (4.13), (4.14), which further impose that the BES power be negative in the charging mode while positive in the discharging mode. The binary variable *u* is used to represent the BES operating state. The BES can discharge only when *u* equals 1 and can charge when u equals 0. Each BES technology has a specific lifecycle, which depends on its associated depth of discharge. The BES cycle is typically defined as a complete charge and discharge cycle. Therefore, computing either the discharging cycles or charging cycles is enough to estimate the total number of cycles. Equation (4.15) is used to determine the BES cycles. The value of ξ will be 1 every time the discharging process is initiated, otherwise it is 0. In a similar way, the BES charging cycles can be computed. The summation of the BES cycles over the planning time horizon cannot exceed the determined lifecycle associated with the chosen depth of discharge and desired project lifetime (4.16). That is, the installed BES does not need to be replaced during the considered project lifetime and therefore the BES replacement cost is

not included in (4.1). The value of κ is determined based on the chosen depth of discharge (Figure 3.2) in which it is assumed that the curve is divided into N segments. *w* is a binary variable that represents the chosen depth of discharge segment. Equation (4.17) ensures that only one depth of discharge value is considered for each installed BES unit. The stored energy in the BES at each time interval equals the stored energy in the preceding interval minus the discharged or charged energy (4.18). The BES cannot be charged more than its rated energy and cannot be discharged below its minimum value which is defined by the determined optimal depth of discharge (4.19).

Finally, the investment cost of the installed BES units is limited by the available budget (4.20).

$$\sum_{i\in \mathrm{B}}\sum_{b\in K}\left(P_{ib}^{\mathrm{R}}\left(CP_i^{\mathrm{a}}+CM_i\right)+C_{ib}^{\mathrm{R}}\left(CE_i^{\mathrm{a}}+CI_i^{\mathrm{a}}\right)\right)\leq \mathrm{BL} \tag{4.20}$$

The problem is solved from a microgrid developer perspective, which means that savings in the upstream grid, such as deferred distribution and transmission upgrades as well as benefits of the reduced congestion, are not included. Figure 4.1 shows a schematic diagram for the comprehensive microgrid-integrated BES planning model.

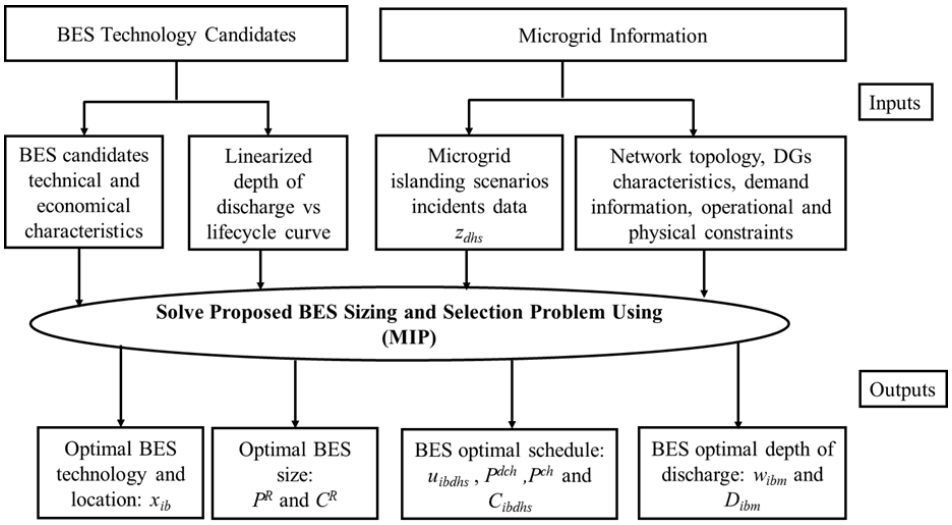

Figure 4.1 Schematic diagram for the comprehensive microgrid-integrated BES planning model [78]

4.2.4 Data Uncertainties Consideration

In the presented microgrid expansion planning formulation above, hourly forecasted data for the renewable DG generation, the load demand, and the electricity price is used. However, forecasting errors may arise as these parameters are affected by uncontrollable factors such as weather conditions, customers' behavior, and congestion or outage incidents. The proposed model can be extended by applying robust optimization method presented in [79] to address the presence of uncertainties in the microgrid expansion problem. Robust optimization determines the worst-case solution by maximizing the minimum value of the objective function (4.1) over uncertainty set Φ (i.e., for renewable DG generation, load demand, and electricity price). The objective function in (4.1) can be rewritten as:

$$\max_{\Phi} \min \sum_{i\in \mathrm{G}}\sum_{d}\sum_{h} F_i(P_{idh0}, I_{idh0}) + \sum_{d}\sum_{h} \rho_{dh} P^{M}_{dh0} + \sum_{s} pr_s \sum_{b\in K}\sum_{d}\sum_{h} LS_{bdhs} v + \sum_{i\in \mathrm{B}}\sum_{b\in K} \left(P^{\mathrm{R}}_{ib} \left(CP^{\mathrm{a}}_{i} + CM_i \right) + C^{\mathrm{R}}_{ib} \left(CE^{\mathrm{a}}_{i} + CI^{\mathrm{a}}_{i} \right) \right) \tag{4.21}$$

Uncertain parameters are associated with a nominal value that can be found from the forecast data. These nominal values, however, expand around a range of uncertainty which define an interval within which the uncertain parameter is presumed to lie. Thus, the uncertain parameters can be expressed as:

$$P_{idhs} = \widetilde{P}_{idhs} + \overline{P}_{idhs}\overline{\chi}^{g}_{idhs} - \underline{P}_{idhs}\underline{\chi}^{g}_{idhs} \qquad \forall i \in \mathrm{W}, \forall d, \forall h, \forall s \tag{4.22}$$

$$D_{bdh} = \widetilde{D}_{bdh} + \overline{D}_{bdh}\overline{\chi}^{l}_{bdh} - \underline{D}_{bdh}\underline{\chi}^{l}_{bdh} \qquad \forall b \in \mathrm{K}, \forall d, \forall h \tag{4.23}$$

$$\widetilde{\rho}_{dh} - \underline{\rho}_{dh}\underline{\chi}^{p}_{dh} \le \rho_{bdh} \le \widetilde{\rho}_{dh} + \overline{\rho}_{dh}\overline{\chi}^{p}_{dh} \qquad \forall b \in \mathrm{K}, \forall d, \forall h \tag{4.24}$$

where the inserted bars in (4.22)-(4.23) represent the upper and lower bounds of each parameter. To ensure only one extreme point is chosen, the following constraints are imposed to the microgrid expansion model at each time interval:

$$\overline{\chi}^{g}_{idhs} + \underline{\chi}^{g}_{idhs} \le 1, \overline{\chi}^{l}_{bdh} + \underline{\chi}^{l}_{bdh} \le 1, \overline{\chi}^{p}_{dh} + \underline{\chi}^{p}_{dh} \le 1 \tag{4.25}$$

However, it must be noted that a trade-off between the solution optimality and robustness must be performed when robust optimization method is used. This can be achieved by imposing a higher cap on the maximum number of uncertain parameters that can reach their bounds in the considered planning horizon. This cap is known as the budget of uncertainty [80]. Increasing the budget of uncertainty value will increase the robustness of the obtained solution at the expense of optimality, and vice versa. If the budget of uncertainty is set to be 0, the problem is solved by ignoring uncertain parameters.

To solve the resulted min-max optimization problem, the duality theory is used to convert the problem into either maximization or minimization problem. For more details about robust optimization formulation and duality theorem, the readers are referred to [79].

4.3 Case Study

Microgrid and BES Data

A 5-bus microgrid that contains a gas generator, a wind turbine, and a solar photovoltaic unit is used to study the proposed microgrid expansion planning model. DGs characteristics and location in the microgrid are given in Table 4.1. The hourly data of renewable DGs generation, local loads, and electricity market price are obtained from [54] for the expansion planning time frame. The local load details and location in the microgrid are given in Table 4.2 while the microgrid distribution network lines characteristics are given in Table 4.3. The point of common coupling (PCC), which connects the microgrid to the utility grid, is located at bus 1.

Table 4.1 Local generation units characteristics

Unit	Bus	Type	Cost Coefficient ($/MWh)	Min-Max Capacity (MW)	Min Up/Down Time (hour)
1	3	Gas unit	90	0-7	1
2	4	PV	0	0-1	-
3	4	Wind	0	0-1.5	-

Table 4.2 Microgrid local demand details (R: residential, C: commercial)

Load	Bus	Peak Load (MW)	Critical Load (%)	Load Type	VOLL ($/MWh)
1	3	6.62	60	C	50,000
2	5	4.41	30	R&C	50,000

Table 4.3 Distribution lines connections and capacities

Line	From Bus	To Bus	Capacity (MW)
1	1	2	8
2	2	3	6
3	2	4	5

4	2	5	5

Four BES technologies are used in the simulation: lead acid, NiCd, Li-ion, and NaS. The characteristics of the BES technologies are borrowed from [70] and shown in Table 4.4. The power rating of each BES technology is constrained by a maximum value, assumed to be 5 MW in this paper. A minimum discharging time of 1 hour and a maximum discharging time of 5 hours are considered. The available budget is assumed to be $5 million. The BES manufacturers data sheets are used to determine the relationship between the depth of discharge and lifecycle of each BES technology [71], [73], [81], [82]. Based on the manufacturer data sheet, ten different depth of discharge values are considered for each BES technology (i.e., N=10) through linearization. Increasing the considered depth of discharge values will increase both the accuracy and the computational requirements. Table 4.5 indicates the lifecycle of the BES technologies at the considered depth of discharge values. In the Li-ion battery case, the given minimum depth of discharge in the manufacturer data is 50% and no information is given for lower depth of discharge values. One-hour islanded scenarios are implemented to evaluate the reliability of the microgrid under islanded modes (i.e., 24 scenarios for each day), with uniform probability (i.e., pr=1/24).

Table 4.4 BES technologies characteristics

Technology	Power Rating Cost ($/kW)	Energy Rating Cost ($/kWh)	Maintenance Cost ($/kW/yr)	Installation Cost ($/kWh)	η (%)
Lead-acid	200	200	50	20	70
NiCd	500	400	20	12	85
Li-ion	900	600	-	3.6	98
NaS	350	300	80	8	95

Table 4.5 BES Lifecycles for Various Depth of Discharge Values

Depth of Discharge (%)	Number of Cycles			
	Lead acid	NiCd	Li-ion	NaS
10	8000	7900	-	100000
20	2500	5800	-	60000
30	1500	3400	-	30000
40	950	2000	-	15000
50	700	1200	8000	10000
55	-	-	7500	-
60	590	900	6900	9000
65	-	-	6200	-
70	500	800	5800	7000
75	-	-	5000	-
80	450	700	4500	6000
85	-	-	4100	-
90	390	600	3700	5000
100	350	500	3000	4000

Results and Discussion

The following four cases are studied in the numerical simulation:

Case 0: Microgrid optimal scheduling (i.e., the BES units installation is not included).

Case 1: Microgrid expansion planning. In this case, the BES installation to reduce both the microgrid operation cost and the cost of unserved energy is considered.

Case 2: This case investigates the impact of ignoring the relationship between the BES depth of discharge and lifecycle on the obtained solution accuracy and practicality.

Case 3: The impact of uncertainties associated with renewable DGs generation and load demand on the obtained solution is studied in this case.

Case 0: To accurately assess the benefits of installing the BES to the microgrid, the pre-expansion case is solved first in order to enable comparisons to the case of BES installation. The microgrid scheduling problem is modeled using (4.2)-(4.10) in this case where the last term in the objective function as well as the second term in (4.1) are set to 0. The results are shown in Table 4.6. The amount of expected unserved energy in this case is 67.5 MWh/year. The associated expected cost of unserved energy is $3,373,488. This of course would happen only when the microgrid is disconnected from the utility grid and operates in the islanded mode.

Case 1: In this case, the BES installation is considered and the proposed mathematical model (i.e., the complete set of equations) is used to model the microgrid expansion problem. In the grid-connected mode, the BES installation reduces the microgrid operation cost by storing energy during low price hours to be used during high price hours toward either supplying local demand (i.e., load shifting) or making economic benefit from selling the stored energy to the utility grid (i.e., energy arbitrage). In the islanded mode, however, the BES reduces the unserved energy, which results in improving the microgrid overall reliability. The obtained results for various project lifetimes are given in Table 4.6. It is clear from the results that installing the BES is economically justifiable, as the total expansion cost for all the considered project lifetimes is less than the cost of operating the microgrid without BES. The BES optimal technology, number, size, depth of discharge, as well as the number of annual cycles performed by the BES in the grid-connected mode are given in Table 4.7.

Table 4.6 Microgrid associated expansion planning costs [78]

Case	BES Lifetime (years)	BES Total Investment Cost ($/year)	Local Generation Cost ($/year)	Cost of Power Exchange ($/year)	Expected Cost of Unserved Energy ($/year)	Total Expansion Cost ($/year)
1	-	-	834,778	1,850,987	3,373,488	6,059,253
2	10	377,682	834,778	1,843,639	64,272	3,120,371
	15	432,445	834,778	1,796,512	10,680	3,074,416
	20	357,420	834,778	1,815,893	24,960	3,033,053

Table 4.7 Installed BESs optimal parameters for case 1 [78]

BES Lifetime (years)	BES Technology	Bus Number	Power Rating (MW)	Energy Rating (MWh)	Depth of Discharge (%)	Number of Cycles (Cycles/year)
10	Lead-acid	2	2.905	5.929	70	48
15	Li-ion	1	1.461	1.886	80	300
	NaS	3	1.444	1.900	80	396
20	Li-ion	1	2.527	2.865	90	168
	Li-ion	4	0.401	0.818	50	396

For the project lifetime of 10 years, a centralized lead acid battery located at bus 2 with the size of 2.905 MW and 5.929 MWh yields the minimum total expansion cost. However, from the BES operation analysis, it is found that the lead acid battery is mostly installed to improve the microgrid reliability under the islanded operation as the number of its cycles in grid-connected operation is low (i.e., 48 cycles). In order for the lead acid battery to perform this number of cycles per year and remains in service for 10 years, its depth of discharge cannot exceed 70%. Installing the lead acid battery is expected to save $7,348/year. However, the big saving is noticed in the islanded operation as the expected unserved energy is reduced by 98.09% compared to Case 0.

When the project lifetime is increased to 15 years, the investment in expensive technologies such as Li-ion and NaS becomes feasible. In this case, it is found that the optimal solution yields when Li-ion and NaS batteries are installed at buses 1 and 3, respectively. As these technologies can perform a high number of cycles before they reach their end of lifetime, they are used to reduce the microgrid operation cost in the grid-connected mode by purchasing power from the utility grid in low price periods and either use it to supply the demand or sell it to the utility grid in high price period. This saves the microgrid operator $54,475 per year and will sum up to $817,125 over the considered expansion timeframe. Both batteries can be discharged up to 80% of their energy rating size. The expected unserved demand in the islanded operation is reduced by 99.68% compared to Case 0.

For a project lifetime of 20 years, the minimum expansion cost is found when two Li-ion batteries are integrated to the microgrid at buses 1 and 4. The optimal size and depth of discharge values for these two BES units are shown in Table 4.7. The BES installed at bus 4, i.e., where the renewable DGs are located, is used to shift the renewable generation from off-peak periods to the peak periods which will reduce the amount of energy that is needed to be imported from the utility grid during the high price periods and therefore reduce the microgrid operation cost. The BES located at bus 1 is used for energy arbitrage. The expected unserved energy in this case is reduced by 99.26% compared to Case 0.

The BES cycles are computed using equation (4.15). Figure 4.2 shows how the proposed model can accurately compute the BES cycles over the planning horizon. It can be seen from the figure that the summation of the BES cycles indicator (ξ) over one week

equals to the number of performed cycles over the same period. This enables microgrid planners to take the impact of the number of BES cycles on its lifetime into consideration during the planning stage. Ignoring this impact may require the BES replacement before the expected end of project which imposes an extra cost to the expansion plan.

The other factor that affects the BES lifetime is the depth of discharge, i.e., the amount of energy that can be taken from the BES in each cycle. Figures 4.3-4.5 depict the SOC for the installed BES units for each considered project lifetime for a sample one week. It must be noted that the optimal depth of discharge value puts a cap on how deep the BES can be discharged based on the relationship between the BES depth of discharge and lifecycle. However, the BES can operate with a depth of discharge value that is less than the determined optimal value as can be seen from the state of charge curves. The determined optimal depth of discharge value, however, will ensure that the installed BES does not need to be replaced during the considered project lifetime which is one of the microgrid planner requirements in this work.

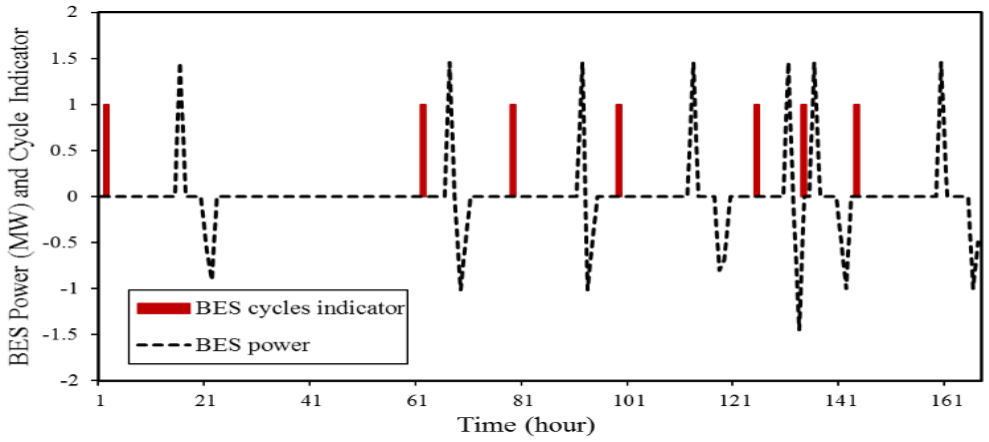

Figure 4.2 The Li-ion battery power and cycles for 15-year project lifetime [78]

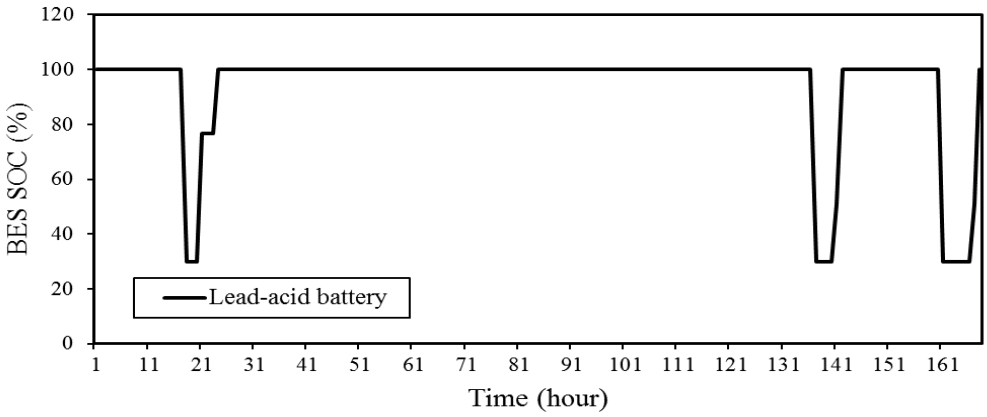

Figure 4.3 The installed Lead-acid battery SOC for one sample week [78]

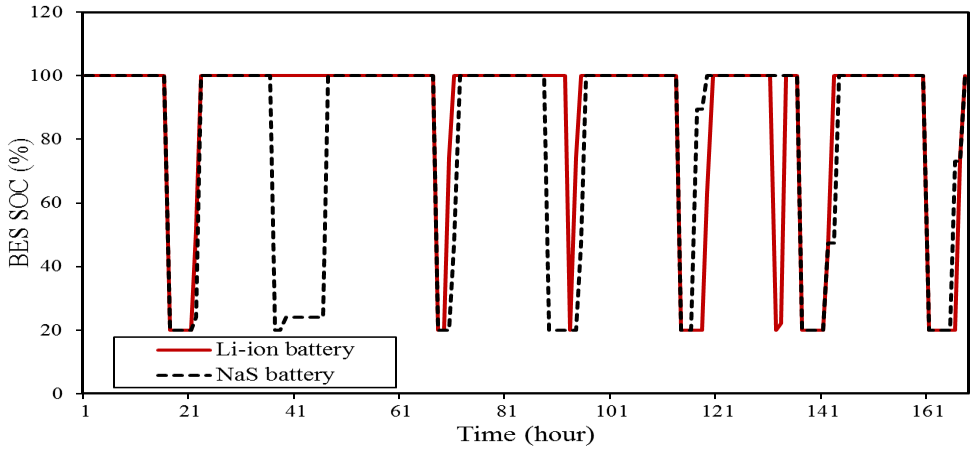

Figure 4.4 The installed Li-ion battery and NaS battery SOC for one sample week [78]

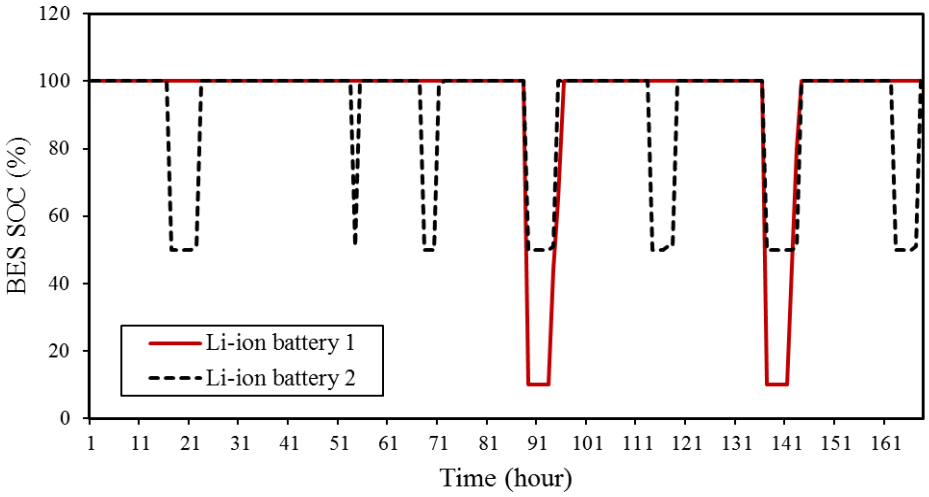

Figure 4.5 The installed Li-ion batteries SOC for one sample week [78]

The reason behind the variation in the obtained optimal BES technology and location in the studied cases stems mainly from two factors: the considered project lifetime and the BES application. These factors are actually correlated to each other as both of them have an impact on the number of cycles performed by the BES. In the 10-year project lifetime case, for example, a lead acid battery is found to be the optimal choice of BES technology to be installed. This BES is used to improve the microgrid reliability during islanding scenarios which rarely occur. This explains why the lead acid battery is selected as the optimal technology in this case as it is characterized with low capital cost and lifecycle. The lead acid battery is located at bus 2 in order to be available to supply both microgrid demand which are located at buses 3 and 5. For longer project lifetimes (i.e., 15 and 20 years) investing in more expensive BES types, which are characterized with high lifecycles such as Li-ion and NaS, becomes feasible. Since these BES technologies have high lifecycles and roundtrip efficiencies, they can be used to perform energy arbitrage and load shifting. The economic revenue gained by these applications combined with the long

project lifetime that the BES will be in service outweigh the high investment cost associated with installing the BES. The optimal locations for the installed BES units are determined by their applications. If the BES is installed to perform energy arbitrage application, it should be placed close to the PCC, which is bus 1 in the studied microgrid. In the other hand, if the BES is installed for load shifting applications, it should be placed close to the microgrid demand or generation units, which are located at buses 3 and 4.

Case 2: In order to accurately estimate the benefits and the optimal parameters of installed BES, the impact of operation factors such as depth of discharge and number of cycles on the BES lifetime must be included into the microgrid expansion problem. In this section, the importance of considering such impact is investigated. The microgrid expansion planning problem is resolved while ignoring the limit on the BES number of cycles. In other words, the relationship between the BES depth of discharge and lifecycle, which is represented by (4.16), is omitted from the proposed formulation. A 10-year BES lifetime case is considered. Table 4.8 shows the obtained results for this case. Since the BES operation impact on its lifetime is not included in the model, the optimal BES technology would be the less expensive BES candidate, which is lead acid battery. Moreover, the optimal maximum depth of discharge is found to be 100%. This result, however, is unrealistic as the installed lead acid battery is expected to perform 792 cycles/year. Based on the relationship between the BES depth of discharge and lifecycle, which is given in Table 4.5, the installed lead acid battery must be replaced within the first 5 months from its installation. This shows how important it is to consider the BES operation

impact on its lifetime in the microgrid expansion problem in order to enhance the accuracy and practicality of the obtained results.

Table 4.8 Numerical simulation results for case 2 [78]

BES Lifetime (years)	Optimal BES Technology	BES Optimal Size (MW/MWh)	Optimal Maximum Depth of Discharge (%)	Number of performed cycles/year	Expected End of Lifetime (months)
10	Lead-acid	0.823/1.306	100	792	5
	Lead-acid	2.105/3.341	100	792	5

Case 3: In this case, the forecast errors in renewable DG generation and load demand impacts on the obtained solution are investigated. The worst-case scenario occurs when a reduction in renewable DG generation and increase in load demand compared to the forecasted data take place. Thus, -20% forecast errors in renewable DGs generation and +10% forecast errors in load demand are considered. These forecast errors are assumed to happen for 1000 hours/year. Increasing or decreasing the number of hours per year at which the uncertainties are considered leads to more conservative or aggressive solution against data uncertainties. In the conservative solution, the obtained results are more robust against uncertainties but at the same time higher microgrid expansion cost is expected. On the other hand, the aggressive solution yields less robust results against uncertainties with lower microgrid expansion total cost compared to the conservative solution. The 1000 hours/year used in this simulation can be considered as a moderate solution. The 10-year BES lifetime case is resolved here using the proposed model with the consideration of uncertainties. From the numerical simulation results, it is found that when the uncertainties associated with renewable DG generation and load demand are taken into consideration, the microgrid

total expansion cost increases to become $3,368,200/year. Moreover, expensive BES technologies, which are characterized with high lifecycle such as NaS battery become economically feasible. The optimally determined parameters of the installed BES units are given in Table 4.9. The reason behind installing NiCd and NaS batteries instead of lead acid battery, which is found to be the optimal BES technology in Case 1, is that considering the uncertainties in the microgrid expansion problem requires the installed BES to be used more frequently in order to overcome the rapid change in the renewable DGs generation and the load demand, especially during islanding operation. Thus, BES technology with high lifecycle is needed in such case. A summary of the studied cases' advantages and disadvantages are shown in Table 4.10.

Table 4.9 Numerical simulation results for Case 3 [78]

BES Lifetime (years)	Optimal BES Technology	BES Optimal Size (MW/MWh)	Optimal Maximum Depth of Discharge (%)	Number of performed cycles/year
10	NiCd	2.483/2.922	100	48
	NaS	1.510/1.987	50	600

Table 4.10 Studied cases summary [78]

Case	Pros	Cons
0	• No BES investment cost as the BES is not installed in this case.	• High microgrid operation cost and low reliability, especially during islanded operation.
1	• Improve the microgrid reliability by supplying demand during islanded incidents. • Reduce operation cost by using BES to perform energy arbitrage application. • Impact of BES depth of discharge on its lifetime is considered.	• Stochastic nature of renewable DGs generation and load demand is not included in the expansion problem.

2	• Microgrid total expansion cost is reduced as the impact of BES depth of discharge on its lifetime is ignored.	• Unrealistic results are obtained and thus the BES will need to be replaced before the end of the desired project lifetime.
3	• The obtained result is robust against renewable generation and load demand uncertainties.	• High microgrid total expansion cost. • The optimality of the obtained solution might be impacted.

General algebraic modeling system (GAMS) is used to solve the optimization problem in both studied cases. The problem is implemented on a 2.4-GHz personal computer using CPLEX 11.0. The obtained solution is found within a 0.05% gap of the optimal solution; hence it provides a near-optimal solution. The gap is adjusted using the built-in functionalities of CPLEX in which in each iteration an upper bound and a lower bound of the current solution are calculated and the relative difference is considered as an optimality gap. It is worth noting that in the long-term planning problem it is not always possible to achieve the optimal solution due to the complexity of the problem and the large number of binary and continuous variables. The computation time, however, depends on the considered case, the number of islanding scenarios, and the optimality gap among other factors. For the first case (i.e., the microgrid scheduling problem without the BES installation) the problem is solved within seconds. When the BES installation is included to the problem, the problem is solved within multiple hours. The highest computational effort is associated with the 20-year project case. The optimal solution is reached within slightly less than 18 hours. However, as the problem in hand is an expansion planning problem, it is solved offline where the computation time is not as important as in operation problem

Chapter 5. Optimal Planning of BES for Non-Microgrid Applications

5.1 Optimal Planning of BES for Commercial and Industrial Customers

5.1.1 Introduction

In addition to the energy consumption charge (in $/kWh), the electricity bill of commercial and industrial (C&I) electricity customers normally contains a demand charge (in $/kW) that accounts for the customer peak demand. This demand charge is high and can reach sometimes up to 50% of the customer electricity bill [83]. Shaving the peak demand will benefit both the customer, by significantly reducing the peak demand payments, as well as the entire grid system, by helping reduce the network congestion and possibly lowering marginal energy prices. There are various methods to shave peak demand, however one common method is to use BES. The BES can be used to store energy during off-peak hours to supply the peak demand. In this case, the customer load profile will not be affected as the shaved demand will be supplied by the BES discharged power, thus the local load is not affected but the net load seen from the utility side is changed. With the implementation of time-based electricity rates, the BES can also be used to further reduce the electricity cost by energy arbitrage. That is, the BES will be charged during low price hours and discharged during high price hours. This is different from peak shaving as the electricity price may vary based on factors other than load profile such as transmission

network congestion or generators' bidding. A viable electricity price prediction technique can be of help in this application to accurately capture the price variations [84].

5.1.2 Problem Formulation

The total annual cost of the commercial customer is divided into three parts: energy consumption cost, monthly peak demand cost, and BES investment cost. The objective function of the optimization problem is to minimize the summation of these costs as:

$$Min\ C^E + C^P + C^B \tag{5.1}$$

The first term in (5.1) denotes the annual energy consumption cost. To reduce this cost, the BES is operated for energy arbitrage. The second term in the objective function represents the annual cost associated demand charges. This cost can be reduced by using the BES to help with peak shaving. The utility measures the commercial customer monthly peak demand and multiply the measured peak power by the demand charge set by the utility. The BES size is the main factor that determines the ability of the BES to adequately perform the energy arbitrage and the peak shaving services. It also determines the BES investment cost, which is the last term in (5.1).

Equation (5.2) is used to calculate the annual energy consumption cost. The power exchanged between the utility and the customer is limited by the capacity of the distribution line connecting them (5.3). It must be noted that power may flow to the grid if the commercial customer has any type of on-site generation sources installed. In this case, *P* would be negative and the customer will be paid at the real-time electricity price.

$$C^E = \sum_m \sum_h \rho_{mh} P^M_{mh} \tag{5.2}$$

$$-PL^{\max} \le P^M_{mh} \le PL^{\max} \qquad \forall m, \forall h \tag{5.3}$$

The contribution of the peak demand on the annual electricity cost is expressed by (5.4). The maximum power drawn from the utility grid at each month can be modeled using (5.5). The value of P^{max} will be determined to be higher than the power exchanged with the utility grid at each time interval during each month. However, since the objective is to minimize the customer electricity cost, the value of P^{max} will be minimized until it eventually become equal to the actual monthly peak demand value.

$$\mathrm{C}^{P} = \sum_{m} \lambda_m P_m^{\max} \tag{5.4}$$

$$P_{mh}^{M} \le P_m^{\max} \le PL^{\max} \qquad \forall m, \forall h \tag{5.5}$$

The BES investment cost is composed of power rating cost and energy rating cost. The optimization problem is solved for one year and therefore the BES investment cost is normalized on an annual basis. The annual BES maintenance cost is included in both annualized power and energy rating costs. Equation (5.6) denotes the investment on the BES. This investment is constrained by the available budget which will further impose a cap on the BES size (5.7). The optimization problem is solved for one year and therefore the BES investment cost is normalized on an annual basis.

$$\mathrm{C}^{B} = CC^{P} P^{R} + CC^{\mathrm{E}} E^{R} \tag{5.6}$$

$$\mathrm{C}^{B} \le BL \tag{5.7}$$

The objective function (5.1) is subject to the following operational constraints which represent the system power balance and the BES operational limits

$$P_{mh}^{PV} + P_{mh}^{B} + P_{mh}^{M} = L_{mh} \qquad \forall m, \forall h \tag{5.8}$$

$$0 \le P_{mh}^{dch} \le P^{R} u_{mh} \qquad \forall m, \forall h \tag{5.9}$$

$$-P^{R}\left(1-u_{mh}\right)\le P_{mh}^{ch}\le 0 \qquad \forall m,\forall h \qquad (5.10)$$

$$P_{mh}^{B}=P_{mh}^{dch}+P_{mh}^{ch} \qquad \forall m,\forall h \qquad (5.11)$$

$$\xi_{mh}=\left(u_{mh}-u_{m(h-1)}\right)u_{mh} \qquad \forall m,\forall h \qquad (5.12)$$

$$\sum_{m}\sum_{h}\xi_{mh}\le N\left(i,T,D\right) \qquad (5.13)$$

$$\left(1-\sum_{k}D_{k}w_{k}\right)\le E_{mh}^{B}\le E^{R} \qquad \forall m,\forall h \qquad (5.14)$$

$$\sum_{k}w_{k}\le 1 \qquad (5.15)$$

$$E_{mh}^{B}=E_{m(h-1)}^{B}-\frac{P_{mh}^{dch}\tau}{\eta}-P_{mh}^{ch}\tau \qquad \forall m,\forall h \qquad (5.16)$$

5.1.3 Case Study

Commercial Customer Data

The developed optimal BES sizing model is validated by testing on a commercial customer. It is assumed that the customer already has a local generation, solar photovoltaic (PV) in this case. The hourly PV generation and local demand are borrowed from [54]. The PV power rating is 1.5 MW and the customer peak demand is 8.49 MW. The commercial customer is connected to the utility grid through a distribution line with 10 MW capacity. The utility offers a real-time pricing rate to charge the customer for its energy consumption. The hourly electricity prices are taken from [85]. Besides the energy consumption charge, a demand charge of $13/kW is considered.

A lithium-ion battery is considered as the selected BES technology, as it is characterized by high efficiency and large number of cycles. The capital cost of lithium-ion batteries has shown a significant decrease during the past few years and is predicted to

exhibit further reduction in the near future. The Li-ion battery technical and economical characteristics are shown in Table 5.1. The relationship between the depth of discharge and the number of cycles that can be performed by the Li-ion battery before it needs to be replaced is taken from [73], which is linearized and shown in Table 5.*2*. If the installed Li-ion battery is desired to be in service for the project lifetime, which is the case in this work, the number of cycles in Table *5.2* must be divided by the project lifetime. In other words, the BES is assumed to perform the same number of cycles each year. The validity of this assumption depends on the annual variation on the customer demand, PV generation, and electricity price.

Table 5.1 Lithium-ion battery characteristics

Power Rating Capital Cost ($/MW)	Energy Rating Capital Cost ($/MWh)	Round Trip Efficiency (%)	Charging/ Discharging duration (hour)	Budget Limit (M$)
30,000	20,000	98	3	1

Table 5.2 Lithium-ion battery number of cycles vs depth of discharge value

Depth of Discharge (%)	50	55	60	65	70
Number of Cycles	8000	7500	6900	6200	5800
Depth of Discharge (%)	75	80	85	90	100
Number of Cycles	5000	4500	4100	3700	3000

Results and Discussion

Three cases are considered in the numerical simulation:

Case 1: Solving the optimization problem without BES (i.e., calculating the commercial customer electricity cost).

Case 2: Solving the optimization problem with BES but without considering the impact of the BES operating parameters on its lifetime.

Case 3: Solving the optimization problem with BES using the developed model.

The results of these cases are summarized in Table *5.3* and Table 5.4. In the first case, the BES optimal parameter is ignored in Table 5.3 as the BES is not yet installed. It is found that the demand charge cost is about 32% of the total electricity cost. The second case studies the general approach used by many papers in the literature. In this case, the limit on the BES number of cycles, i.e., (5.13), is not considered. Since the depth of discharge does not affect the BES lifetime in this scenario, the optimal value as expected is determined to be 100%. Moreover, the BES optimal size is found to be large. Installing the BES reduces the total planning cost (i.e., the total electricity cost and the BES investment cost) by 3.75% which saves the customer $109,326 per year. The energy arbitrage application reduces the annual customer energy consumption cost by 8.86%, while the peak shaving application reduces the annual peak demand related cost by 9.95%. However, based on the number of performed cycles over the year and the relationship between the BES depth of discharge and number of cycles in Table 5.2, it can be said that the installed BES will need to be replaced after two years. This of course imposes extra cost that was not considered in the problem.

Table 5.3 Obtained optimal parameters for the Li-ion battery

Case	Power Rating (MW)	Energy Rating (MWh)	Depth of Discharge (%)	Number of Cycles
2	1.772	5.316	100	1451
3	0.340	1.020	55	485

Table 5.4 Obtained commercial customer costs for the considered cases

Case	BES Investment Cost ($/year)	Energy Consumption Cost ($/year)	Peak Demand Cost ($/year)	Total Cost ($/year)
1	-	1,976,918	940,420	2,917,338
2	159,489	1,801,601	846,884	2,807,976
3	30,600	1,959,873	900,444	2,890,917

To get more realistic results, the optimization problem is solved again using the proposed model. The desired project lifetime is chosen to be 15 years. It is noticed that the optimal BES size is smaller compared to Case 2. Moreover, the optimal depth of discharge is found to be 55%. With this depth of discharge, the BES can perform up to 500 cycles per year. In the obtained results, the performed number of cycles is 485. The total planning cost is reduced by 0.91% compared to the total electricity cost in Case 1. Using the BES in energy arbitrage application reduces the annual energy consumption cost by 0.86%, whereas using the BES for peak shaving application reduces the annual peak demand related cost by 4.2%. Although it seems that this reduction is smaller than the reduction in Case 2, the aggregated economic benefits over the project lifetime is actually higher. In Case 2, the aggregated saving is $218,652 whereas in this Case 3, aggregated saving is $396,300. Hence, it can be said that considering the impact of the BES depth of discharge and number of cycles on the BES lifetime does not only improve the practicality of the obtained results but also increases the gained economic benefits. Fig. 2 depicts the reduction on the peak demand associated with each case.

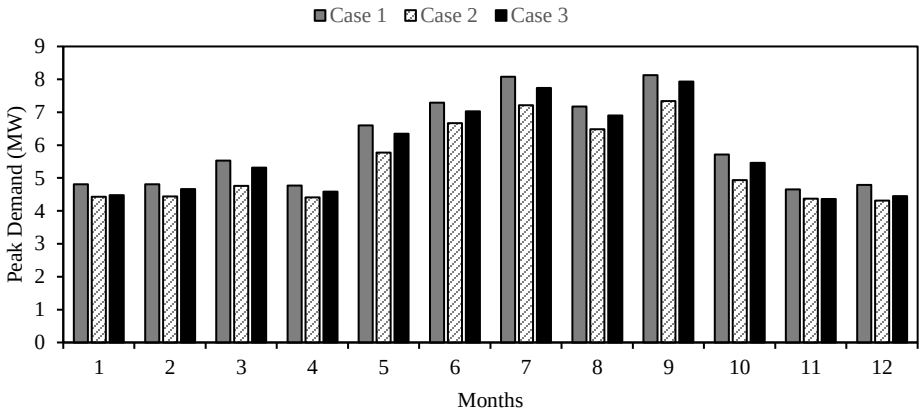

Figure 5.1 Commercial customer monthly peak demand reduction

It is worth mentioning that the obtained optimal BES size may not be available in the market as the BES manufacturers produce a range of predetermined sizes. However, the obtained results can be used as a basis for the BES size selection. Moreover, the obtained results are greatly impacted by economical and technical factors such as BES capital cost, charging/discharging duration, project lifetime, electricity prices, demand charges, and local solar generation capacity. Therefore, sensitivity analyses are conducted to investigate the impact of some of the aforementioned factors on the optimization results.

Table 5.5 shows the impact of changing the BES discharging/charging duration on the obtained results. For a 1-hour charging duration, the installation of the BES is not feasible as can be seen from the results. As the charging/discharging duration increases, the BES benefits outweigh its investment cost which makes the investment in the BES economically viable. The total planning cost reduces as the discharge duration increases until it reaches 5 hours, after which the total planning cost increases again. However, the impact of the discharge duration on the BES size and depth of discharge are not proportional.

Table 5.5 Sensitivity analysis for different BES charging/discharging duration

Discharging/ Charging duration (hour)	Power Rating (MW)	Depth of Discharge (%)	Number of Cycles	Total Cost ($/year)
1	-	-	-	2,917,338
2	0.489	50	513	2,895,899
3	0.340	55	485	2,890,918
4	0.390	80	300	2,888,167
5	0.393	85	262	2,885,066
6	0.440	60	459	2,897,278

As expected, increasing the demand charge will increase the total planning cost, shown in Table 5.6. It is also noticed that increasing the demand charges causes the BES size and depth of discharge to increase. The explanation of this will be that as the demand charges increase, the economic benefit of installing the BES to shave the commercial customer peak demand becomes clearer and therefore investing in larger BES size turns out to be feasible.

Table 5.6 Sensitivity analysis for different demand charge values

Demand Charges ($/kW)	Power Rating (MW)	Depth of Discharge (%)	Number of Cycles	Total Cost ($/year)
9	0.285	50	508	2,622,421
11	0.326	50	523	2,758,814
13	0.340	55	485	2,890,918
15	0.562	55	495	3,025,571
17	0.632	85	272	3,159,407

The last sensitivity analysis is performed to examine the PV capacity impact on the BES optimal size and depth of discharge. Since the PV is assumed to be already installed in the system, it is not necessary to include its total planning cost into this analysis. From

Table 5.7, it can be seen that as the solar generation increases, the BES size increases. However, the analysis results do not show a clear relationship between the PV capacity and the optimal depth of discharge value.

Table 5.7 Sensitivity analysis for different PV capacities

PV Capacity (MW)	Power Rating (MW)	Depth of Discharge (%)	Number of Cycles
1	0.357	80	280
1.5	0.340	55	485
2	0.622	50	524
2.5	0.785	65	388

5.2 Optimal Planning of BES for Distribution Network Expansion

5.2.1 Introduction

To meet the forecasted load growth and to maintain an acceptable quality of service, electric utilities need to continuously expand and upgrade their existing distribution networks. Failing to determine the appropriate expansion plan may increase the distribution network operation cost and reduce its reliability. Thus, efficient distribution network expansion models are of great importance for electric utilities. Traditionally, expansion and upgrade of distribution networks involved building new distribution lines, transformers, and substations. However, due to the rapid advancement in distributed energy resources, especially distributed battery energy storage, new expansion paradigms are emerging. If the distributed BES units are optimally sized and placed within the distribution network, they can potentially lead to a reduction in the total expansion cost, which includes investment cost and system operation cost, while at the same time help achieve economic, reliability, and power quality objectives [86], [87]. Moreover, the distributed BES units

can provide the distribution network with other benefits such as loss reduction and voltage profile enhancement which may not be readily available using traditional expansion methods.

Different approaches have been proposed to solve the distribution network expansion planning problem. The work in [86] and [87] review many of the existing distribution network expansion planning models. Traditional distribution network expansion models are proposed in [88]–[93] that focus on adding or replacing substations, transformers, and distribution lines. On the other hand, the works in [94]–[97] consider only the installation of distributed BES units and accordingly propose planning models to find the optimal size and location of the installed distributed BES units within the distribution network. Few published works consider simultaneous investment on both traditional options and distributed BES [82]–[86]. The distribution network expansion models in [98]–[100] use dynamic programming, a method that is characterized by high computation burden. In [101] mixed integer nonlinear programming is used to formulate the distribution network expansion planning problem and thus the solution optimality is not guaranteed. The work in [102] assumes that the installed distributed BES size is known in advance. This assumption reduces the practicality of the proposed method knowing that the BES investment cost is mainly related to its size.

In this section, a distribution network expansion planning model is developed to determine the optimal expansion plan that minimizes the total expansion cost while benefitting from distributed BES units installation. Linearized distribution power flow is used to examine the network constraints, i.e., voltage magnitude and line flow, to ensure

the feasibility of the obtained expansion plan. Mixed integer linear programming (MIP) is used to formulate the problem. The solution of the problem will be the optimal size and location of the distributed BES units to be installed in the network.

5.2.2 Problem Formulation

The objective of the distribution network expansion is defined as to minimize the total expansion cost, which is a summation of the investment cost associated with installing new distribution lines and distributed BES units as well as the load interruption cost as given in (5.17).

$$Min \left\{ \sum_{ij \in L_c} CL_{ij}\ z_{ij} + \sum_{s \in S_m} \left(CC_s^P\ P_s^R + CC_s^E\ E_s^R \right) + \sum_t v_t LS_t \right\} \tag{5.17}$$

The first term in (5.17) indicates the investment cost of building new distribution lines, which is obtained from line capacity and length. The second term is the distributed BES units investment cost, which comprises two terms associated with power rating cost and energy rating cost. The cost of the power electronics needed to interface the BES units with the distribution network is assumed to be embedded into the BES power rating cost. The last term in the objective represents the cost associated with failing to supply the load demand. This cost depends on the interrupted load type, location, and time. This objective is minimized subject to the distribution network and the distributed BES units operational and budget constraints as further discussed in the following.

Distribution Network Operational Constraints

These set of constraints ensure an adequate and reliable operation for the distribution network. The first constraint that must be fulfilled all times is the active and reactive power balance constraint (5.18) and (5.19).

$$P_t^M + \sum_{s\in \mathrm{S_m}} P_{st} + \sum_{j\in \mathrm{B}_m} PL_{ijt} = PD_{it} \qquad \forall i, \forall t \tag{5.18}$$

$$Q_t^M + \sum_{s\in \mathrm{S_m}} Q_{st} + \sum_{j\in \mathrm{B_m}} QL_{ijt} = QD_{it} \qquad \forall i, \forall t \tag{5.19}$$

The active and reactive line flow equations, as shown respectively in (5.20) and (5.21), are nonlinear in nature.

$$PL_{ijt} = g_{ij}V_{it}^2 - V_{it}V_{jt}\left(g_{ij}\cos\left(\theta_{it}-\theta_{jt}\right) + b_{ij}\sin\left(\theta_{it}-\theta_{jt}\right)\right) \qquad \forall ij \in \mathrm{L_e}, \forall t \tag{5.20}$$

$$QL_{ijt} = b_{ij}V_{it}^2 - V_{it}V_{jt}\left(-b_{ij}\cos\left(\theta_{it}-\theta_{jt}\right) + g_{ij}\sin\left(\theta_{it}-\theta_{jt}\right)\right) \qquad \forall ij \in \mathrm{L_e}, \forall t \tag{5.21}$$

Since the bus voltage angles in adjacent buses in distribution networks are normally close, the difference between these angles can be considered close to zero. Keeping this in mind, the trigonometric terms in (5.20) and (5.21) can be approximated as $\sin(\theta_{it}-\theta_{jt})\approx(\theta_{it}-\theta_{jt})$ and $\cos(\theta_{it}-\theta_{jt})\approx 1$. Besides, the bus voltage magnitude and angle can be expressed using the voltage and angle deviation at each bus with respect to the slack bus (i.e., the bus at which the distribution network is connected to the higher voltage subtransmission network). That is, the bus voltage magnitude and angle can be redefined as $V_{it}=1+\Delta V_{it}$ and $\theta_{it}=1+\Delta\theta_{it}$.

By substituting the trigonometric terms approximation and the new bus voltage magnitude and angle definitions into the line flow equations, (5.22) and (5.23) are obtained.

$$PL_{ijt} = g_{ij}(\Delta V_i - \Delta V_j) - b_{ij}(\Delta\theta_i - \Delta\theta_j) + g_{ij}\Delta\hat{V}_i(\Delta V_i - \Delta V_j) \quad \forall ij \in \mathrm{L_e}, \forall t \tag{5.22}$$

$$QL_{ijt} = -b_{ij}(\Delta V_i - \Delta V_j) - g_{ij}(\Delta\theta_i - \Delta\theta_j) - b_{ij}\Delta\hat{V}_i(\Delta V_i - \Delta V_j) \quad \forall ij \in \mathrm{L_e}, \forall t \tag{5.23}$$

In this work, the distribution power flow problem is solved in two steps. In the first step, the third term in (5.22) and (5.23) is omitted by setting $\Delta\hat{V}_i$ =0. In this step, a lossless power flow solution is obtained. The bus voltage deviation that is calculated in the first step is recorded as $\Delta\hat{V}_i$ and used in the second step. The distribution power flow is then solved in the second step using (5.22) and (5.23). In this way, the nonlinear distribution power flow is linearized and thus can be used in the developed distribution network expansion model. The line flow in each distribution line is constrained by its associated capacity limits for active and reactive power, respectively as in (5.24) and (5.25).

$$-PL_{ij}^{\max} \le PL_{ijt} \le PL_{ij}^{\max} \qquad \forall ij \in \mathrm{L_e}, \forall t \tag{5.24}$$

$$-QL_{ij}^{\max} \le QL_{ijt} \le QL_{ij}^{\max} \qquad \forall ij \in \mathrm{L_e}, \forall t \tag{5.25}$$

For candidate lines, the line flow equations are modified, as in (5.26)-(5.29), to include a binary variable z that represents the distribution line investment state. If a new line between buses *i* and *j* is built, z_{ij} is 1, otherwise it is 0. Note that when z_{ij} is 0, (5.26) and (5.27) are relaxed and the line flow is set to 0 by (5.28) and (5.29). On the other hand, when z_{ij} is 1, (5.26) and (5.27) treat the candidate line as an existing line, i.e., impose similar

equation for line flow as in existing lines, and (5.28) and (5.29) add the active and reactive capacity limits, respectively.

$$-\mathrm{K}(1-z_{ij}) \le PL_{ijt} - (g_{ij}(\Delta V_i - \Delta V_j) - b_{ij}(\Delta\theta_i - \Delta\theta_j) + g_{ij}\Delta\hat{V}_i(\Delta V_i - \Delta V_j)) \le \mathrm{K}(1-z_{ij}) \qquad \forall ij \in \mathrm{L_c}, \forall t \tag{5.26}$$

$$-\mathrm{K}(1-z_{ij}) \le QL_{ijt} - (-b_{ij}(\Delta V_i - \Delta V_j) - g_{ij}(\Delta\theta_i - \Delta\theta_j) - b_{ij}\Delta\hat{V}_i(\Delta V_i - \Delta V_j)) \le \mathrm{K}(1-z_{ij}) \qquad \forall ij \in \mathrm{L_c}, \forall t \tag{5.27}$$

$$-PL_{ij}^{\max} z_{ij} \le PL_{ijt} \le PL_{ij}^{\max} z_{ij} \qquad \forall ij \in \mathrm{L_c}, \forall t \tag{5.28}$$

$$-QL_{ij}^{\max} z_{ij} \le QL_{ijt} \le QL_{ij}^{\max} z_{ij} \qquad \forall ij \in \mathrm{L_c}, \forall t \tag{5.29}$$

Lastly, the bus voltage magnitude is limited by maximum and minimum limits (5.30).

$$\Delta V_i^{\min} \le \Delta V_{it} \le \Delta V_i^{\max} \qquad \forall i, \forall t \tag{5.30}$$

DBES units Operational Constraints

The distributed BES units investment and operation can be modeled using (5.31)-(5.37). The distributed BES units charging and discharging power cannot exceed the optimal power rating size (5.31)-(5.32). The distributed BES units operating state indicator *u* ensures that the distributed BES units is either charging or discharging and is not in both states simultaneously. The distributed BES power is positive when the BES is discharging and negative when the BES is charging. The distributed BES units are assumed to be used only for active power applications. The distributed BES units' power used in (5.18) at any time interval is determined as the summation of the DBES charging and discharging power (5.33). The amount of energy stored in the DBES is calculated by (5.34). To protect the distributed BES units from overcharging or undercharging situations, the amount of hourly

stored energy is constrained by associated maximum and minimum limits based on the optimal energy rating and the allowable depth of discharge (5.35). The optimal power rating size is limited by the available technology/module size (5.36). The distributed BES units energy rating is determined based on the energy to power ratio in (5.37).

$$0 \le P_{st}^{\mathrm{dch}} \le P_s^R u_{st}^{\mathrm{dch}} \qquad \forall s \in \mathrm{S}_i, \forall t \tag{5.31}$$

$$-P_s^R (1-u_{st}^{\mathrm{dch}}) \le P_{st}^{\mathrm{ch}} \le 0 \qquad \forall s \in \mathrm{S}_i, \forall t \tag{5.32}$$

$$P_{st} = P_{st}^{\mathrm{dch}} + P_{st}^{\mathrm{ch}} \qquad \forall s \in \mathrm{S}_i, \forall t \tag{5.33}$$

$$E_{st}^{B} = E_{s(t-1)}^{\mathrm{B}} - \frac{P_{st}^{\mathrm{dch}} \tau}{\eta_s} - P_{st}^{\mathrm{ch}} \tau \qquad \forall s \in \mathrm{S}_i, \forall t \tag{5.34}$$

$$(1-D_s)\, E_s^R \le E_{st}^B \le E_s^R \qquad \forall s \in \mathrm{S}_i, \forall t \tag{5.35}$$

$$P_s^{\min} x_s \le P_s^R \le P_s^{\max} x_s \qquad \forall s \in \mathrm{S}_i, \forall t \tag{5.36}$$

$$P_s^R \sigma_s^{\min} \le E_s^R \le P_s^R \sigma_s^{\max} \qquad \forall s \in \mathrm{S}_i, \forall t \tag{5.37}$$

The desired values from the BES planning model, when considered within the expansion planning model, are *x*, which represents the decision to install the distributed BES units as well as its location, and E^R and P^R, which represent the size of the installed distributed BES units.

Distribution Network Expansion Budget Limit

Each expansion project has an available budget limit that cannot be exceeded. This limit will impact the selected expansion plan such as the type of the technology to be used, the location and the optimal size (5.38).

$$\sum_{ij \in L_c} CL_{ij}\ z_{ij} + \sum_{s \in S_i} \left(CC_s^P\ P_s^R + CC_s^E\ C_s^R \right) \leq BL \tag{5.38}$$

5.2.3 Case Study

Distribution Network and DBES Data

The IEEE 33-bus system, shown in Figure 5.2, is used to study the proposed distribution network expansion planning model. The hourly load demand data are borrowed from [54] and scaled to be suitable for this system. The forecasted load growth is given in Table 5.8. This load growth is assumed for active load and the reactive load growth is determined accordingly based on a fixed power factor. The cost of failing to supply loads is assumed to be $20/kWh. The candidate distribution lines data is given in Table 5.9. The line investment cost is determined based on the information given in [103]. A lead acid battery is selected as the selected distributed BES technology. However, other BES technologies can be used without loss of generality. The lead acid battery characteristics are retrieved from [70] and shown in Table 5.10. The annualized capital cost is calculated assuming 10% interest rate, along with a lifetime of 20 years and 10 years for the lines and the distributed BES units, respectively.

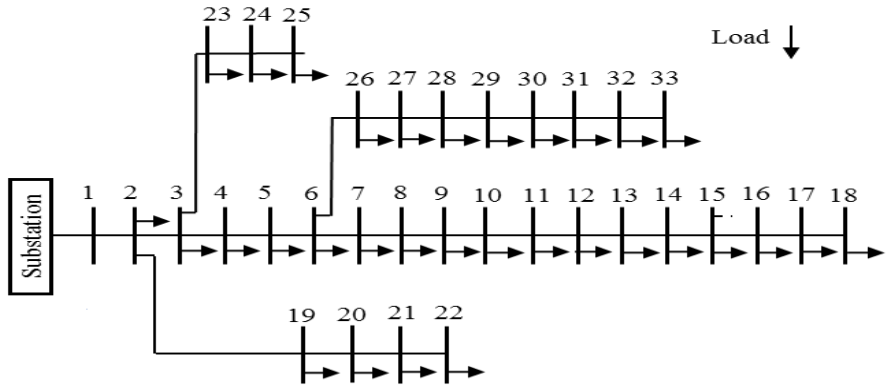

Figure 5.2 IEEE 33-bus single line diagram

Table 5.8 Forecasted load growth

Bus Number	1	2	3	4	5
Load Growth (%)	0	12	10	2	3
Bus Number	6	7	8	9	10
Load Growth (%)	5	1.5	6	0.5	2.3
Bus Number	11	12	13	14	15
Load Growth (%)	5	0	0.5	8	6
Bus Number	16	17	18	19	20
Load Growth (%)	2	8	4	3	15
Bus Number	21	22	23	24	25
Load Growth (%)	2	0.3	10	0	5
Bus Number	26	27	28	29	30
Load Growth (%)	8	4	0	0.5	5
Bus Number	31	32	33	-	-
Load Growth (%)	6	0.3	0	-	-

Table 5.9 Candidate distribution lines data

Candidate Line	From Bus	To Bus	R (Ohms)	X (Ohms)	Capacity (kW)	Inv. Cost ($/year)
1	1	2	0.0922	0.0470	4600	21811.72
2	2	3	0.4930	0.2511	4100	103951.77
3	3	4	0.3660	0.1864	2900	54585.86
4	4	5	0.3811	0.1941	2900	56837.9
5	5	6	0.8190	0.7070	2900	122147.05
6	6	7	0.1872	0.6188	1500	14441.03
7	7	8	0.7114	0.2351	1050	38415.3
8	8	9	1.0300	0.7400	1050	55619.56
9	9	10	1.0440	0.7400	1050	56375.56

10	10	11	0.1966	0.0650	1050	10616.32
11	11	12	0.3744	0.1298	1050	20217.44
12	12	13	1.4680	1.1550	500	37748.28
13	13	14	0.5416	0.7129	450	12534.07
14	14	15	0.5910	0.5260	300	9118.215
15	15	16	0.7463	0.5450	250	9595.21
16	16	17	1.2890	1.7210	250	16572.72
17	17	18	0.7320	0.5740	100	3764.54
18	2	19	0.1640	0.1565	500	4217.11
19	19	20	1.5042	1.3554	500	38679.12
20	20	21	0.4095	0.4784	210	4422.56
21	21	22	0.7089	0.9373	110	4010.31
22	3	23	0.4512	0.3083	1050	24364.61
23	23	24	0.8980	0.7091	1050	48491.62
24	24	25	0.8960	0.7011	500	23039.82
25	6	26	0.2030	0.1034	1500	15659.87
26	26	27	0.2842	0.1447	1500	21923.83
27	27	28	1.0590	0.9337	1500	81693.65
28	28	29	0.8042	0.7006	1500	62037.80
29	29	30	0.5075	0.2585	1500	39149.69
30	30	31	0.9744	0.9630	500	25055.80
31	31	32	0.3105	0.3619	500	7984.22

Table 5.10 Lead acid battery characteristics

Min./Max. Power Rating (kW)	Capital Cost		Depth of Discharge (%)	Min./Max Energy to Power Ratio
	($/kW)	($/kWh)		
0/200	300	200	85	1/5

Results and Discussion

Three cases are studied in this simulation:

Case 1: The distribution network power flow is solved without considering the network expansion to determine the amount of potentially curtailed load.

Case 2: A traditional distribution network expansion problem is solved in which the load growth will be met by installing new distribution lines.

Case 3: The proposed distribution expansion planning model is used to meet the forecasted load growth. The expansion plan is expected to be either installing new distribution lines, installing distributed BES units, or a combination of these two.

The obtained results for each case are presented below:

Case 1: In this case, it is found that 6684 kWh of load must be curtailed each year for the distribution network to operate in a secure manner. The curtailed loads are located at buses 18, 25, and 33. This load curtailment costs $133,680/year based on the considered value of lost load. This is however the worst-case scenario when the electric utility chooses not to expand their network. In practice, electric utilities are obligated to meet certain reliability standards. The distribution network reliability is measured using reliability indices such as customer average interruption duration index (CAIDI) and system average interruption duration index (SAIDI) among others [104], significantly limiting permitted load curtailments.

Case 2: In this case, the traditional distribution network expansion planning model is employed to find the expansion plan. It is assumed that the distribution network substation has the adequate capacity and is not required to be replaced or upgraded. In this case, the only available expansion option is to build new distribution lines to meet the forecasted growth in the load demand. In this case the load curtailment is reduced to 814.19 kWh/year when four new distribution lines, namely candidate lines 1, 12, 14, and 17, are installed. The curtailed load demand is located at buses number 18 and 25. The load demand located at bus 33 does not experience any load interruption in this case compared to Case 1. The total distribution network expansion cost is $88726.628/year.

Case 3: This case represents the optimal distribution network expansion plan based on the proposed model. Here, a combination of building new distribution lines and installing distributed BES units is considered. The optimal plan will be the one that yields the minimum total expansion cost. The solution of this problem is to install three distributed BES units at buses 18, 25, and 33, which are buses that initially experienced load curtailment. It can be noticed that the optimal distributed BES units size is small compared to the network total load. This is due to the fact that the installed distributed BES units are needed only to shave the peak demand which results in significant savings for the electric utility company in terms of reduced load curtailment and also deferred/prevented distribution line installation. Installing the distributed BES units reduces the load curtailment to 0, which means the expanded distribution network should be able to meet the forecasted load growth. The optimal distributed BES units' sizes are given in Table 5.11. A summary of the results for the studied cases is provided in Table 5.12.

Table 5.11 Installed distributed BES optimal size and location for case 3

Optimal Power	Optimal Energy Rating Size	Optimal Location
35.05	140.19	18
15.88	29.54	25
18.23	23.46	33

Table 5.12 Obtained results for the considered cases

Case	1	2	3
No. of Installed Lines	-	4	-
Installed Lines	-	1,12,14,17	

No. of Installed BES	-	-	3
Total Power Loss (MW)	2285.515	2305.022	2288.232
Load Curtailment (KWh/year)	6684	814.19	0
Interruption Cost ($/year)	133680	16283.87	0
Investment Cost ($/year)	-	72442.75	9663.04
Total Cost ($/year)	133680	88726.628	9663.04

To investigate the impact of the installed distributed BES units on the distribution network voltage profile, the voltage magnitude at each bus is calculated for the three studied cases. Figure 5.3 shows the voltage magnitude at each bus in the system at a specific time interval. As expected, the buses that experience load curtailment are the weakest in the system in terms of voltage magnitude. However, building new lines or installing distributed BES units equally enhance the voltage profile at those buses as can be seen from the figure. It is expected that with more stringent requirement in voltage deviation limit (i.e., equation 96), voltage profile will be enhanced even more with the optimal distributed BES units. This of course will be associated with larger distributed BES units size.

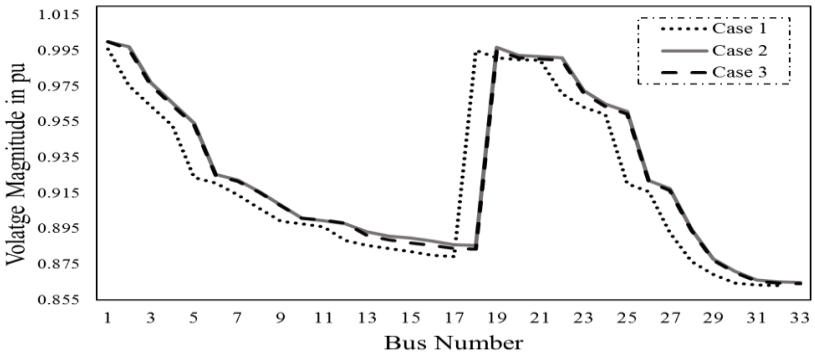

Figure 5.3 Voltage profile for the IEEE 33-bus system at a specific time interval

5.3 Optimal Planning of BES for Solar PV Ramp Rate Control

5.3.1 Introduction

The penetration of solar photovoltaic (PV) units in power system has shown an increase in the past few years and is expected to continue growing in the near future. This is due to several factors such as the drop in solar PV technology cost, the advancements in power electronics and control methodologies, and the implementation of new regulations that allow solar PV owners to make profit when connected to the grid. If not properly controlled and managed, high solar PV penetration may introduce some challenges to the power system operation. One of the main challenges is caused by the fact that the primary source of solar PV is the solar irradiance which changes over the time causing the solar PV power to fluctuate. The variation in the solar PV ramp rate can be categorized into small ramp rates and large ramp rates due to weather changes and cloud passage. Both types of PV ramp rates must be addressed and controlled to ensure a reliable grid operation [105], [106].

Various methods have been discussed to solve the solar PV power variation issue and to control the ramp rate of the power injected to the grid. These methods include

voltage regulating control [107], active power reserve [108], geographical dispersion [109], and energy storage integration [110]. However, it is shown that energy storage integration is the most attractive option as the installed storage can be used for other applications, such as energy arbitrage and regulation services, which increase the economic value of energy storage. Among the various available energy storage technologies, battery energy storage (BES) stands out to be the most mature technology that can be used for solar PV ramp rate control.

The main challenge that faces BES installation is the associated high investment cost. The BES investment cost is greatly related to the selected technology and size. Sizing BES for solar PV ramp rate control is addressed in literature and different methods are proposed to find the optimal size of the installed BES. The work in [111] derives an analytical method to determine the required BES maximum power and minimum capacity for controlling PV ramp rate. A statistical approach is adopted in [112] to determine the BES size required to smooth the solar PV output power. The work in [113] uses a moving average technique to investigate BES sizing for commercial solar PV system. In [114], the BES size is found based on an economic dispatch solution. Although extensive, the reviewed literature only considers the installation of one BES to control solar PV ramp rate and further ignores the variation between the BES technologies characteristics which results in a higher total investment cost.

The solar PV ramp rate changes according to weather conditions. In the worst case, solar PV ramp rate may reach up to 100% of its rated capacity. If one BES is used to control the solar PV ramp rate, it will need to have both high lifecycle and high capacity. A BES

with such characteristics is expensive and might not be economically viable to be purchased and installed. However, analyzing PV ramp rate variations reveals that large ramp rates rarely occur unlike small ramp rates. Thus, in this model, the small and large solar PV ramp rate controls are decoupled and two different BES technologies are used to perform the PV ramp rate control. The BES technology with higher cost and lifecycle, such as a Li-ion battery, will be used to control small solar PV ramp rates while the BES with lower cost and lifecycle, such as a lead acid battery, will be used to control large solar PV ramp rates. A coordinated BES sizing method is proposed to determine the optimal size for both BES units in order to minimize the overall investment cost while satisfying the grid ramp rate control requirements.

5.3.2 Problem Formulation

Figure 5.4 shows the structure of the PV-BES system studied in this paper. This system is connected to the grid via DC/AC inverter. For the sake of simplicity, the power electronic converters are not shown in the figure. The solar PV power signal fluctuates with time due to the variation in solar irradiance. If the PV power is fed to the grid as it is, it may negatively impact grid voltage values and cause considerable load-generation mismatch. Therefore, BES units are integrated to the solar PV to control the ramp rate and to ensure a mitigated solar PV output. BES 1 is installed to handle the large solar PV ramp rate while BES 2 is used to mitigate the small solar PV ramp rate. It must be noted that BES 2 is expected to perform high number of charging/discharging cycles while BES 1 is expected to perform long charging/discharging periods. The produced PV power signal must comply with the grid ramp rate requirements as shown in Figure 5.4.

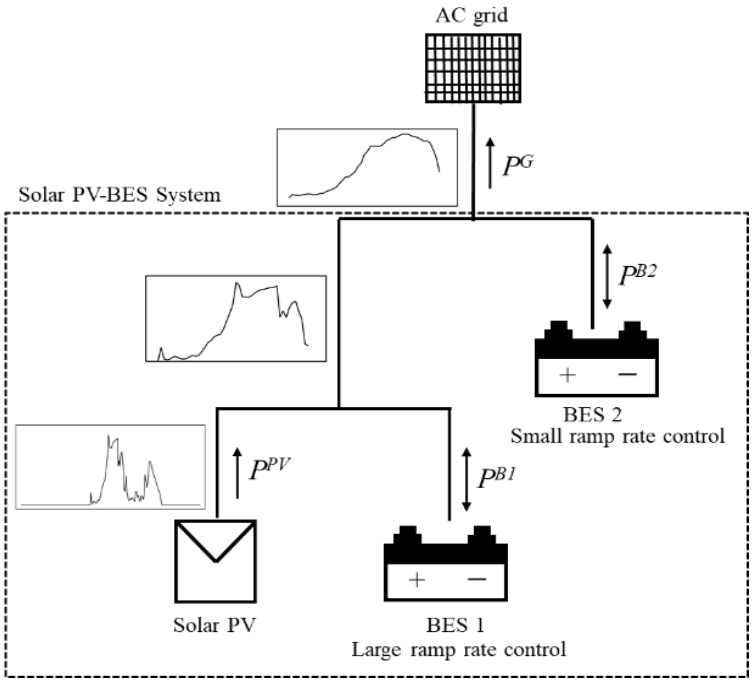

Figure 5.4 Studied PV-BES system structure for ramp rate control application

The objective of the BES optimal planning problem is to minimize the overall investment cost associated with installing the BES units while satisfying the grid ramp rate requirement. The BES investment cost can be divided into two parts: power rating cost in \$/kW and energy rating cost in \$/kWh. The objective function is defined by (5.39).

$$\min \sum_{s \in S} \left(CC_s^P \; P_s^R + CC_s^E \; E_s^R \right) \tag{5.39}$$

The power transferred to the grid (P^G) is the summation of the solar PV power (P^{PV}) and the installed BES power (P^B) as given by (5.40). Indices *d* and *t* represent days and considered time periods within each day, respectively. That is, if each hour is divided into an identical set of minutes (*n*), then the considered time periods for each day (*t*) is equal to 24×(60/*n*). In this work, a 5 minutes solar PV data is used (i.e., *n*=5). Since the BES planning problem is solved for one year, a total number of 105,120 time periods will be

considered. The change in the power transferred to the grid in all of the considered time periods should follow a permissible ramp rate limit imposed by the grid operator (5.41).

$$P_{dt}^{\mathrm{G}} = P_{dt}^{PV} + \sum_{s \in S} P_{sdt}^{B} \qquad \forall d, \forall t \tag{5.40}$$

$$\left| P_{dt}^{\mathrm{G}} - P_{d(t-1)}^{\mathrm{G}} \right| \le \Delta \qquad \forall d, \forall t \tag{5.41}$$

The installed BES units are governed by a set of constraints that model their operation as follow:

$$P_{sdt}^{\mathrm{B}} = P_{sdt}^{dch} + P_{sdt}^{ch} \qquad \forall s \in S, \forall d, \forall t \tag{5.42}$$

$$0 \le P_{sdt}^{\mathrm{dch}} \le P_{s}^{R} u_{sdt} \qquad \forall s \in S, \forall d, \forall t \tag{5.43}$$

$$-P_{s}^{R}(1-u_{sdt}) \le P_{sdt}^{\mathrm{ch}} \le 0 \qquad \forall s \in \mathrm{S}, \forall d, \forall t \tag{5.44}$$

$$u_{sdt} - u_{sd(t-1)} \le \xi_{sdt} \le \frac{(u_{sdt} - u_{sd(t-1)}) + 1}{2} \qquad \forall s \in S, \forall d, \forall t \tag{5.45}$$

$$E_{sdt}^{B} = E_{sd(t-1)}^{\mathrm{B}} - \frac{P_{sdt}^{\mathrm{dch}} \tau}{\eta_{s}} - P_{sdt}^{\mathrm{ch}} \tau \qquad \forall s \in \mathrm{S}, \forall d, \forall t \tag{5.46}$$

$$(1-D_{s})\, E_{s}^{R} \le E_{sdt}^{R} \le E_{s}^{R} \qquad \forall i \in \mathrm{S}, \forall d, \forall t \tag{5.47}$$

The BES power (P^{B}) given in (5.40) is the summation of the BES charging power and discharging power at each time period (5.42). The charging and discharging power of the installed BES are modeled using (5.43)-(5.44). The binary variable u indicates the BES operation state, that is the BES is discharging when u=1 and either charging or in idle state when u=0, thus it is ensured that the BES does not charge and discharge at the same time period. This binary variable is used in (5.45) to indicate the BES cycle completion, i.e., BES charging/discharging cycle is completed when the value of ξ is 1. The stored energy

within the BES at each time period is defined as the stored energy at the previous time period minus the BES charging/discharging power (5.46). The value of τ in (5.46) depends on the considered time periods. It must be noted how the BES charging/discharging power are defined in (5.43) and (5.44), which will result in a negative value for BES charging power and positive value for the BES discharging power. Keeping this in mind the stored energy within the BES will increase if the BES is charging and decrease if the BES is discharging. In general, the stored energy within the BES is limited by the maximum and minmum values, normally provided by the BES manufacturer, to protect the BES from excessive charging and discharging conditions. These limits are different from one BES technology to another. In this work, it is assumed that the BES can be charged up to its rated capacity and can be discharged up to an allowable depth of discharge value (D) decided based on the considered BES technology (5.47).

5.3.3 Case Study

Solar PV and BES Technologies Data

The proposed model is tested on a 1 MW solar PV unit. The solar PV power data are retrieved from [115] with a 5-minute time resolution. Figure 5.5 shows the PV power profile for one month while Figure 5.6 shows the associated ramp rate values. As can be seen that the solar PV power profile is different from one day to another. Most of the presented days, however, show a typical solar PV power profile that is associated with small ramp rate variation. For these days, a small BES is sufficient to control the variations and maintain the power sent to the grid within the required ramp rate limit. Due to weather changes, the PV profile at certain days exhibit a rapid change which results in high ramp

rate variations. In this case, a large BES is needed to either absorb or produce the difference between the PV output power and the power that should be sent to the grid in order to satisfy the grid operator ramp rate limit.

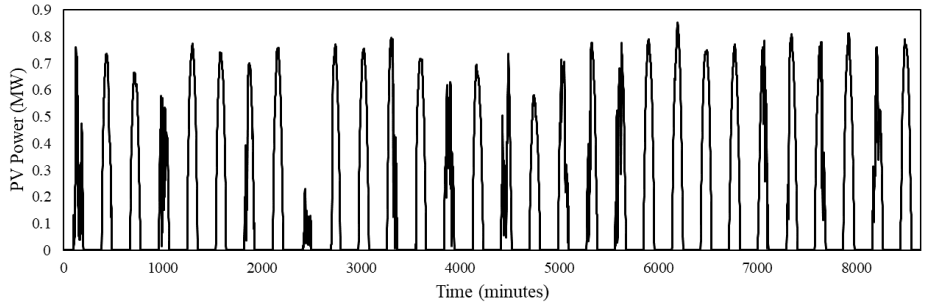

Figure 5.5 Solar PV power for one month period

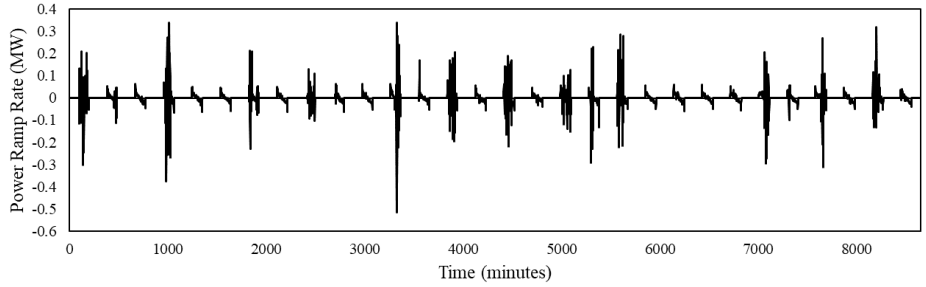

Figure 5.6 Solar PV ramp rate for one month period

In this work, two BES technologies with different characteristic and capital costs, as shown in Table 5.13, are utilized to control the solar PV ramp rate. An 8% interest rate and a 10-year lifetime is assumed to calculate the annualized capital costs.

Table 5.13 BES technologies characteristics

BES Technology	Power Rating Cost ($/kW)	Energy Rating Cost ($/kWh)	Depth of Discharge (%)	Round Trip Efficiency (%)
Lead acid	600	400	70	75
Li-ion	1300	800	90	95

Results and Discussion

The ramp rate limit is assumed to be 0.05 MW (i.e., 5% of PV rated power). The optimal size for the installed BES units along with the corresponding annualized investment cost are calculated as in Table 5.14. The overall investment cost is found to be $36,475/year. Figure 5.7 shows PV power, output power after using lead acid battery for large ramp rate control, and the output power after using Li-ion battery for small ramp rate control. Besides the difference in the installed size, it is noticed that the lead acid battery performs around 66% less cycles than the Li-ion battery (2136 cycles/year for lead acid and 6312 cycles/year for Li-ion). Table 5.15 shows how many times in a year the ramp rates value has exceeded a given percentage of the solar PV rated power ramp rate values. It can be seen that large ramp rates (i.e., >15%) are mitigated using lead acid battery. After mitigating large ramp rates, the Li-ion battery is used to control the small ramp rates (i.e., <10%) to satisfy the grid ramp rate limit.

Table 5.14 Numerical Simulation Results

BES Technology	Optimal Power Rating (KW)	Optimal Energy Rating (KWh)	Investment Cost ($/year)
Lead acid	205	96	24,048.6
Li-ion	58	10	12,426.6

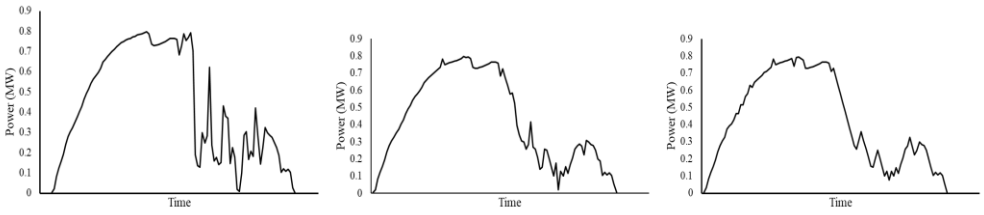

(a) (b) (c)

Figure 5.7 (a) PV power, (b) output power after using lead acid battery for large variation control, (c) output power after using Li-ion for small variation control (i.e., power transferred to the grid)

Table 5.15 Ramp Rate Analysis

Ramp Rate Percentage	No. of violations		
	in original Solar PV	after using BES 1	after using BES 2
5	2040	1104	0
10	828	12	0
15	444	0	0
20	228	0	0

Chapter 6. Conclusion and Future Research

BES is perceived to be a vital component in ensuring a cost-effective and reliable microgrid operation during both the grid-connected and the islanded operation modes. However, to add a BES to an existing microgrid requires the consideration of some decisive and critical factors, such as the BES size, integration configuration, technology, and depth of discharge. This dissertation explained the impact of these BES planning parameters on the BES operation and further developed a comprehensive expansion models to optimally determine their values for various BES technologies and microgrid types.

The developed BES planning models aimed at minimizing the microgrid total expansion planning cost, i.e., the summation of the microgrid operation cost, the cost of unserved energy, and the storage investment cost. Numerical simulations performed on test microgrids validated the effectiveness of the proposed microgrid-integrated BES planning models. The obtained results showed that the developed models were able to determine the optimal BES size, integration configuration, technologies, and depth of discharge that minimizes the total microgrid expansion planning cost.

Besides microgrid application, this research investigated the utilization of BES in reducing I&C customers electricity bill, expanding distribution network, and accommodating solar PV ramp rate. Three planning models of BES used for each of the aforementioned applications are proposed to ensure economic and reliable BES

installation. The ability of the proposed models to find optimal planning parameters of the installed BES while taking into consideration the impact of BES operation on its lifetime were validated through numerical simulations.

Although the developed BES planning models in this dissertation cover a wide range of BES applications in distribution network, more investigations are required on using the BES for multiple stacked applications [116]. This will increase the BES economic value and therefore increase its deployment in the power system. Such research requires the development of comprehensive models that can accurately quantify each application that can be performed by the BES and accordingly select the optimal applications that maximize the benefits of installing the BES from either the grid prospective or the owner prospective. However, a modification in the existing regulations and market arrangements, especially those that prevent the utilization of BES in some of power applications, needs to be done to realize the full capabilities provided by BES.

References

[1] Department of Energy Office of Electricity Delivery and Energy Reliability. (2012). Summary Report: 2012 DOE Microgrid Workshop [Online]. Available: http://energy.gov/sites/prod/files/2012%20Microgrid%20Workshop%20Report%20 09102012.pdf. [Accessed: Nov-1-2015].

[2] C. Gouveia, J. Moreira, C. L. Moreira, and J. A. P. Lopes, "Coordinating Storage and Demand Response for Microgrid Emergency Operation," *IEEE Trans. Smart Grid*, vol. 4, no. 4, pp. 1898–1908, Dec. 2013.

[3] W. A. Omran, M. Kazerani, and M. M. A. Salama, "Investigation of Methods for Reduction of Power Fluctuations Generated From Large Grid-Connected Photovoltaic Systems," *IEEE Trans. Energy Convers.*, vol. 26, no. 1, pp. 318–327, Mar. 2011.

[4] A. Khodaei, "Provisional Microgrids," *IEEE Trans. Smart Grid*, vol. 6, no. 3, pp. 1107–1115, May 2015.

[5] A. Khodaei, "Provisional Microgrid Planning," *IEEE Trans. Smart Grid*, vol. 8, no. 3, pp. 1096–1104, May 2017.

[6] S. Gill, E. Barbour, I. A. G. Wilson, and D. Infield, "Maximising revenue for non-firm distributed wind generation with energy storage in an active management scheme," *IET Renew. Power Gener.*, vol. 7, no. 5, pp. 421–430, Sep. 2013.

[7] S. Parhizi, H. Lotfi, A. Khodaei, and S. Bahramirad, "State of the Art in Research on Microgrids: A Review," *IEEE Access*, vol. 3, pp. 890–925, 2015.

[8] J. Eyer and G. Corey, "Energy storage for the electricity grid: Benefits and market potential assessment guide," *Sandia Natl. Lab.*, vol. 20, no. 10, p. 5, 2010.

[9] Q. Fu, A. Hamidi, A. Nasiri, V. Bhavaraju, S. B. Krstic, and P. Theisen, "The Role of Energy Storage in a Microgrid Concept: Examining the opportunities and promise of microgrids.," *IEEE Electrification Mag.*, vol. 1, no. 2, pp. 21–29, Dec. 2013.

[10] I. Alsaidan, A. Alanazi, W. Gao, H. Wu, and A. Khodaei, "State-Of-The-Art in Microgrid-Integrated Distributed Energy Storage Sizing," *Energies*, vol. 10, no. 9, p. 1421, Sep. 2017.

[11] S. Bahramirad and H. Daneshi, "Optimal sizing of smart grid storage management system in a microgrid," in *2012 IEEE PES Innovative Smart Grid Technologies (ISGT)*, 2012, pp. 1–7.

[12] S. Bahramirad, W. Reder, and A. Khodaei, "Reliability-Constrained Optimal Sizing of Energy Storage System in a Microgrid," *IEEE Trans. Smart Grid*, vol. 3, no. 4, pp. 2056–2062, Dec. 2012.

[13] E. Hajipour, M. Bozorg, and M. Fotuhi-Firuzabad, "Stochastic Capacity Expansion Planning of Remote Microgrids With Wind Farms and Energy Storage," *IEEE Trans. Sustain. Energy*, vol. 6, no. 2, pp. 491–498, Apr. 2015.

[14] H. Alharbi and K. Bhattacharya, "Optimal Sizing of Battery Energy Storage Systems for Microgrids," in *2014 IEEE Electrical Power and Energy Conference (EPEC)*, 2014, pp. 275–280.

[15] J. P. Fossati, A. Galarza, A. Martín-Villate, and L. Fontán, "A method for optimal sizing energy storage systems for microgrids," *Renew. Energy*, vol. 77, pp. 539–549, May 2015.
[16] G. Carpinelli, G. Celli, S. Mocci, F. Mottola, F. Pilo, and D. Proto, "Optimal Integration of Distributed Energy Storage Devices in Smart Grids," *IEEE Trans. Smart Grid*, vol. 4, no. 2, pp. 985–995, Jun. 2013.
[17] N. Zhou, N. Liu, J. Zhang, and J. Lei, "Multi-Objective Optimal Sizing for Battery Storage of PV-Based Microgrid with Demand Response," *Energies*, vol. 9, no. 8, p. 591, Jul. 2016.
[18] B. Jiao, C. Wang, and L. Guo, "Scenario Generation for Energy Storage System Design in Stand-alone Microgrids," *Energy Procedia*, vol. 61, pp. 824–828, 2014.
[19] H. Khorramdel, J. Aghaei, B. Khorramdel, and P. Siano, "Optimal Battery Sizing in Microgrids Using Probabilistic Unit Commitment," *IEEE Trans. Ind. Inform.*, vol. 12, no. 2, pp. 834–843, Apr. 2016.
[20] H. Xiao, W. Pei, Y. Yang, and L. Kong, "Sizing of battery energy storage for micro-grid considering optimal operation management," in *2014 International Conference on Power System Technology (POWERCON)*, 2014, pp. 3162–3169.
[21] T. Kerdphol, Y. Qudaih, and Y. Mitani, "Optimum battery energy storage system using PSO considering dynamic demand response for microgrids," *Int. J. Electr. Power Energy Syst.*, vol. 83, pp. 58–66, Dec. 2016.
[22] T. Kerdphol, Y. Qudaih, and Y. Mitani, "Battery energy storage system size optimization in microgrid using particle swarm optimization," in *IEEE PES Innovative Smart Grid Technologies, Europe*, 2014, pp. 1–6.
[23] X. Xie, H. Wang, S. Tian, and Y. Liu, "Optimal capacity configuration of hybrid energy storage for an isolated microgrid based on QPSO algorithm," in *2015 5th International Conference on Electric Utility Deregulation and Restructuring and Power Technologies (DRPT)*, 2015, pp. 2094–2099.
[24] B. Bahmani-Firouzi and R. Azizipanah-Abarghooee, "Optimal sizing of battery energy storage for micro-grid operation management using a new improved bat algorithm," *Int. J. Electr. Power Energy Syst.*, vol. 56, pp. 42–54, Mar. 2014.
[25] S. Sharma, S. Bhattacharjee, and A. Bhattacharya, "Grey wolf optimisation for optimal sizing of battery energy storage device to minimise operation cost of microgrid," *Transm. Distrib. IET Gener.*, vol. 10, no. 3, pp. 625–637, 2016.
[26] S. Mohammadi and A. Mohammadi, "Stochastic scenario-based model and investigating size of battery energy storage and thermal energy storage for micro-grid," *Int. J. Electr. Power Energy Syst.*, vol. 61, pp. 531–546, Oct. 2014.
[27] T. A. Nguyen, M. L. Crow, and A. C. Elmore, "Optimal Sizing of a Vanadium Redox Battery System for Microgrid Systems," *IEEE Trans. Sustain. Energy*, vol. 6, no. 3, pp. 729–737, Jul. 2015.
[28] M. Ross, R. Hidalgo, C. Abbey, and G. Joós, "Analysis of Energy Storage sizing and technologies," in *2010 IEEE Electric Power and Energy Conference (EPEC)*, 2010, pp. 1–6.

[29] S. X. Chen and H. B. Gooi, "Sizing of energy storage system for microgrids," in *2010 IEEE 11th International Conference on Probabilistic Methods Applied to Power Systems (PMAPS)*, 2010, pp. 6–11.
[30] S. X. Chen, H. B. Gooi, and M. Q. Wang, "Sizing of Energy Storage for Microgrids," *IEEE Trans. Smart Grid*, vol. 3, no. 1, pp. 142–151, Mar. 2012.
[31] J. Dong, F. Gao, X. Guan, Q. Zhai, and J. Wu, "Storage-Reserve Sizing With Qualified Reliability for Connected High Renewable Penetration Micro-Grid," *IEEE Trans. Sustain. Energy*, vol. 7, no. 2, pp. 732–743, Apr. 2016.
[32] H. J. Khasawneh, A. Mondal, M. S. Illindala, B. L. Schenkman, and D. R. Borneo, "Evaluation and sizing of energy storage systems for microgrids," in *2015 IEEE/IAS 51st Industrial Commercial Power Systems Technical Conference (I CPS)*, 2015, pp. 1–8.
[33] S. Koohi-Kamali, N. A. Rahim, and H. Mokhlis, "New algorithms to size and protect battery energy storage plant in smart microgrid considering intermittency in load and generation," in *3rd IET International Conference on Clean Energy and Technology (CEAT) 2014*, 2014, pp. 1–7.
[34] K. Keskamol and N. Hoonchareon, "Sizing of battery energy storage system for sustainable energy in a remote area," in *Smart Grid Technologies - Asia (ISGT ASIA), 2015 IEEE Innovative*, 2015, pp. 1–4.
[35] A. Beiranvand, M. M. Aghdam, L. Li, S. Zhu, and J. Zheng, "Finding the optimal place and size of an energy storage system for the daily operation of microgrids considering both operation modes simultaneously," in *2016 IEEE International Conference on Power System Technology (POWERCON)*, 2016, pp. 1–6.
[36] C. Sun and Y. Yuan, "Sizing of hybrid energy storage system in independent microgrid based on BP neural network," in *Renewable Power Generation Conference (RPG 2013), 2nd IET*, 2013, pp. 1–4.
[37] T. Kerdphol, R. N. Tripathi, T. Hanamoto, Khairudin, Y. Qudaih, and Y. Mitani, "ANN based optimized battery energy storage system size and loss analysis for distributed energy storage location in PV-microgrid," in *Smart Grid Technologies - Asia (ISGT ASIA), 2015 IEEE Innovative*, 2015, pp. 1–6.
[38] K. Hongesombut, T. Piroon, and Y. Weerakamaeng, "Evaluation of battery energy storage system for frequency control in microgrid system," in *2013 10th International Conference on Electrical Engineering/Electronics, Computer, Telecommunications and Information Technology (ECTI-CON)*, 2013, pp. 1–4.
[39] M. R. Aghamohammadi and H. Abdolahinia, "A new approach for optimal sizing of battery energy storage system for primary frequency control of islanded Microgrid," *Int. J. Electr. Power Energy Syst.*, vol. 54, pp. 325–333, Jan. 2014.
[40] A. Toliyat and A. Kwasinski, "Energy storage sizing for effective primary and secondary control of low-inertia microgrids," in *2015 IEEE 6th International Symposium on Power Electronics for Distributed Generation Systems (PEDG)*, 2015, pp. 1–7.
[41] H. Jia, Y. Mu, and Y. Qi, "A statistical model to determine the capacity of battery–supercapacitor hybrid energy storage system in autonomous microgrid," *Int. J. Electr. Power Energy Syst.*, vol. 54, pp. 516–524, Jan. 2014.

[42] G. Muñoz-Delgado, J. Contreras, and J. M. Arroyo, "Joint Expansion Planning of Distributed Generation and Distribution Networks," *IEEE Trans. Power Syst.*, vol. 30, no. 5, pp. 2579–2590, Sep. 2015.
[43] S. de la Torre, A. J. Conejo, and J. Contreras, "Transmission Expansion Planning in Electricity Markets," *IEEE Trans. Power Syst.*, vol. 23, no. 1, pp. 238–248, Feb. 2008.
[44] A. Khodaei, M. Shahidehpour, and S. Kamalinia, "Transmission Switching in Expansion Planning," *IEEE Trans. Power Syst.*, vol. 25, no. 3, pp. 1722–1733, Aug. 2010.
[45] J. C. Smith and Z. C. Taskin, "A tutorial guide to mixed-integer programming models and solution techniques," *Optim. Med. Biol.*, pp. 521–548, 2008.
[46] A. J. Conejo, Ed., *Decomposition techniques in mathematical programming: engineering and science applications*. Berlin ; New York: Springer, 2006.
[47] A. Khodaei and M. Shahidehpour, "Microgrid-Based Co-Optimization of Generation and Transmission Planning in Power Systems," *IEEE Trans. Power Syst.*, vol. 28, no. 2, pp. 1582–1590, May 2013.
[48] LONDON ECONOMICS, 2013. "Estimating the Value of Lost Load". Briefing paper prepared for the Electricity Reliability Council of Texas, Inc. by London Economics International LLC. June 17th 2013.
[49] L. Xu, X. Ruan, C. Mao, B. Zhang, and Y. Luo, "An Improved Optimal Sizing Method for Wind-Solar-Battery Hybrid Power System," *IEEE Trans. Sustain. Energy*, vol. 4, no. 3, pp. 774–785, Jul. 2013.
[50] J. Cui, K. Li, Y. Sun, Z. Zou, and Y. Ma, "Distributed energy storage system in wind power generation," in *2011 4th International Conference on Electric Utility Deregulation and Restructuring and Power Technologies (DRPT)*, 2011, pp. 1535–1540.
[51] W. Li and G. Joos, "Performance Comparison of Aggregated and Distributed Energy Storage Systems in a Wind Farm For Wind Power Fluctuation Suppression," in *2007 IEEE Power Engineering Society General Meeting*, 2007, pp. 1–6.
[52] I. Alsaidan, A. Khodaei, and W. Gao, "Distributed energy storage sizing for microgrid applications," in *2016 IEEE/PES Transmission and Distribution Conference and Exposition (T D)*, 2016, pp. 1–5.
[53] M. Gitizadeh and H. Fakharzadegan, "Battery capacity determination with respect to optimized energy dispatch schedule in grid-connected photovoltaic (PV) systems," *Energy*, vol. 65, pp. 665–674, Feb. 2014.
[54] "Microgrid at Illinois Institute of Technology." [Online]. Available: http://iitmicrogrid.net/microgrid.aspx. [Accessed: 21-Mar-2017].
[55] N. Saito, T. Niimura, K. Koyanagi, and R. Yokoyama, "Trade-off analysis of autonomous microgrid sizing with PV, diesel, and battery storage," in *Power & Energy Society General Meeting, 2009. PES'09. IEEE*, 2009, pp. 1–6.
[56] G. Merei, C. Berger, and D. U. Sauer, "Optimization of an off-grid hybrid PV–Wind–Diesel system with different battery technologies using genetic algorithm," *Sol. Energy*, vol. 97, pp. 460–473, Nov. 2013.

[57] X. Zhang, S.-C. Tan, G. Li, J. Li, and Z. Feng, “Components sizing of hybrid energy systems via the optimization of power dispatch simulations,” *Energy*, vol. 52, pp. 165–172, Apr. 2013.
[58] H. Chen, T. N. Cong, W. Yang, C. Tan, Y. Li, and Y. Ding, “Progress in electrical energy storage system: A critical review,” *Prog. Nat. Sci.*, vol. 19, no. 3, pp. 291–312, Mar. 2009.
[59] K. C. Divya and J. Østergaard, “Battery energy storage technology for power systems—An overview,” *Electr. Power Syst. Res.*, vol. 79, no. 4, pp. 511–520, Apr. 2009.
[60] I. Alsaidan, A. Khodaei, and W. Gao, “Determination of battery energy storage technology and size for standalone microgrids,” in *2016 IEEE Power and Energy Society General Meeting (PESGM)*, 2016, pp. 1–5.
[61] M. Koller, T. Borsche, A. Ulbig, and G. Andersson, “Defining a degradation cost function for optimal control of a battery energy storage system,” in *PowerTech (POWERTECH), 2013 IEEE Grenoble*, 2013, pp. 1–6.
[62] C. Ju and P. Wang, “Energy management system for microgrids including batteries with degradation costs,” in *Power System Technology (POWERCON), 2016 IEEE International Conference on*, 2016, pp. 1–6.
[63] Y. Zhang and M.-Y. Chow, “Microgrid cooperative distributed energy scheduling (CoDES) considering battery degradation cost,” in *Industrial Electronics (ISIE), 2016 IEEE 25th International Symposium on*, 2016, pp. 720–725.
[64] K. Abdulla, J. De Hoog, V. Muenzel, F. Suits, K. Steer, A. Wirth, and S. Halgamuge, “Optimal operation of energy storage systems considering forecasts and battery degradation,” *IEEE Trans. Smart Grids*, in press. [Online]. Available http://ieeexplore.ieee.org/stamp/stamp.jsp?tp=&arnumber=7562406&isnumber=5446437.
[65] E. Hajipour, M. Bozorg, and M. Fotuhi-Firuzabad, “Stochastic Capacity Expansion Planning of Remote Microgrids With Wind Farms and Energy Storage,” *IEEE Trans. Sustain. Energy*, vol. 6, no. 2, pp. 491–498, Apr. 2015.
[66] A. Bocca, A. Sassone, D. Shin, A. Macii, E. Macii, and M. Poncino, “An equation-based battery cycle life model for various battery chemistries,” in *Very Large Scale Integration (VLSI-SoC), 2015 IFIP/IEEE International Conference on*, 2015, pp. 57–62.
[67] L. H. Thaller, “Expected Cycle Life vs. Depth of Discharge Relationships of Well-Behaved Single Cells and Cell Strings,” *J. Electrochem. Soc.*, vol. 130, no. 5, pp. 986–990, 1983.
[68] N. Omar *et al.*, “Lithium iron phosphate based battery – Assessment of the aging parameters and development of cycle life model,” *Appl. Energy*, vol. 113, pp. 1575–1585, Jan. 2014.
[69] I. Alsaidan, A. Khodaei, and W. Gao, “Determination of optimal size and depth of discharge for battery energy storage in standalone microgrids,” in *2016 North American Power Symposium (NAPS)*, 2016, pp. 1–6.

[70] X. Luo, J. Wang, M. Dooner, and J. Clarke, “Overview of current development in electrical energy storage technologies and the application potential in power system operation,” *Appl. Energy*, vol. 137, pp. 511–536, Jan. 2015.
[71] “ODYSSEY battery - Official Manufacturer’s Site.” [Online]. Available: http://www.odysseybattery.com/. [Accessed: 21-Mar-2017].
[72] I. Alsaidan, W. Gao, and A. Khodaei, “Optimal design of battery energy storage in stand-alone brownfield microgrids,” in *2017 North American Power Symposium (NAPS)*, 2017, pp. 1–6.
[73] “C&D Technologies Home.” [Online]. Available: http://www.cdtechno.com/. [Accessed: 21-Mar-2017].
[74] A. Gabash and P. Li, “Active-Reactive Optimal Power Flow in Distribution Networks With Embedded Generation and Battery Storage,” *IEEE Trans. Power Syst.*, vol. 27, no. 4, pp. 2026–2035, Nov. 2012.
[75] A. Gabash and P. Li, “Flexible Optimal Operation of Battery Storage Systems for Energy Supply Networks,” *IEEE Trans. Power Syst.*, vol. 28, no. 3, pp. 2788–2797, Aug. 2013.
[76] A. Gabash and P. Li, “Variable reverse power flow-Part I: AR-OPF with reactive power of wind stations,” in *Environment and Electrical Engineering (EEEIC), 2015 IEEE 15th International Conference on*, 2015, pp. 21–26.
[77] A. Gabash and P. Li, “Variable reverse power flow-part II: Electricity market model and results,” in *Environment and Electrical Engineering (EEEIC), 2015 IEEE 15th International Conference on*, 2015, pp. 27–32.
[78] I. Alsaidan, A. Khodaei, and W. Gao, “A Comprehensive Battery Energy Storage Optimal Sizing Model for Microgrid Applications,” *IEEE Trans. Power Syst.*, in press. [Online]. Available: http://ieeexplore.ieee.org.du.idm.oclc.org/stamp/stamp.jsp?tp=&arnumber=8094981
[79] A. Khodaei, S. Bahramirad, and M. Shahidehpour, “Microgrid Planning Under Uncertainty,” *IEEE Trans. Power Syst.*, vol. 30, no. 5, pp. 2417–2425, Sep. 2015.
[80] A. Thiele, T. Terry, and M. Epelman, “Robust linear optimization with recourse,” *Rapp. Tech.*, pp. 4–37, 2009.
[81] “Alpha Industrial - Industrial Power.” [Online]. Available: http://industrial.alpha.com/index.php/products. [Accessed: 21-Mar-2017].
[82] N. Lu, M. R. Weimar, Y. V. Makarov, and C. Loutan, “An evaluation of the NaS battery storage potential for providing regulation service in California,” in *2011 IEEE/PES Power Systems Conference and Exposition*, 2011, pp. 1–9.
[83] J. Neubauer and M. Simpson, “Deployment of behind-the-meter energy storage for demand charge reduction,” *Natl. Renew. Energy Lab. Tech Rep NRELTP-5400-63162*, 2015.
[84] A. H. Mohsenian-Rad and A. Leon-Garcia, “Optimal Residential Load Control With Price Prediction in Real-Time Electricity Pricing Environments,” *IEEE Trans. Smart Grid*, vol. 1, no. 2, pp. 120–133, Sep. 2010.
[85] “Home | ComEd’s Hourly Pricing Program.” [Online]. Available: https://hourlypricing.comed.com/. [Accessed: 14-Apr-2017].

[86] S. K. Khator and L. C. Leung, “Power distribution planning: A review of models and issues,” *IEEE Trans. Power Syst.*, vol. 12, no. 3, pp. 1151–1159, 1997.
[87] S. S. Tanwar and D. K. Khatod, “A review on distribution network expansion planning,” in *India Conference (INDICON), 2015 Annual IEEE*, 2015, pp. 1–6.
[88] E. G. Carrano, F. G. Guimaraes, R. H. C. Takahashi, O. M. Neto, and F. Campelo, “Electric Distribution Network Expansion Under Load-Evolution Uncertainty Using an Immune System Inspired Algorithm,” *IEEE Trans. Power Syst.*, vol. 22, no. 2, pp. 851–861, May 2007.
[89] T. Asakura, T. Genji, T. Yura, N. Hayashi, and Y. Fukuyama, “Long-term distribution network expansion planning by network reconfiguration and generation of construction plans,” *IEEE Trans. Power Syst.*, vol. 18, no. 3, pp. 1196–1204, Aug. 2003.
[90] N. Jahanyari, A. Amini, N. Taghizadeghan, and S. Najafi Ravadanegh, “Smart distribution grid multistage expansion planning under load forecasting uncertainty,” *IET Gener. Transm. Distrib.*, vol. 10, no. 5, pp. 1136–1144, Apr. 2016.
[91] D. T. C. Wang, L. F. Ochoa, and G. P. Harrison, “Modified GA and Data Envelopment Analysis for Multistage Distribution Network Expansion Planning Under Uncertainty,” *IEEE Trans. Power Syst.*, vol. 26, no. 2, pp. 897–904, May 2011.
[92] R. H. Fletcher and K. Strunz, “Optimal Distribution System Horizon Planning ndash;Part I: Formulation,” *IEEE Trans. Power Syst.*, vol. 22, no. 2, pp. 791–799, May 2007.
[93] R. H. Fletcher and K. Strunz, “Optimal Distribution System Horizon Planning ndash;Part II: Application,” *IEEE Trans. Power Syst.*, vol. 22, no. 2, pp. 862–870, May 2007.
[94] C. MacRae, M. Ozlen, A. Ernst, and S. Behrens, “Locating and sizing energy storage systems for distribution feeder expansion planning,” in *TENCON 2015 - 2015 IEEE Region 10 Conference*, 2015, pp. 1–6.
[95] L. B. Arruda, A. M. Schetinger, B. S. M. C. Borba, D. H. N. Dias, R. S. Maciel, and B. H. Dias, “Maximum PV Penetration Under Voltage Constraints Considering Optimal Sizing of BESS on Brazilian Secondary Distribution Network,” *IEEE Lat. Am. Trans.*, vol. 14, no. 9, pp. 4063–4069, Sep. 2016.
[96] M. Farrokhifar, S. Grillo, and E. Tironi, “Optimal placement of energy storage devices for loss reduction in distribution networks,” in *IEEE PES ISGT Europe 2013*, 2013, pp. 1–5.
[97] H. Nazaripouya, Y. Wang, P. Chu, H. R. Pota, and R. Gadh, “Optimal sizing and placement of battery energy storage in distribution system based on solar size for voltage regulation,” in *2015 IEEE Power Energy Society General Meeting*, 2015, pp. 1–5.
[98] G. Celli, G. G. Soma, F. Pilo, E. Ghiani, R. Cicoria, and S. Corti, “Comparison of planning alternatives for active distribution networks,” in *CIRED 2012 Workshop: Integration of Renewables into the Distribution Grid*, 2012, pp. 1–4.
[99] G. Celli, S. Mocci, F. Pilo, and M. Loddo, “Optimal integration of energy storage in distribution networks,” in *2009 IEEE Bucharest PowerTech*, 2009, pp. 1–7.

[100] G. Celli *et al.*, "A comparison of distribution network planning solutions: Traditional reinforcement versus integration of distributed energy storage," in *PowerTech (POWERTECH), 2013 IEEE Grenoble*, 2013, pp. 1–6.
[101] H. Cheng, P. Zeng, H. Xing, and Y. Zhang, "Active distribution network expansion planning integrating dispersed energy storage systems," *IET Gener. Transm. Distrib.*, vol. 10, no. 3, pp. 638–644, Feb. 2016.
[102] X. Shen, M. Shahidehpour, Y. Han, S. Zhu, and J. Zheng, "Expansion Planning of Active Distribution Networks With Centralized and Distributed Energy Storage Systems," *IEEE Trans. Sustain. Energy*, vol. 8, no. 1, pp. 126–134, Jan. 2017.
[103] State highway administration research report " Cost benefits for overhead/underground utilities: Edwards and Kelcey, Inc/Exeter Associates, Inc." Available: http://www.roads.maryland.gov/OPR_Research/MD-03-SP208B4C-Cost-Benefits-for-Overhead-vs-Underground-Utility-Study_Report.pdf. [Accessed: 2-Jan-2018]
[104] R.-L. Chen, K. Allen, and R. Billinton, "Value-based distribution reliability assessment and planning," *IEEE Trans. Power Deliv.*, vol. 10, no. 1, pp. 421–429, Jan. 1995.
[105] M. Morjaria, D. Anichkov, V. Chadliev, and S. Soni, "A Grid-Friendly Plant: The Role of Utility-Scale Photovoltaic Plants in Grid Stability and Reliability," *IEEE Power Energy Mag.*, vol. 12, no. 3, pp. 87–95, May 2014.
[106] M. Alam, K. Muttaqi, D. Sutanto, "A Novel Approach for Ramp-Rate Control of Solar PV Using Energy Storage to Mitigate Output Fluctuations Caused by Cloud Passing," *IEEE Trans. Energy Convers.*, vol. 29, no. 2, pp. 507–518, Jun. 2014.
[107] M. Chamana, B. H. Chowdhury, and F. Jahanbakhsh, "Distributed Control of Voltage Regulating Devices in the Presence of High PV Penetration to Mitigate Ramp-Rate Issues," *IEEE Trans. Smart Grid*, in press. [Online]. Available: http://ieeexplore.ieee.org.du.idm.oclc.org/stamp/stamp.jsp?tp=&arnumber=7484323
[108] B.-I. Craciun, T. Kerekes, D. Sera, R. Teodorescu, and U. D. Annakkage, "Power Ramp Limitation Capabilities of Large PV Power Plants With Active Power Reserves," *IEEE Trans. Sustain. Energy*, vol. 8, no. 2, pp. 573–581, Apr. 2017.
[109] J. Marcos, L. Marroyo, E. Lorenzo, and M. García, "Smoothing of PV power fluctuations by geographical dispersion: Smoothing of PV power fluctuations," *Prog. Photovolt. Res. Appl.*, vol. 20, no. 2, pp. 226–237, Mar. 2012.
[110] I. de la Parra, J. Marcos, M. García, and L. Marroyo, "Dynamic ramp-rate control to smooth short-term power fluctuations in large photovoltaic plants using battery storage systems," in *Industrial Electronics Society, IECON 2016-42nd Annual Conference of the IEEE*, 2016, pp. 3052–3057.
[111] J. Marcos, O. Storkël, L. Marroyo, M. Garcia, and E. Lorenzo, "Storage requirements for PV power ramp-rate control," *Sol. Energy*, vol. 99, pp. 28–35, Jan. 2014.
[112] C. Gavriluta, I. Candela, J. Rocabert, I. Etxeberria-Otadui, and P. Rodriguez, "Storage system requirements for grid supporting PV-power plants," in *Energy Conversion Congress and Exposition (ECCE), 2014 IEEE*, 2014, pp. 5323–5330.
[113] Y. Moumouni, Y. Baghzouz, and R. F. Boehm, "Power 'smoothing' of a commercial-size photovoltaic system by an energy storage system," in *Harmonics*

and Quality of Power (ICHQP), 2014 IEEE 16th International Conference on, 2014, pp. 640–644.
[114] Q. Zhao, K. Wu, and A. M. Khambadkone, "Optimal sizing of energy storage for PV power ramp rate regulation," in *Energy Conversion Congress and Exposition (ECCE), 2016 IEEE*, 2016, pp. 1–6.
[115] "Solar Power Data for Integration Studies | Grid Modernization | NREL." [Online]. Available: https://www.nrel.gov/grid/solar-power-data.html. [Accessed: 05-Aug-2017].
[116] G.Strbac, M. Aunedi, L. Konstantelos, R. Moreira, F. Teng, R. Moreno, D. Pudjianto, A. Laguna, and P. Papadopoulos, "Opportunities for Energy Storage", IEEE Power & Energy Magazine, September/October 2017
[117] A. Brooke, D. Kendrick, A. Meeraus, R. Raman, and R. E. Rosenthal, "Gams," Users Guide GAMS Dev. Corp., 2005.

Appendix A

Linearization of bilinear terms: if variable y is equal to the multiplication of continuous variable β and k binary variables $\delta_1, \delta_2, \delta_3, \ldots, \delta_k$ such as illustrated in (A1), it can be described by 2(k+1) constraints as shown in (A2)-(A3). M is a large positive constant.

$$y = \beta\,\delta_1\delta_2\delta_3\ldots\delta_k \tag{A1}$$

$$\beta - \sum_{j=1}^{k} M\left(1-\delta_j\right) \le y \le \beta + \sum_{j=1}^{k} M\left(1-\delta_j\right) \tag{A2}$$

$$-M\delta_j \le y \le M\delta_j \qquad \forall j \in (1,2,3,\ldots,k) \tag{A3}$$

If at least one binary variable is zero, according to (A3), y would be zero, and (A2) would be relaxed. If all binary variables are one, all k constraints in (A3) would be relaxed, and according to (A2), y would be equal to β. Therefore, the equation is linearized, and the results of the constraints defined in (A2)-(A3) conform to the original equation in (A1).

Appendix B

A commonly used approach to solve MIP problems, such as the one presented in this paper, is the branch and bound approach. Before explaining how this approach works, a concept of MIP relaxation must be introduced. A relaxed MIP problem can be defined based on the following two characteristics:

1) Any solution to the original MIP problem is also a feasible solution to the relaxed problem.

2) The objective function value associated with the original MIP solution is larger than or equal to the objective function value associated with the relaxed problem solution.

A typical relaxed MIP problem is its corresponding LP problem, which can be found by removing any integrality constraints in the original MIP problem. To this end, solving the corresponding LP problem will yield one of three possible cases: infeasible solution, feasible solution that satisfies the original MIP integrality constraints, or feasible solution that does not satisfy the original MIP problem integrality constraints. If there is no solution to the LP problem, then the problem is said to be infeasible and some of the constraints must be relaxed or the problem should be reformulated. In case of a feasible solution, if the obtained LP solution happens to satisfy the original MIP integrality constraints, then the LP solution is the optimal solution for the original MIP problem. However, such optimistic case does not happen often and the LP solution normally tends not to comply with the MIP integrality constraints. In this case, the LP problem is divided into two sub-problems. This process is known as branching as the LP problem is branched into sub-problems. These sub-problems are solved and the obtained solutions are compared

with each other. If the solutions of both sub-problems satisfy the integrality conditions, they must be compared and the sub-problem solution that is associated with smaller objective function value for minimization problem or larger objective function value for maximization problem is selected as the optimal solution. If only one sub-problem solution satisfies the MIP integrality conditions, then this solution is saved as incumbent solution (i.e., the optimal solution if no better solution is found) while the branching process is continued on the second sub-problem searching for a better solution that satisfies the MIP integrality conditions. Powerful solvers such as CPLEX, Xpress-MP, and SYMPHONEY implement a combination of branch and bound techniques and cutting-plane techniques to accelerate the computation time associated with solving MIP problems, which allows large MIP problems to be solved using personal computers. The resulted MIP problem can be solved using GAMS. More information about GAMS can be found in [117]. The branching and bounding steps are shown in the following figure.

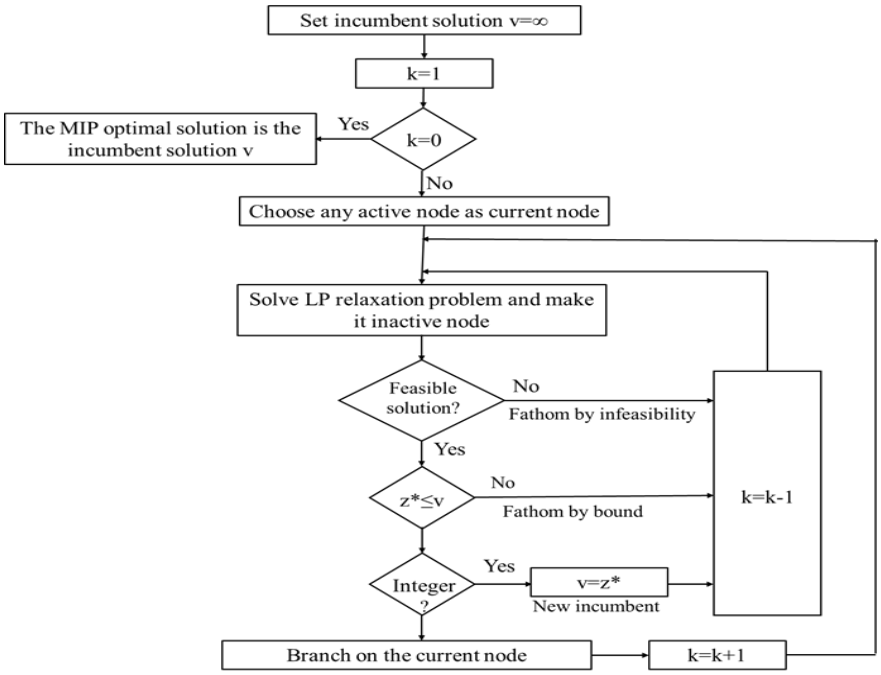

List of Publications

- I. Alsaidan, A. Alanazi, W. Gao, H. Wu, and A. Khodaei, "State-Of-The-Art in Microgrid-Integrated Distributed Energy Storage Sizing," *Energies*, vol. 10, no. 9, p. 1421, Sep. 2017.

- I. Alsaidan, A. Khodaei, and W. Gao, "A Comprehensive Battery Energy Storage Optimal Sizing Model for Microgrid Applications," *IEEE Trans. Power Syst.*, in press. [Online]. Available http://ieeexplore.ieee.org.du.idm.oclc.org/document/8094981/

- I. Alsaidan, A. Khodaei, and W. Gao, "Distributed energy storage sizing for microgrid applications," in *2016 IEEE/PES Transmission and Distribution Conference and Exposition (T&D)*, 2016, pp. 1–5.

- I. Alsaidan, A. Khodaei, and W. Gao, "Determination of battery energy storage technology and size for standalone microgrids," in *2016 IEEE Power and Energy Society General Meeting (PESGM)*, 2016, pp. 1–5.

- I. Alsaidan, A. Khodaei, and W. Gao, "Determination of optimal size and depth of discharge for battery energy storage in standalone microgrids," in *2016 North American Power Symposium (NAPS)*, 2016, pp. 1–6.

- I. Alsaidan, W. Gao, and A. Khodaei, "Battery Energy Storage Sizing for Commercial Customers," in *2017 IEEE Power and Energy Society General Meeting (PESGM)*, 2017.

- I. Alsaidan, W. Gao, and A. Khodaei, "Optimal design of battery energy storage in stand-alone brownfield microgrids," in *2017 North American Power Symposium (NAPS)*, 2017, pp. 1–6.

- I. Alsaidan, W. Gao, A. Khodaei, E. A. Paaso, and S. Bahramirad, "Coordinated Battery Energy Storage Systems Sizing for Photovoltaic Ramp Rate Control," in *CIGRE Grid of the Future Symposium, 2017.*

- I. Alsidan, W. Gao, and A. Khodaei "Distribution Network Expansion through Optimally Sized and Placed Distributed Energy Storage," in *2018 IEEE/PES Transmission and Distribution Conference and Exposition (T&D)*, 2018.